Lecture Notes
in Control and Information Sciences 298

Editors: M. Thoma · M. Morari

Springer

Berlin
Heidelberg
New York
Hong Kong
London
Milan
Paris
Tokyo

Youngjin Choi · Wan Kyun Chung

PID Trajectory Tracking Control for Mechanical Systems

With 22 Figures and 12 Tables

Springer

Series Advisory Board

A. Bensoussan · P. Fleming · M.J. Grimble · P. Kokotovic · A.B. Kurzhanski · H. Kwakernaak · J.N. Tsitsiklis

Authors

Dr. Youngjin Choi
Korea Institute of Science and Technology (KIST)
Intelligent Robotics Research Center
Sungbuk-Gu, Seoul, 136-791, Korea
E-Mail: cyj@kist.re.kr

Prof. Wan Kyun Chung
Pohang University of Science and Technology (POSTECH)
Dept. of Mechanical Engineering
San 31, Hyoja-Dong
Pohang, 790-784, Korea
E-Mail: wkchung@postech.edu

ISSN 0170-8643

ISBN 3-540-20567-5 Springer-Verlag Berlin Heidelberg New York

Cataloging-in-Publication Data applied for
A catalog record for this book is available from the Library of Congress.
Bibliographic information published by Die Deutsche Bibliothek
Die Deutsche Bibliothek lists this publication in the Deutsche Nationalbibliografie; detailed bibliographic data is available in the Internet at <http://dnb.ddb.de>.

Springer-Verlag is a part of Springer Science+Business Media

springeronline.com

Printed in Germany

Typesetting: Data conversion by the authors.
Final processing by PTP-Berlin Protago-TeX-Production GmbH, Berlin
Cover-Design: design & production GmbH, Heidelberg
Printed on acid-free paper 62/3020Yu - 5 4 3 2 1 0

I would like to dedicate this book to my parents, to my daughter Yuhyun and to my wife Seoyoung.
- Dr. Youngjin Choi

For Jinhwa and Kiseo, my family.
- Dr Wan Kyun Chung

Preface

Though PID control has a long history as much as its life force since Ziegler and Nichols published the empirical tuning rules in 1942, surprisingly, it has never been changed in the structure itself. The strength of PID control lies in the simplicity, lucid meaning, and clear effect. Though it must be a widely accepted controller for mechanical control systems, it is still short of theoretical bases, *e.g.*, optimality, performance tuning rules, automatic performance tuning method, and output feedback PID control have not been clearly presented for mechanical control systems. These subjects will be thoroughly discussed in this book. There are many books of PID controller for the purpose of process control, but it is hard to find a book on the characteristics of PID control for mechanical systems.

In the first place, when nonlinear optimal control theory is applied to mechanical systems, a class of Hamilton-Jacobi (HJ) equations is derived as a result of optimization. There are two methods to solve a class of HJ equations: a direct method using an approximation and inverse method finding the performance index from a class of HJ equations. Also, there are two control methods according to the objective: the set-point regulation control and trajectory tracking control. The trajectory tracking control is basically different from set-point regulation one in that the desired configuration, velocity and acceleration profiles according to time progress are added to the motion of mechanical system. This book is focusing on an inverse optimization method and the trajectory tracking control system.

Second, the PID control is shown to be an optimal one for a performance index found inversely from a class of HJ equations. In other words, this book reveals algebraic relationships between the individual PID gains and $\mathcal{H}_\infty$ performance index. Especially, an inverse optimal PID controller is newly defined from the extended disturbance input-to-state stability (ISS) and an inverse optimization method. It is proved that an inverse optimal PID control exists if and only if the mechanical system is extended disturbance input-to-state stable (ISS). Also, selection guidelines for gains are suggested using the time derivative of Lyapunov function.

Third, the performance tuning methods of PID control are derived from performance limitations expressed by a state vector and composite error, respectively. They are suggested for trajectory tracking models of mechanical systems. To begin with, two simple performance tuning rules are suggested for an inverse optimal PID controller: the square tuning rule and linear one. And then, the compound performance tuning rule is suggested unifying both square tuning and linear one. Also, many experiments are performed to show the effectiveness of those tuning rules.

Fourth, an automatic performance tuning method of PID control is derived from the direct adaptive control scheme, because above three tuning methods are all passive in that the control performance can not be directly estimated by them because they are composed of proportional relations. The quasi-equilibrium region is firstly defined to show the existence of target performance for PID controller. Also, it is proved that the control performance is enhanced by applying an auto-tuning law to the PID controller. The experimental results show the validity of auto-tuning law for PID control.

Finally, PID state observer is suggested to accomplish output feedback PID controller, similar to the design method for high-gain observer. The observer gains of PID state observer are found from the robustness against disturbances. Also, it is proved that the output feedback PID control system including a PID state observer can be disturbance input-to-state stable under the condition for observer gain. Additionally, the reduced-order PID (ID) state observer is suggested according to the same procedures with a PID state observer.

We hope this book helps to understand the characteristics of PID controller and finally to better use it.

Korea, Inst. of Sci. & Tech. (KIST), Seoul, Korea,
Oct., 2003 *Youngjin Choi*

Pohang Univ. of Sci. & Tech. (POSTECH), Korea,
Oct., 2003 *Wan Kyun Chung*

Contents

List of Figures

List of Tables

List of Abbreviations

EISS	Extended disturbance Input-to-State Stability
GAS	Global Asymptotic Stability
Hamiltonian system	Hamiltonian control system
HJ	Hamilton-Jacobi equation
HJB	Hamilton-Jacobi-Bellman equation
HJI	Hamilton-Jacobi-Isaacs equation
ID	Integral-Derivative state observer
IOSS	Input-Output-to-State Stability
ISS	Input-to-State Stability
ISS-CLF	Input-to-State Stabilizable Control Lyapunov Function
Lagrangian system	Lagrangian control system
LQG	Linear Quadratic Gaussian control
Modified-CTC	Modified Computed Torque Control
NPDE	Nonlinear Partial Differential Equation
PD	Proportional-Derivative control
PI	Performance Index
PID	Proportional-Integral-Derivative control
SGAS	Semi-Global Asymptotic Stability
SGUUB	Semi-Global Uniform Ultimate Boundedness
UUB	Uniform Ultimate Boundedness

1

Introduction

1.1 Motivation

Since Ziegler and Nichols' PID tuning rules had been published in 1942 [68], the PID control has survived the challenge of advanced control theories, *e.g.*, *LQG* and $\mathcal{H}_\infty$ control [20, 67], adaptive (backstepping) control [28, 38] and so forth. The PID's long life force comes from its clear meaning and effectiveness in practice. In PID control, the P-control (Proportional control) is the present effort making a present state into desired state, I-control (Integral control) is the accumulated effort using the experience information of bygone state and D-control (Derivative control) is the predictive effort reflecting the tendency information for ongoing state. Also, PID control has been utilized irrespective of linear system or nonlinear one, electrical system or mechanical one, time-invariant system or time-varying one. Though the PID control has been widely accepted in industry, PID control itself is still short of the theoretical basis, *e.g.*, the optimality of PID control, performance tuning rules of PID control, automatic performance tuning method and the PID state observer have not been clearly presented especially for the trajectory tracking control of mechanical systems.

As we can see in [3, 26, 66], the PID control has been an intensive research topic for process control systems, but it has not attracted one's interest so much for electrical and mechanical control systems. For electrical control systems, there have been a lot of control methods because the linear characteristics is dominant near operating region, *e.g.*, lead/lag compensator, LQG control, $\mathcal{H}_\infty$ control and so on. On the contrary, since most mechanical systems show nonlinear characteristics generally, there has been only a few control methods for mechanical systems. The representative control method for nonlinear mechanical systems is a feedback linearization method such as computed-torque one. The feedback linearization method is applicable to the case that the mechanical parameters such as moment of Inertia, center of mass and a variety of friction parameters are all identified exactly. If they are not possible to be identified all, then the feedback linearization with an adaptive

Y. Choi, W.K. Chung: PID Trajectory Tracking Control for Mechanical Systems, LNCIS 298, pp. 3–7, 2004.

control scheme in [23, 30, 56] can be applied to nonlinear systems. Though the adaptive control is useful for uncertain mechanical systems, it has brought tremendous complexity in controller. According to the survey reported in [35], since n-link robot manipulators have $10n$ parameters to be identified by adaptation, a great deal of algebraic calculations are required to make use of an adaptive control according to the increase of the number of linkage. Actually, industrial robot manufacturing company has used basically the simple PID control with compensation, in spite of the development of adaptive and/or modern control assuring better performance, because of its simplicity.

The strongest advantage of PID control is a 'simplicity' itself. The simple control is preferable to the complex control at least in industry, if the performance enhanced by using complex control does not stand in different levels. Inspired by this idea, the author tried to extend the theoretical basis of PID control to both robust control theory and direct adaptive ones including several issues such as optimality, performance limitation, performance tuning rule, auto-tuning law, and observer design.

1.2 Historic PD and PID

In Table 1.1, the stability brought by applying either PD or PID control to mechanical systems is largely classified according to the regulation control or tracking one. After that Takegaki and Arimoto had proved the global asymptotic stability (GAS) by PD control in [60], many kinds of stability have been proved under various conditions as shown in Table 1.1.

For mechanical system including the external disturbance such as Coulomb friction, the GAS of PID control was proved in [2]. Even for the mechanical system under gravity effect, Tomei proved the GAS of PD control in [63] by using an adaptation for gravity term. On the other hand, Ortega *et al.* showed in [46] that the PI^{2}D control could bring the semi-global asymptotic stability (SGAS) in the existence of gravity effect and bounded external disturbances. Also, Angeli proved in [1] that the PD control could achieve the input-output-to-state stability (IOSS) for mechanical systems. Recently, Ramirez *et al.* proved the semi-global asymptotic stability (SGAS) with conditions for PID gains in [51].

The trajectory tracking control system is quite different from the regulation control system in that the desired configurations which are functions of time are inserted in equation of motion for mechanical system. Hence, the trajectory tracking system has the time-varying characteristics because of desired configurations. As a primitive work, Qu and Dorsey proved in [50] that the PD control could bring uniform ultimate boundedness (UUB). Also, Berghuis and Nijmeijer proposed the output feedback PD control which brought the semi-global uniform ultimate boundedness (SGUUB) in [7] under gravity and a bounded disturbance. Recently, Choi *et al.* suggested an inverse optimal PID control in [14]. As shown in Table 1.1, it assures the extended disturbance

input-to-state stability (EISS) and $\mathcal{H}_\infty$ optimality for a given performance index. These characteristics will be discussed in chapter 3.

Table 1.1. Stability classification achieved by applying PD/PID control to mechanical systems : where PD+A : PD plus adaptation for gravity term, PD+NI : PD plus a nonlinear integral control, and PD+O : PD plus linear state observer

	Gravity	Disturbance	Optimality	Stability	Year
PD Regulation	x	x	x	GAS	1981 [60]
PID Regulation	x	o	x	GAS	1984 [2]
PD+A Regulation	o	x	x	GAS	1991 [63]
PI^2D Regulation	o	o	x	SGAS	1995 [46]
PD+NI Regulation	o	x	x	GAS	1998 [32]
PD Regulation	x	x	x	IOSS	1999 [1]
PID Regulation	o	o	x	SGAS	2000 [51]
PD Tracking	o	x	x	UUB	1991 [50]
PD+O Tracking	o	o	x	SGUUB	1994 [7]
PID Tracking	o	o	o	EISS	2001 [14]

GAS : global asymptotic stability,
SGAS : semi-global asymptotic stability,
IOSS : input-output-to-state stability,
UUB : uniform ultimate boundedness,
SGUUB : semi-global uniform ultimate boundedness,
EISS : extended disturbance input-to-state stability,

1.3 Book Preview

This book is organized as shown in Fig. 1.1. Chapter 2 describes the characteristics of mechanical system. Also, optimal control methods for mechanical system are discussed from the viewpoint of both direct and inverse optimization approaches. The direct one is an approximate method and an inverse one has been used in [18, 47, 50] based on the primitive work by Kalman. Some kinds of Hamilton-Jacobi equations, *e.g.*, Hamilton-Jacobi-Bellman (HJB) equation and Hamilton-Jacobi-Isaacs (HJI) equation, are obtained from the optimization similar to Riccati equation in linear systems.

In chapter 3, it is discussed that the PID control for mechanical systems can be optimal for what performance index. Actually, although nonlinear $\mathcal{H}_\infty$ optimal control theory has been developed for nonlinear mechanical systems, application examples are few and, if any, it is very restrictive in applying to multi-variable mechanical systems. Therefore, it is important to reveal the relationship between $\mathcal{H}_\infty$ optimal control and PID one. Also, we can confirm a $\mathcal{H}_\infty$ optimality of PID through the performance estimation by optimality.

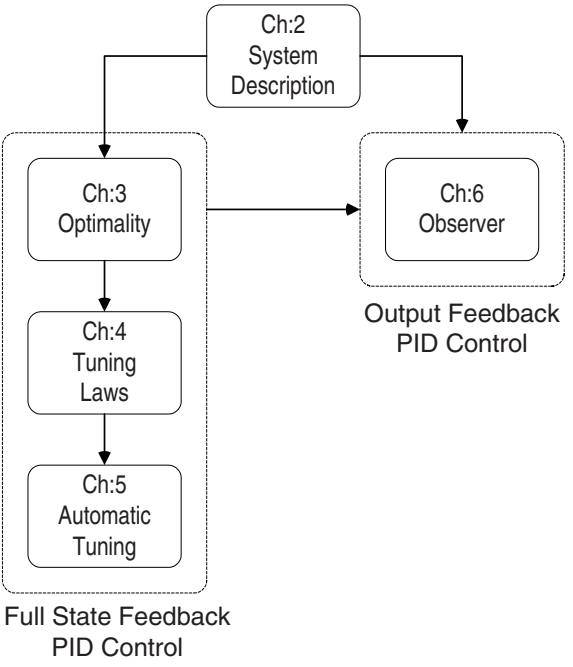

Fig. 1.1. Relations among the chapters

In chapter 4, two simple performance tuning rules are derived from the performance limitation of PID control system, *e.g.*, the square tuning rule and linear one. Actually, square tuning rule and linear one have an obvious importance in an engineering sense because of their simplicity. And then, a compound performance tuning rule is suggested unifying both square rule and linear one. Also, experimental results for a robotic manipulator show the effectiveness of those tuning rules.

In chapter 5, an automatic performance tuning rule is proposed for mechanical systems, with an extension of the idea about above passive tuning rules derived from the performance limitation. A lot of automatic performance tuning methods for PID control system have been proposed for the chemical process control systems as we can see in [3, 66], however, they can not be directly applied to mechanical systems because most process systems show very slow responses and time-delay. Though they have attracted one's interest, there has been still no auto-tuning law for mechanical systems. According to the direct adaptive control scheme, the auto-tuning law of PID controller and the performance improvement enhanced by using an auto-tuning law are suggested in this chapter.

In chapter 6, an output feedback PID controller is considered instead of the full state feedback one. Actually, the mechanical systems are usually equipped

with only position measurement devices, *e.g.*, the optical encoder is utilized as an exact position measurement device of low cost, hence, the observer is required to estimate the remaining states, *e.g.*, velocity and integral of position. A kind of high-gain observer is chosen as the PID state observer. Additionally, the reduced-PID (ID) state observer is derived from a PID state observer. Finally, chapter 7 concludes the results.

1.4 Notations

Following notations are used in this book. First, a continuous function $\alpha : [0, a) \to \Re_+$ is said to belong to class $\mathcal{K}$, if it is strictly increasing and $\alpha(0) = 0$. If $a = \infty$ and $\alpha(r) \to \infty$ as $r \to \infty$, then the function $\alpha(r)$ is said to belong to class $\mathcal{K}_\infty$. Second, a continuous function $\beta : [0, a) \times \Re_+ \to \Re_+$ is said to belong to class $\mathcal{KL}$ if, for each fixed s, the mapping $\beta(r, s)$ belongs to class $\mathcal{K}$ with respect to r and, for each fixed r, the mapping $\beta(r, s) \to 0$ as $s \to \infty$. Third, the Euclidean norm of signal vector $\boldsymbol{x}(t)$ is defined by

$$|\boldsymbol{x}| \triangleq \sqrt{\boldsymbol{x}(t)^T \boldsymbol{x}(t)}, \tag{1.1}$$

the $\mathcal{L}_2$ norm of signal vector $\boldsymbol{x}(t)$ is defined as follows:

$$\|\boldsymbol{x}\| \triangleq \sqrt{\int_0^t \boldsymbol{x}(\sigma)^T \boldsymbol{x}(\sigma) d\sigma}, \tag{1.2}$$

and the $\mathcal{L}_\infty$ norm is defined as the maximum among Euclidean norms of signal vector $\boldsymbol{x}(t)$ as following form:

$$\|\boldsymbol{x}\|_\infty \triangleq \max_{0 \le \sigma \le t} |\boldsymbol{x}(\sigma)|. \tag{1.3}$$

2

Robust and Optimal Control for Mechanical Systems

2.1 Introduction

There are three methods to describe the equation of motion for mechanical system: Newtonian mechanics, Lagrangian one and Hamiltonian one. Newtonian mechanics has been used for simple mechanical systems because it is an intuitive and non-systematic method. On the contrary, Lagrangian and Hamiltonian ones can be used for complex multi-body mechanical systems because they are systematic approaches. In this chapter, either Lagrangian or Hamiltonian mechanics is used as a representation for motion of mechanical systems.

Also, a class of Hamilton-Jacobi (HJ) equations in [8, 65] should be solved to get the optimality for some performance index. However, since they are nonlinear partial differential equations, it is hard or impossible to solve them exactly. There are several trials to solve them: the one is a direct optimization method by using approximation and the other is an inverse optimization method which finds a performance index from HJ equation conversely. First, the approximation method was suggested to approximately solve the HJ equation in [12, 64, 65]. For a given performance index, it produces directly an approximate solution for the HJ equation, as the sweep method for Riccati equation in linear systems. Second, the inverse optimal method in [18, 36, 47] suggests the solution first, and then it finds the performance index conversely from the solution of HJ equation. In this chapter, both direct and inverse methods are suggested and explained as a background in regard to nonlinear optimal control.

According to the objective of mechanical control systems, there are two control types: set-point regulation and trajectory tracking control. Since the set-point regulation system shows nonlinear time-invariant characteristics, nonlinear $\mathcal{H}_\infty$ control method can be directly applied to mechanical systems. On the contrary, the trajectory tracking system has the nonlinear time-varying characteristics. To show the optimality of trajectory tracking system, the authors of [18, 47] used the modified computed torque control (Modified-CTC).

Y. Choi, W.K. Chung: PID Trajectory Tracking Control for Mechanical Systems, LNCIS 298, pp. 9–26, 2004.

This chapter is organized as follows: section 2.2 arranges two representation methods for mechanical systems, the optimal control methods for the set-point regulation and trajectory tracking are surveyed in section 2.3 and 2.4, respectively.

2.2 Nonlinear Mechanical Control Systems

Mechanical system is generally described by nonlinear equation where *Lagrangian* and *Hamiltonian* mechanics are used to represent the behavior of mechanical system. Let us consider a mechanical system with n degrees of freedom, locally represented by n generalized configuration (position) coordinates $\boldsymbol{q} = (q_1, \cdots, q_n)$. In classical mechanics, the following equation of motion is derived

$$\frac{d}{dt}\left(\frac{\partial T}{\partial \dot{q}_i}\right) - \frac{\partial T}{\partial q_i} = F_i, \qquad i = 1, 2, \cdots, n.$$

Here $T(\boldsymbol{q}, \dot{\boldsymbol{q}})$ denotes the total kinetic energy of the system, while F_i is the force acting on the system. Usually, the force F_i is decomposed of conservative forces, *i.e.*, forces that are derivable from a potential energy, and remaining part F_i^e, consisting of dissipative and generalized external forces as

$$F_i = -\frac{\partial V}{\partial q_i} + F_i^e, \qquad i = 1, 2, \cdots, n,$$

with the potential energy function $V(\boldsymbol{q})$.

Defining the Lagrangian function $L_0(\boldsymbol{q}, \dot{\boldsymbol{q}})$ as $T(\boldsymbol{q}, \dot{\boldsymbol{q}}) - V(\boldsymbol{q})$, one arrives at the Euler-Lagrange equations

$$\frac{d}{dt}\left(\frac{\partial L_0}{\partial \dot{q}_i}\right) - \frac{\partial L_0}{\partial q_i} = F_i^e, \qquad i = 1, 2, \cdots, n. \tag{2.1}$$

In general, for a mechanical system with a Lagrangian $L(\boldsymbol{q}, \dot{\boldsymbol{q}}, \boldsymbol{u})$ depending directly on u_i corresponding to the generalized external force F_i^e, we obtain the equation of motion as follow:

$$\frac{d}{dt}\left(\frac{\partial L}{\partial \dot{q}_i}\right) - \frac{\partial L}{\partial q_i} = 0, \qquad i = 1, 2, \cdots, n. \tag{2.2}$$

Notice that (2.1) can be regarded as a special case of (2.2) by taking the Lagrangian

$$L(\boldsymbol{q}, \dot{\boldsymbol{q}}, \boldsymbol{u}) = L_0(\boldsymbol{q}, \dot{\boldsymbol{q}}) + \sum_{i=1}^{n} q_i u_i, \tag{2.3}$$

where u_i is decomposed of the control input variable τ_i and external input disturbance d_i, *i.e.*, $\boldsymbol{u} = \boldsymbol{\tau} + \boldsymbol{d}$. We will call (2.2) a Lagrangian control system, in short *Lagrangian system.*

Let us now formulate a Hamiltonian control system. For the Lagrangian control system of (2.2), the generalized momentum is defined as follows:

$$p_i = \frac{\partial L(\boldsymbol{q}, \dot{\boldsymbol{q}}, \boldsymbol{u})}{\partial \dot{q}_i}, \qquad i = 1, 2, \cdots, n. \tag{2.4}$$

In general, since the $n \times n$ matrix with (i, j)-th element $\frac{\partial^2 L}{\partial \dot{q}_i \partial \dot{q}_j}$ will be nonsingular everywhere, Hamiltonian function $H(\boldsymbol{q}, \boldsymbol{p}, \boldsymbol{u})$ is defined as the Legendre transform of $L(\boldsymbol{q}, \dot{\boldsymbol{q}}, \boldsymbol{u})$, *i.e.*,

$$H(\boldsymbol{q}, \boldsymbol{p}, \boldsymbol{u}) = \sum_{i=1}^{n} p_i \dot{q}_i - L(\boldsymbol{q}, \dot{\boldsymbol{q}}, \boldsymbol{u}), \tag{2.5}$$

where $\dot{\boldsymbol{q}}$ and $\boldsymbol{p}$ are related by (2.4). Here, with (2.4) and (2.5), the Lagrangian control system (2.2) can be transformed into the Hamiltonian control system as following forms:

$$\dot{q}_i = \frac{\partial H(\boldsymbol{q}, \boldsymbol{p}, \boldsymbol{u})}{\partial p_i} \tag{2.6}$$

$$\dot{p}_i = -\frac{\partial H(\boldsymbol{q}, \boldsymbol{p}, \boldsymbol{u})}{\partial q_i}. \tag{2.7}$$

As a matter of fact, (2.7) follows from substituting (2.4) into (2.2), while (2.6) follows from (2.5). Also, above Hamiltonian control system is called as *Hamiltonian system* briefly. The main advantage of Hamiltonian system in comparison with Lagrangian system is that Hamiltonian system immediately constitutes a control system in standard state space form, with state variables $(\boldsymbol{q}, \boldsymbol{p})$. In particular, if $L(\boldsymbol{q}, \dot{\boldsymbol{q}}, \boldsymbol{u})$ is given as in (2.3), then it immediately follows that

$$H(\boldsymbol{q}, \boldsymbol{p}, \boldsymbol{u}) = H_0(\boldsymbol{q}, \boldsymbol{p}) - \sum_{i=1}^{n} q_i u_i,$$

where $H_0(\boldsymbol{q}, \boldsymbol{p})$ is the Legendre transform of $L_0(\boldsymbol{q}, \dot{\boldsymbol{q}})$.

2.2.1 Lagrangian System

To begin with, let us obtain the Lagrangian system (Lagrangian control system) for typical mechanical systems. The kinetic energy of mechanical system is characterized by using Inertia matrix $\boldsymbol{M}(\boldsymbol{q})$. If the Lagrangian is given as follows:

$$L(\boldsymbol{q}, \dot{\boldsymbol{q}}, \boldsymbol{u}) = \frac{1}{2} \dot{\boldsymbol{q}}^T \boldsymbol{M}(\boldsymbol{q}) \dot{\boldsymbol{q}} - V(\boldsymbol{q}) + \boldsymbol{q}^T \boldsymbol{u}, \tag{2.8}$$

then we can obtain the description of Lagrangian system using (2.2) as follows:

$$\boldsymbol{M}(\boldsymbol{q}) \ddot{\boldsymbol{q}} + \left[\dot{\boldsymbol{M}}(\boldsymbol{q}) - \frac{1}{2} \frac{\partial}{\partial \boldsymbol{q}} \{ \dot{\boldsymbol{q}}^T \boldsymbol{M}(\boldsymbol{q}) \} \right] \dot{\boldsymbol{q}} + \frac{\partial V(\boldsymbol{q})}{\partial \boldsymbol{q}} - \boldsymbol{u} = \boldsymbol{0}, \tag{2.9}$$

because the components of (2.2) are calculated as following forms:

$$\frac{d}{dt}\left(\frac{\partial L(\boldsymbol{q},\dot{\boldsymbol{q}},\boldsymbol{u})}{\partial \dot{\boldsymbol{q}}}\right) = \frac{d}{dt}\left(\boldsymbol{M}(\boldsymbol{q})\dot{\boldsymbol{q}}\right)$$
$$\frac{\partial L(\boldsymbol{q},\dot{\boldsymbol{q}},\boldsymbol{u})}{\partial \boldsymbol{q}} = \frac{1}{2}\left[\frac{\partial}{\partial \boldsymbol{q}}\left\{\dot{\boldsymbol{q}}^T\boldsymbol{M}(\boldsymbol{q})\right\}\right]\dot{\boldsymbol{q}} - \frac{\partial V(\boldsymbol{q})}{\partial \boldsymbol{q}} + \boldsymbol{u}.$$

If the Coriolis and centrifugal matrix is defined as following form:

$$\boldsymbol{C}(\boldsymbol{q},\dot{\boldsymbol{q}}) = \dot{\boldsymbol{M}}(\boldsymbol{q}) - \frac{1}{2}\frac{\partial}{\partial \boldsymbol{q}}\left\{\dot{\boldsymbol{q}}^T\boldsymbol{M}(\boldsymbol{q})\right\}, \tag{2.10}$$

and the gravitational torque/force is defined as $\boldsymbol{g}(\boldsymbol{q}) = \frac{\partial V(\boldsymbol{q})}{\partial \boldsymbol{q}}$ with $\boldsymbol{u} = \boldsymbol{\tau} - \boldsymbol{d}$, then Lagrangian system (2.9) is simplified as following well-known equation:

$$\boldsymbol{M}(\boldsymbol{q})\ddot{\boldsymbol{q}} + \boldsymbol{C}(\boldsymbol{q},\dot{\boldsymbol{q}})\dot{\boldsymbol{q}} + \boldsymbol{g}(\boldsymbol{q}) + \boldsymbol{d} = \boldsymbol{\tau}, \tag{2.11}$$

where $\boldsymbol{d}$ is the unknown external input disturbance and $\boldsymbol{\tau}$ is control input. Here, we should notice that the sign of unknown external input disturbance $\boldsymbol{d}$ is of no importance.

2.2.2 Hamiltonian System

First of all, the Hamiltonian is derived from the generalized momentum (2.4) and Legendre transform (2.5) as follows:

$$H(\boldsymbol{q},\boldsymbol{p},\boldsymbol{u}) = \frac{1}{2}\boldsymbol{p}^T\boldsymbol{M}^{-1}(\boldsymbol{q})\boldsymbol{p} + V(\boldsymbol{q}) - \boldsymbol{q}^T\boldsymbol{u}. \tag{2.12}$$

Next, let us express the Hamiltonian system (Hamiltonian control system) for a mechanical system as simple as possible. When the Hamiltonian is given as (2.12), the Hamiltonian system (2.6) and (2.7) are calculated as follows:

$$\begin{aligned}
\dot{\boldsymbol{q}}^T &= \frac{\partial H(\boldsymbol{q},\boldsymbol{p},\boldsymbol{u})}{\partial \boldsymbol{p}^T} \\
&= \boldsymbol{p}^T\boldsymbol{M}^{-1}(\boldsymbol{q}) \\
\dot{\boldsymbol{p}}^T &= -\frac{\partial H(\boldsymbol{q},\boldsymbol{p},\boldsymbol{u})}{\partial \boldsymbol{q}^T} \\
&= -\frac{1}{2}\boldsymbol{p}^T\left[\frac{\partial \boldsymbol{M}^{-1}}{\partial q_1}\boldsymbol{p}\middle|\ldots\middle|\frac{\partial \boldsymbol{M}^{-1}}{\partial q_n}\boldsymbol{p}\right] - \frac{\partial V(\boldsymbol{q})}{\partial \boldsymbol{q}^T} + \boldsymbol{u}^T.
\end{aligned}$$

By using $\frac{\partial \boldsymbol{M}^{-1}}{\partial q_i} = -\boldsymbol{M}^{-1}\frac{\partial \boldsymbol{M}}{\partial q_i}\boldsymbol{M}^{-1}$, above equation can be rewritten as

$$\begin{aligned}
\dot{\boldsymbol{p}} &= \frac{1}{2}\left[\frac{\partial \boldsymbol{M}}{\partial q_1}\dot{\boldsymbol{q}}\middle|\ldots\middle|\frac{\partial \boldsymbol{M}}{\partial q_n}\dot{\boldsymbol{q}}\right]^T\boldsymbol{M}^{-1}(\boldsymbol{q})\boldsymbol{p} - \boldsymbol{g}(\boldsymbol{q}) + \boldsymbol{u}. \\
&= \frac{1}{2}\left[\frac{\partial}{\partial \boldsymbol{q}}\left\{\dot{\boldsymbol{q}}^T\boldsymbol{M}(\boldsymbol{q})\right\}\right]\boldsymbol{M}^{-1}(\boldsymbol{q})\boldsymbol{p} - \boldsymbol{g}(\boldsymbol{q}) + \boldsymbol{u}.
\end{aligned} \tag{2.13}$$

Here, we should note that the derivative of Inertia matrix can be decomposed like this

$$\dot{\boldsymbol{M}}(\boldsymbol{q}) = \frac{1}{2}\left[\frac{\partial}{\partial \boldsymbol{q}}\left\{\dot{\boldsymbol{q}}^T \boldsymbol{M}(\boldsymbol{q})\right\}\right] + \frac{1}{2}\left[\frac{\partial}{\partial \boldsymbol{q}}\left\{\dot{\boldsymbol{q}}^T \boldsymbol{M}(\boldsymbol{q})\right\}\right]^T. \tag{2.14}$$

Finally, if we introduce the Coriolis and centrifugal matrix (2.10) to above equations, then the Hamiltonian system is described with coordinates $(q_1, q_2, \ldots, q_n, p_1, p_2, \ldots, p_n)$ as follows:

$$\begin{aligned} \dot{\boldsymbol{q}} &= \boldsymbol{M}^{-1}(\boldsymbol{q})\boldsymbol{p} \\ \dot{\boldsymbol{p}} &= \boldsymbol{C}^T(\boldsymbol{q}, \dot{\boldsymbol{q}})\boldsymbol{M}^{-1}(\boldsymbol{q})\boldsymbol{p} - \boldsymbol{g}(\boldsymbol{q}) + \boldsymbol{d} + \boldsymbol{\tau}, \end{aligned} \tag{2.15}$$

using $\boldsymbol{u} = \boldsymbol{\tau} + \boldsymbol{d}$ in (2.13). Additionally, we can obtain the following Lemma for the relationship between Inertia matrix and Coriolis and centrifugal one.

Lemma 1. *For Lagrangian system (2.11) and Hamiltonian system (2.15), the following properties are always satisfied:*

1. $\dot{\boldsymbol{M}}(\boldsymbol{q}) = \boldsymbol{C}(\boldsymbol{q}, \dot{\boldsymbol{q}}) + \boldsymbol{C}^T(\boldsymbol{q}, \dot{\boldsymbol{q}})$.
2. $\dot{\boldsymbol{M}}(\boldsymbol{q}) - 2\boldsymbol{C}(\boldsymbol{q}, \dot{\boldsymbol{q}})$ *is skew symmetric.*
3. $\dot{\boldsymbol{M}}(\boldsymbol{q}) - 2\boldsymbol{C}^T(\boldsymbol{q}, \dot{\boldsymbol{q}})$ *is skew symmetric.*

Above Lemma can be easily proved using (2.10) and (2.14). Also, above Lemma plays a core role in proving either the stability or optimality in following sections.

2.3 Set-Point Regulation Control

In this section, we survey the set-point regulation (point-to-point) position control for Hamiltonian systems. The stability achieved by applying a PD control to Hamiltonian system was investigated for the first time by Arimoto *et al.* in [2, 60]. Also, Van der schaft showed in [64, 65] that the optimality for nonlinear systems can be accomplished by the solution for Hamilton-Jacobi (HJ) equation. Since it is hard to solve directly the HJ equation, however, the approximation method to solve HJ equation was suggested for Hamiltonian system by Choi *et al.* in [12].

2.3.1 Global Asymptotic Stability [Arimoto *et al.*]

For Hamiltonian system (2.15), assume that there exist no gravity force and external disturbance, *i.e.*, $\boldsymbol{g}(\boldsymbol{q}) = \boldsymbol{0}$ and $\boldsymbol{d} = \boldsymbol{0}$. Putting a PD control as following form:

$$\boldsymbol{\tau} = -\boldsymbol{K}_D\dot{\boldsymbol{q}} - \boldsymbol{K}_P(\boldsymbol{q} - \boldsymbol{q}_s)$$

into (2.15), the closed-loop control system is obtained as follows:

$$\begin{aligned}\dot{\boldsymbol{q}} &= \boldsymbol{M}^{-1}(\boldsymbol{q})\boldsymbol{p} \\ \dot{\boldsymbol{p}} &= \boldsymbol{C}^T(\boldsymbol{q},\dot{\boldsymbol{q}})\boldsymbol{M}^{-1}(\boldsymbol{q})\boldsymbol{p} - \boldsymbol{K}_D\boldsymbol{M}^{-1}(\boldsymbol{q})\boldsymbol{p} - \boldsymbol{K}_P(\boldsymbol{q}-\boldsymbol{q}_s),\end{aligned} \tag{2.16}$$

where $\boldsymbol{K}_D > \boldsymbol{0}, \boldsymbol{K}_P > \boldsymbol{0}$ are constant diagonal gain matrices and $\boldsymbol{q}_s$ is the set-point to be regulated. Now, it is possible to prove the GAS of equilibrium point $(\boldsymbol{p}=\boldsymbol{0}, \boldsymbol{q}=\boldsymbol{q}_s)$ with an aid of Lyapunov direct method. If the following Lyapunov function

$$V(\boldsymbol{p},\boldsymbol{q}) = \frac{1}{2}\boldsymbol{p}^T\boldsymbol{M}^{-1}(\boldsymbol{q})\boldsymbol{p} + \frac{1}{2}(\boldsymbol{q}-\boldsymbol{q}_s)^T\boldsymbol{K}_P(\boldsymbol{q}-\boldsymbol{q}_s) \tag{2.17}$$

is utilized, then its time derivative is obtained along the solution trajectory of (2.16) as follows:

$$\begin{aligned}\dot{V} &= \boldsymbol{p}^T\boldsymbol{M}^{-1}(\boldsymbol{q})\dot{\boldsymbol{p}} + \frac{1}{2}\boldsymbol{p}^T\dot{\boldsymbol{M}}^{-1}(\boldsymbol{q})\boldsymbol{p} + (\boldsymbol{q}-\boldsymbol{q}_s)^T\boldsymbol{K}_P\dot{\boldsymbol{q}} \\ &= \boldsymbol{p}^T\boldsymbol{M}^{-1}(\boldsymbol{q})\boldsymbol{C}^T(\boldsymbol{q},\dot{\boldsymbol{q}})\boldsymbol{M}^{-1}(\boldsymbol{q})\boldsymbol{p} \\ &\quad -\boldsymbol{p}^T\boldsymbol{M}^{-1}(\boldsymbol{q})\boldsymbol{K}_D\boldsymbol{M}^{-1}(\boldsymbol{q})\boldsymbol{p} + \frac{1}{2}\boldsymbol{p}^T\dot{\boldsymbol{M}}^{-1}(\boldsymbol{q})\boldsymbol{p}.\end{aligned}$$

Since $\dot{\boldsymbol{M}}^{-1} = -\boldsymbol{M}^{-1}\dot{\boldsymbol{M}}\boldsymbol{M}^{-1}$ and $\dot{\boldsymbol{M}}(\boldsymbol{q}) - 2\boldsymbol{C}^T(\boldsymbol{q},\dot{\boldsymbol{q}})$ is skew symmetric as stated in Lemma 1, it is easy to see that

$$\begin{aligned}\dot{V} &= \frac{1}{2}\boldsymbol{p}^T\boldsymbol{M}^{-1}(\boldsymbol{q})\left[2\boldsymbol{C}^T(\boldsymbol{q},\dot{\boldsymbol{q}}) - \dot{\boldsymbol{M}}(\boldsymbol{q})\right]\boldsymbol{M}^{-1}(\boldsymbol{q})\boldsymbol{p} \\ &\quad -\boldsymbol{p}^T\boldsymbol{M}^{-1}(\boldsymbol{q})\boldsymbol{K}_D\boldsymbol{M}^{-1}(\boldsymbol{q})\boldsymbol{p} \\ &= -\boldsymbol{p}^T\boldsymbol{M}^{-1}(\boldsymbol{q})\boldsymbol{K}_D\boldsymbol{M}^{-1}(\boldsymbol{q})\boldsymbol{p}.\end{aligned} \tag{2.18}$$

At this stage, it is necessary to recall the well-known LaSalle Theorem (Invariance Theorem). If there exists such a function $V(\boldsymbol{x})$ defined in a certain domain Ω of the state space of $\boldsymbol{x} = (\boldsymbol{p},\boldsymbol{q})$ containing the equilibrium point $\boldsymbol{x}_0 = (\boldsymbol{0},\boldsymbol{q}_s)$, then for any initial condition $\boldsymbol{x}(0) = (\boldsymbol{p}(0),\boldsymbol{q}(0))$ in a neighborhood of $\boldsymbol{x}_0$, the solution trajectory $(\boldsymbol{p}(t),\boldsymbol{q}(t))$ of equation (2.16) approaches asymptotically to the maximal invariant set $\mathcal{M}$ contained in the set

$$\mathcal{E} = \left\{\boldsymbol{x} = (\boldsymbol{p},\boldsymbol{q}) \in \Omega : \dot{V} = 0\right\}.$$

In our case, according to equation (2.18), $\dot{V} = 0$ means $\boldsymbol{p} = \boldsymbol{0}$ because $\boldsymbol{K}_D > \boldsymbol{0}$. Therefore, it holds along any solution trajectory in $\mathcal{E}$ that

$$\dot{\boldsymbol{p}} = -\boldsymbol{K}_P(\boldsymbol{q}-\boldsymbol{q}_s).$$

This in turn implies that $\mathcal{M}$ is composed of the single point $\boldsymbol{x}_0 = (\boldsymbol{p}=\boldsymbol{0}, \boldsymbol{q}=\boldsymbol{q}_s)$. Also, since Lyapunov function (2.17) is unbounded function for $\boldsymbol{x}$, *i.e.*, $V \to \infty$ as $|\boldsymbol{x}| \to \infty$, the global asymptotic stability (GAS) of the equilibrium point $\boldsymbol{x}_0 = (\boldsymbol{0},\boldsymbol{q}_s)$ can be proved by PD control.

2.3.2 Direct $\mathcal{H}_\infty$ Control [Choi *et al.*]

For Hamiltonian system (2.15), let us assume that there exists no gravity force, *i.e.*, $\boldsymbol{g}(\boldsymbol{q}) = \boldsymbol{0}$. Since the equilibrium point is $\boldsymbol{p} = \boldsymbol{0}$ and $\boldsymbol{q} = \boldsymbol{q}_s$, if we define the state vector as follows:

$$\boldsymbol{x} \triangleq \begin{bmatrix} \boldsymbol{x}_1 \\ \boldsymbol{x}_2 \end{bmatrix} = \begin{bmatrix} \boldsymbol{q} - \boldsymbol{q}_s \\ \boldsymbol{p} \end{bmatrix} \in \Re^{2n},$$

then state space representation of Hamiltonian system (2.15) can be written as follows:

$$\dot{\boldsymbol{x}} = \boldsymbol{A}(\boldsymbol{q}, \dot{\boldsymbol{q}})\boldsymbol{x} + \boldsymbol{B}\boldsymbol{d} + \boldsymbol{B}\boldsymbol{\tau},$$

where

$$\boldsymbol{A}(\boldsymbol{q}, \dot{\boldsymbol{q}}) = \begin{bmatrix} \boldsymbol{0} & \boldsymbol{M}^{-1}(\boldsymbol{q}) \\ \boldsymbol{0} & \boldsymbol{C}^T(\boldsymbol{q}, \dot{\boldsymbol{q}})\boldsymbol{M}^{-1}(\boldsymbol{q}) \end{bmatrix}$$
$$\boldsymbol{B} = \begin{bmatrix} \boldsymbol{0} \\ \boldsymbol{I} \end{bmatrix}.$$

Here, we should notice that $\boldsymbol{A}(\boldsymbol{q}, \dot{\boldsymbol{q}})$ is function of state vector, because $\boldsymbol{q}(= \boldsymbol{q}_s + \boldsymbol{x}_1)$ and $\dot{\boldsymbol{q}}(= \boldsymbol{M}^{-1}(\boldsymbol{x}_1 + \boldsymbol{q}_s)\boldsymbol{x}_2)$ are the function of state vector.[1] Let us consider the typical $\mathcal{H}_\infty$ Performance Index (PI) as following form:

$$\int_0^\infty \left[\boldsymbol{x}^T\boldsymbol{Q}\boldsymbol{x} + \boldsymbol{u}^T\boldsymbol{R}\boldsymbol{u}\right] dt \leq \gamma^2 \int_0^\infty |\boldsymbol{d}|^2 dt \tag{2.19}$$

where $\boldsymbol{Q}$ is the state weighting matrix and $\boldsymbol{R}$ the control input weighting. The Hamilton-Jacobi (HJ) equation for above PI can be found in following Lemma, also in [64].

Lemma 2. *Let $\gamma > 0$, Suppose there exists a smooth function $V(\boldsymbol{x}) > 0$ with $V(\boldsymbol{0}) = 0$ that satisfies*

$$HJ = \boldsymbol{V}_x\boldsymbol{A}\boldsymbol{x} + \frac{1}{2\gamma^2}\boldsymbol{V}_x\boldsymbol{B}\boldsymbol{B}^T\boldsymbol{V}_x^T - \frac{1}{2}\boldsymbol{V}_x\boldsymbol{B}\boldsymbol{R}^{-1}\boldsymbol{B}^T\boldsymbol{V}_x^T + \frac{1}{2}\boldsymbol{x}^T\boldsymbol{Q}\boldsymbol{x} = 0, \tag{2.20}$$

where $\boldsymbol{V}_x \triangleq \frac{\partial V}{\partial \boldsymbol{x}^T}$ is a row vector, then the following control law

$$\boldsymbol{\tau} = -\boldsymbol{R}^{-1}\boldsymbol{B}^T\boldsymbol{V}_x^T \tag{2.21}$$

minimizes the $\mathcal{H}_\infty$ PI (2.19) with a given $\mathcal{L}_2$-gain γ.

[1] The set-point $\boldsymbol{q}_s$ is a constant vector.

Approximated Solution of Hamilton-Jacobi (HJ) Equation [van der Schaft]

Consider the Hamiltonian vector fields on Hamilton-Jacobi equation (2.20) with Hamiltonian $\mathcal{H} : N^{2n} \to \Re$ and equilibrium $\boldsymbol{z}_0$,

$$\dot{\boldsymbol{z}} = \boldsymbol{X}_{\mathcal{H}}(\boldsymbol{z}), \quad \boldsymbol{X}_{\mathcal{H}}(\boldsymbol{z}_0) = \boldsymbol{0},$$

and local coordinate system of Hamiltonian vector fields is $(x_1, x_2, \ldots, x_n, \lambda_1 = \frac{\partial V}{\partial x_1}(\boldsymbol{x}), \lambda_2 = \frac{\partial V}{\partial x_2}(\boldsymbol{x}), \ldots, \lambda_n = \frac{\partial V}{\partial x_n}(\boldsymbol{x}))$ and the vector fields take the well known local form as

$$\begin{aligned} \dot{x}_i &= \frac{\partial \mathcal{H}}{\partial \lambda_i}(\boldsymbol{x}, \boldsymbol{\lambda}) \\ \dot{\lambda}_i &= -\frac{\partial \mathcal{H}}{\partial x_i}(\boldsymbol{x}, \boldsymbol{\lambda}) \quad i = 1, 2, \ldots, n. \end{aligned}$$

Now, suppose that $\boldsymbol{z}_0$ is a hyperbolic equilibrium for $\boldsymbol{X}_{\mathcal{H}}$, *i.e.*, the Jacobian matrix $D\boldsymbol{X}_{\mathcal{H}}(\boldsymbol{z}_0)$ given as

$$\begin{bmatrix} \ddot{\boldsymbol{x}} \\ \ddot{\boldsymbol{\lambda}} \end{bmatrix} = \begin{bmatrix} \frac{\partial}{\partial \boldsymbol{x}^T}\left(\frac{\partial \mathcal{H}}{\partial \boldsymbol{\lambda}}\right) & \frac{\partial}{\partial \boldsymbol{\lambda}^T}\left(\frac{\partial \mathcal{H}}{\partial \boldsymbol{\lambda}}\right) \\ -\frac{\partial}{\partial \boldsymbol{x}^T}\left(\frac{\partial \mathcal{H}}{\partial \boldsymbol{x}}\right) & -\frac{\partial}{\partial \boldsymbol{\lambda}^T}\left(\frac{\partial \mathcal{H}}{\partial \boldsymbol{x}}\right) \end{bmatrix} \begin{bmatrix} \dot{\boldsymbol{x}} \\ \dot{\boldsymbol{\lambda}} \end{bmatrix}, \tag{2.22}$$

has no imaginary eigenvalues. As a matter of fact, the matrix of (2.22) is called as the *Hamiltonian matrix*. Also, using the definition of local coordinate $\lambda_i = \frac{\partial V}{\partial x_i}$, the $\boldsymbol{V}_x^T$ can be represented by the series expansion at an equilibrium point $\boldsymbol{z}_0$ as follow:

$$\dot{\boldsymbol{\lambda}} = \frac{d}{dt}\boldsymbol{V}_x^T = \frac{d}{dt}\left[\boldsymbol{V}_x^T(\boldsymbol{z}_0) + \frac{\partial \boldsymbol{V}_x}{\partial \boldsymbol{x}}(\boldsymbol{z}_0)\boldsymbol{x} + \frac{1}{2!}\frac{\partial^2 \boldsymbol{V}_x}{\partial \boldsymbol{x}^2}(\boldsymbol{z}_0)\boldsymbol{x}^2 + \frac{1}{3!}\frac{\partial^3 \boldsymbol{V}_x}{\partial \boldsymbol{x}^3}(\boldsymbol{z}_0)\boldsymbol{x}^3 \ldots\right].$$

If the higher order terms are neglected, then the approximated relation is obtained as follow:

$$\dot{\boldsymbol{\lambda}} \approx \frac{d}{dt}\left[\boldsymbol{V}_x^T(\boldsymbol{z}_0) + \frac{\partial \boldsymbol{V}_x}{\partial \boldsymbol{x}}(\boldsymbol{z}_0)\boldsymbol{x}\right].$$

Here, without loss of generality, we can let the equilibrium as $\boldsymbol{z}_0 = \boldsymbol{0}$, *i.e.*, $\boldsymbol{x} = \boldsymbol{0}$ and $\boldsymbol{\lambda} = \boldsymbol{V}_x^T(\boldsymbol{0}) = \boldsymbol{0}$. Therefore, we can get the following:

$$\begin{aligned} \dot{\boldsymbol{\lambda}} &\approx \frac{d}{dt}\left(\frac{\partial \boldsymbol{V}_x}{\partial \boldsymbol{x}}(\boldsymbol{0})\boldsymbol{x}\right), \\ &= \frac{\partial \boldsymbol{V}_x}{\partial \boldsymbol{x}}(\boldsymbol{0})\dot{\boldsymbol{x}}, \\ &= \left[\frac{\partial}{\partial \boldsymbol{x}}\left(\frac{\partial V}{\partial \boldsymbol{x}^T}\right)\right](\boldsymbol{0})\dot{\boldsymbol{x}}, \\ &\triangleq \boldsymbol{P}\dot{\boldsymbol{x}} \end{aligned}$$

where $\boldsymbol{P}$ is a solution of Riccati operator[2] for Hamiltonian matrix (2.22). Actually, this method to solve HJ equation is similar to well-known *sweep method* in solving a Riccati equation for time-invariant linear system.

Hamiltonian Matrix for Set-Point Regulation Control

For Hamilton-Jacobi equation of (2.20), by letting $\boldsymbol{\lambda}^T = \boldsymbol{V}_x$, we can rewrite the Hamilton-Jacobi (HJ) equation as follows

$$\mathcal{H}(\boldsymbol{x}, \boldsymbol{\lambda}) = \boldsymbol{\lambda}^T \boldsymbol{A}(\boldsymbol{q}, \dot{\boldsymbol{q}})\boldsymbol{x} + \frac{1}{2\gamma^2}\boldsymbol{\lambda}^T \boldsymbol{B}\boldsymbol{B}^T\boldsymbol{\lambda} - \frac{1}{2}\boldsymbol{\lambda}^T \boldsymbol{B}\boldsymbol{R}^{-1}\boldsymbol{B}^T\boldsymbol{\lambda} + \frac{1}{2}\boldsymbol{x}^T\boldsymbol{Q}\boldsymbol{x} = \boldsymbol{0}.$$

First, we get the following by a differentiation:

$$\frac{\partial \mathcal{H}}{\partial \boldsymbol{\lambda}^T} = \boldsymbol{x}^T \boldsymbol{A}^T(\boldsymbol{q}, \dot{\boldsymbol{q}}) + \frac{1}{\gamma^2}\boldsymbol{\lambda}^T \boldsymbol{B}\boldsymbol{B}^T - \boldsymbol{\lambda}^T \boldsymbol{B}\boldsymbol{R}^{-1}\boldsymbol{B}^T,$$

also, we can calculate the followings:

$$\begin{aligned} \frac{\partial}{\partial \boldsymbol{x}^T}\left(\frac{\partial \mathcal{H}}{\partial \boldsymbol{\lambda}}\right) &= \frac{\partial}{\partial \boldsymbol{x}^T}\left[\left(\frac{\partial \mathcal{H}}{\partial \boldsymbol{\lambda}^T}\right)^T\right] \\ &= \frac{\partial}{\partial \boldsymbol{x}^T}\left[\boldsymbol{A}(\boldsymbol{q}, \dot{\boldsymbol{q}})\boldsymbol{x}\right] \qquad (2.23) \\ \frac{\partial}{\partial \boldsymbol{\lambda}^T}\left(\frac{\partial \mathcal{H}}{\partial \boldsymbol{\lambda}}\right) &= \frac{\partial}{\partial \boldsymbol{\lambda}^T}\left[\left(\frac{\partial \mathcal{H}}{\partial \boldsymbol{\lambda}^T}\right)^T\right] \\ &= \frac{1}{\gamma^2}\boldsymbol{B}\boldsymbol{B}^T - \boldsymbol{B}\boldsymbol{R}^{-1}\boldsymbol{B}^T. \qquad (2.24) \end{aligned}$$

Second,

$$\frac{\partial \mathcal{H}}{\partial \boldsymbol{x}^T} = \boldsymbol{\lambda}^T \boldsymbol{A}(\boldsymbol{q}, \dot{\boldsymbol{q}}) + \boldsymbol{x}^T\boldsymbol{Q}$$

also,

$$\begin{aligned} \frac{\partial}{\partial \boldsymbol{\lambda}^T}\left(\frac{\partial \mathcal{H}}{\partial \boldsymbol{x}}\right) &= \frac{\partial}{\partial \boldsymbol{\lambda}^T}\left[\left(\frac{\partial \mathcal{H}}{\partial \boldsymbol{x}^T}\right)^T\right] \\ &= \frac{\partial}{\partial \boldsymbol{\lambda}^T}\left[\boldsymbol{A}^T(\boldsymbol{q}, \dot{\boldsymbol{q}})\boldsymbol{\lambda}\right] \qquad (2.25) \\ \frac{\partial}{\partial \boldsymbol{x}^T}\left(\frac{\partial \mathcal{H}}{\partial \boldsymbol{x}}\right) &= \frac{\partial}{\partial \boldsymbol{x}^T}\left[\left(\frac{\partial}{\partial \boldsymbol{x}^T}\right)^T\right] \\ &= \boldsymbol{Q}. \qquad (2.26) \end{aligned}$$

[2] See chapter 13 in [67] for more detail explanation

Therefore, two components (2.23) and (2.25) of Hamiltonian matrix around an equilibrium point ($\boldsymbol{x} = \mathbf{0}, \boldsymbol{\lambda} = \mathbf{0}$) can be calculated as following set:

$$\left[\frac{\partial}{\partial \boldsymbol{x}^T}\left(\frac{\partial \mathcal{H}}{\partial \boldsymbol{\lambda}}\right)\right](\mathbf{0},\mathbf{0}) = \boldsymbol{A}(\boldsymbol{q}_s,\mathbf{0}),$$
$$\left[\frac{\partial}{\partial \boldsymbol{\lambda}^T}\left(\frac{\partial \mathcal{H}}{\partial \boldsymbol{x}}\right)\right](\mathbf{0},\mathbf{0}) = \boldsymbol{A}^T(\boldsymbol{q}_s,\mathbf{0}).$$

Therefore, the Hamiltonian matrix for set-point regulation control has the following form:

$$\boldsymbol{P} = Ric\begin{bmatrix} \boldsymbol{A}(\boldsymbol{q}_s,\mathbf{0}) & \frac{1}{\gamma^2}\boldsymbol{B}\boldsymbol{B}^T - \boldsymbol{B}\boldsymbol{R}^{-1}\boldsymbol{B}^T \\ -\boldsymbol{Q} & -\boldsymbol{A}^T(\boldsymbol{q}_s,\mathbf{0}) \end{bmatrix}. \tag{2.27}$$

where $\boldsymbol{P}$ is a solution of Riccati operator for above Hamiltonian matrix. As a matter of fact, the symmetric matrix $\boldsymbol{P} = \left[\frac{\partial}{\partial \boldsymbol{x}}\left(\frac{\partial V}{\partial \boldsymbol{x}^T}\right)\right](\mathbf{0})$ is the stabilizing solution of an algebraic Riccati equation, *i.e.*, the Hessian matrix of Lyapunov function $V(\boldsymbol{x})$ at $\boldsymbol{x} = 0$.

The solution $\boldsymbol{P}$ of Riccati equation depends only on the set-point ($\boldsymbol{q}_s$) as shown in (2.27). Since $\boldsymbol{V}_x^T \approx \left[\frac{\partial}{\partial \boldsymbol{x}}\left(\frac{\partial V}{\partial \boldsymbol{x}^T}\right)\right](\mathbf{0})\boldsymbol{x} = \boldsymbol{P}\boldsymbol{x}$, therefore, the control input (2.21) has the following form:

$$\boldsymbol{\tau} = -\boldsymbol{R}^{-1}\boldsymbol{B}^T\boldsymbol{P}\boldsymbol{x}. \tag{2.28}$$

Here, we only need to solve Riccati equation (2.27) once for the set-point. Also, the Lyapunov function can be estimated as $V(\boldsymbol{x}) \approx \frac{1}{2}\boldsymbol{x}^T\boldsymbol{P}\boldsymbol{x}$. Till now, we showed that an approximate solution of HJ equation (2.20) is equal to a solution of Riccati operator for Hamiltonian matrix. In other words, this section suggests an optimal control method for the set-point regulation control system.

2.4 Trajectory Tracking Control

Trajectory tracking control is basically different from the set-point regulation control in that the desired configuration, velocity and its acceleration profiles are added to typical Lagrangian systems. As a matter of fact, putting the desired configuration, velocity and acceleration into Lagrangian system makes it difficult to prove the stability or optimality of the controller. Following sections explain briefly the optimal control and $\mathcal{H}_\infty$ control as a part of a modified computed torque controller (Modified-CTC), respectively.

2.4.1 Optimal Control of a Modified-CTC [Dawson *et al.*]

There has been much discussion related to the computed-torque control technique. Also, there has been some works related with applying optimal control

technique to Lagrangian systems, especially robotic manipulators, after it has been feedback linearized. The optimal control using a modified computed-torque controller (Modified-CTC) was proposed in [18]. To be an optimal control for a given performance index, the Hamilton-Jacobi-Bellman (HJB) equation should be solved to achieve the optimality. However, it is difficult to solve HJB equation analytically, because HJB equation is the form of nonlinear partial differential equation (NPDE).

For Lagrangian systems (2.11), let us assume that there exist no external disturbances, *i.e.*, $\boldsymbol{d}(t) = \boldsymbol{0}$. Also, the errors should be defined to deal with trajectory tracking control system, *i.e.*, $\boldsymbol{e} \triangleq \boldsymbol{q}_d - \boldsymbol{q}$ and $\dot{\boldsymbol{e}} \triangleq \dot{\boldsymbol{q}}_d - \dot{\boldsymbol{q}}$. If we adopt the modified computed-torque control input as following form:

$$\boldsymbol{\tau} = \boldsymbol{M}(\boldsymbol{q})(\ddot{\boldsymbol{q}}_d + \boldsymbol{K}_P\dot{\boldsymbol{e}}) + \boldsymbol{C}(\boldsymbol{q},\dot{\boldsymbol{q}})(\dot{\boldsymbol{q}}_d + \boldsymbol{K}_P\boldsymbol{e}) + \boldsymbol{g}(\boldsymbol{q}) - \boldsymbol{u}, \tag{2.29}$$

where $\boldsymbol{u}$ is an auxiliary control input vector, then the resultant system dynamics is given by

$$\boldsymbol{M}(\boldsymbol{q})(\ddot{\boldsymbol{e}} + \boldsymbol{K}_P\dot{\boldsymbol{e}}) + \boldsymbol{C}(\boldsymbol{q},\dot{\boldsymbol{q}})(\dot{\boldsymbol{e}} + \boldsymbol{K}_P\boldsymbol{e}) = \boldsymbol{u}. \tag{2.30}$$

Here, if we define the state vector as

$$\boldsymbol{x} \triangleq \begin{bmatrix} \boldsymbol{x}_1 \\ \boldsymbol{x}_2 \end{bmatrix} = \begin{bmatrix} \boldsymbol{e} \\ \dot{\boldsymbol{e}} \end{bmatrix} \in \Re^{2n},$$

then the state space representation of the system (2.30) can be simply written by

$$\dot{\boldsymbol{x}} = \boldsymbol{A}(\boldsymbol{x},t)\boldsymbol{x} + \boldsymbol{B}(\boldsymbol{x},t)\boldsymbol{u} \tag{2.31}$$

where

$$\boldsymbol{A}(\boldsymbol{x},t) = \begin{bmatrix} \boldsymbol{0} & \boldsymbol{I} \\ -\boldsymbol{M}^{-1}\boldsymbol{C}\boldsymbol{K}_P & -\boldsymbol{M}^{-1}\boldsymbol{C} - \boldsymbol{K}_P \end{bmatrix}$$
$$\boldsymbol{B}(\boldsymbol{x},t) = \begin{bmatrix} \boldsymbol{0} \\ \boldsymbol{M}^{-1} \end{bmatrix}.$$

Also, we should notice that $\boldsymbol{A}(\boldsymbol{x},t)$ and $\boldsymbol{B}(\boldsymbol{x},t)$ are functions of time and state vector, because $\boldsymbol{q}(= \boldsymbol{q}_d - \boldsymbol{x}_1)$ and $\dot{\boldsymbol{q}}(= \dot{\boldsymbol{q}}_d - \boldsymbol{x}_2)$ are the function of state vector and time[3]. Let us consider the quadratic performance index (PI) as following form:

$$\int_0^\infty \left[\boldsymbol{x}^T\boldsymbol{Q}(\boldsymbol{x},t)\boldsymbol{x} + \boldsymbol{u}^T\boldsymbol{R}(\boldsymbol{x},t)\boldsymbol{u}\right] dt \tag{2.32}$$

where $\boldsymbol{Q}(\boldsymbol{x},t)$ is the state weighting matrix and $\boldsymbol{R}(\boldsymbol{x},t)$ the auxiliary control input weighting. The HJB equation for the above PI (2.32) can be found in the following Lemma, also in [18].

[3] The desired configuration and velocity $(\boldsymbol{q}_d, \dot{\boldsymbol{q}}_d)$ are function of time.

Lemma 3. *Suppose there exists a smooth function* $V(\boldsymbol{x},t) > 0$ *with* $V(\boldsymbol{0},t) = 0$ *that satisfies*

$$HJB = V_t + \boldsymbol{V}_x\boldsymbol{A}\boldsymbol{x} - \frac{1}{2}\boldsymbol{V}_x\boldsymbol{B}\boldsymbol{R}^{-1}\boldsymbol{B}^T\boldsymbol{V}_x^T + \frac{1}{2}\boldsymbol{x}^T\boldsymbol{Q}\boldsymbol{x} = 0, \tag{2.33}$$

where $V_t = \frac{\partial V}{\partial t}$ *and* $\boldsymbol{V}_x = \frac{\partial V}{\partial \boldsymbol{x}^T}$, *then the auxiliary control*

$$\boldsymbol{u} = -\boldsymbol{R}^{-1}\boldsymbol{B}^T\boldsymbol{V}_x^T \tag{2.34}$$

minimizes the PI (2.32).

To make active use of above Lemma, Dawson *et al.* suggested the Lyapunov function $V(\boldsymbol{x},t) = \frac{1}{2}\boldsymbol{x}^T\boldsymbol{P}(\boldsymbol{x},t)\boldsymbol{x}$ for tracking system model (2.31) as following form:

$$\boldsymbol{P}(\boldsymbol{x},t) = \begin{bmatrix} \boldsymbol{K}_P\boldsymbol{M}\boldsymbol{K}_P + \boldsymbol{K}_P\boldsymbol{K} & \boldsymbol{K}_P\boldsymbol{M} \\ \boldsymbol{M}\boldsymbol{K}_P & \boldsymbol{M} \end{bmatrix}, \tag{2.35}$$

where the positive definiteness of $\boldsymbol{P}(\boldsymbol{x},t)$ requires the condition of $\boldsymbol{K} > \boldsymbol{0}$. Here, the tracking system model (2.31) and the Lyapunov matrix (2.35) were slightly changed in that $\boldsymbol{K}_P > \boldsymbol{0}$ is a diagonal matrix, not a scalar $\alpha > 0$ in [18, 50]. From now on, we obtain the differential Riccati equation from HJB (2.33). First, we simplify the HJB equation, which is indeed a nonlinear partial differential equation, to an ordinary matrix differential equation, *i.e.*, the differential Riccati equation. Note that

$$V_t = \frac{1}{2}\boldsymbol{x}^T\frac{\partial \boldsymbol{P}}{\partial t}\boldsymbol{x}, \quad \boldsymbol{V}_x = \frac{1}{2}\boldsymbol{x}^T\frac{\partial \boldsymbol{P}}{\partial \boldsymbol{x}^T}\boldsymbol{x} + \boldsymbol{x}^T\boldsymbol{P}$$

and $\boldsymbol{P}(\boldsymbol{x},t)$ is not a function of $\boldsymbol{x}_2 = \dot{\boldsymbol{e}}$, then we have the following:

$$\boldsymbol{V}_x = \frac{1}{2}\boldsymbol{x}^T\left[\frac{\partial \boldsymbol{P}}{\partial \boldsymbol{x}_1^T}\boldsymbol{x} \quad \boldsymbol{0}\right] + \boldsymbol{x}^T\boldsymbol{P}.$$

Hence,

$$\begin{aligned}\boldsymbol{V}_x\boldsymbol{A}\boldsymbol{x} &= \frac{1}{2}\boldsymbol{x}^T\boldsymbol{P}\boldsymbol{A}\boldsymbol{x} + \frac{1}{2}\boldsymbol{x}^T\boldsymbol{A}^T\boldsymbol{P}\boldsymbol{x} + \frac{1}{2}\boldsymbol{x}^T\left[\frac{\partial \boldsymbol{P}}{\partial \boldsymbol{x}_1^T}\boldsymbol{x} \quad \boldsymbol{0}\right]\begin{pmatrix}\boldsymbol{x}_2 \\ *\end{pmatrix} \\ &= \frac{1}{2}\boldsymbol{x}^T\left\{\boldsymbol{P}\boldsymbol{A} + \boldsymbol{A}^T\boldsymbol{P} + \frac{\partial \boldsymbol{P}}{\partial \boldsymbol{x}_1^T}\dot{\boldsymbol{x}}_1\right\}\boldsymbol{x}\end{aligned}$$

and

$$\begin{aligned}V_t + \boldsymbol{V}_x\boldsymbol{A}\boldsymbol{x} &= \frac{1}{2}\boldsymbol{x}^T\left\{\frac{\partial \boldsymbol{P}}{\partial t} + \frac{\partial \boldsymbol{P}}{\partial \boldsymbol{x}_1^T}\dot{\boldsymbol{x}}_1 + \boldsymbol{P}\boldsymbol{A} + \boldsymbol{A}^T\boldsymbol{P}\right\}\boldsymbol{x} \\ &= \frac{1}{2}\boldsymbol{x}^T\left\{\dot{\boldsymbol{P}} + \boldsymbol{P}\boldsymbol{A} + \boldsymbol{A}^T\boldsymbol{P}\right\}\boldsymbol{x}.\end{aligned}$$

Also, $\boldsymbol{V}_x\boldsymbol{B}$ is simplified to

$$\boldsymbol{V}_x\boldsymbol{B} = \boldsymbol{x}^T\boldsymbol{P}\boldsymbol{B} + \frac{1}{2}\boldsymbol{x}^T\left[\frac{\partial \boldsymbol{P}}{\partial \boldsymbol{x}^T}\boldsymbol{x}\right]\boldsymbol{B} = \boldsymbol{x}^T\boldsymbol{P}\boldsymbol{B}$$

since

$$\left[\frac{\partial \boldsymbol{P}}{\partial \boldsymbol{x}^T}\boldsymbol{x}\right]\boldsymbol{B} = \left[\frac{\partial \boldsymbol{P}}{\partial \boldsymbol{x}_1^T}\boldsymbol{x} \;\; \boldsymbol{0}\right]\begin{bmatrix}\boldsymbol{0}\\ \boldsymbol{M}^{-1}\end{bmatrix} = \boldsymbol{0}.$$

Hence, the HJB (2.33) is arranged to:

$$\frac{1}{2}\boldsymbol{x}^T\left\{\dot{\boldsymbol{P}} + \boldsymbol{P}\boldsymbol{A} + \boldsymbol{A}^T\boldsymbol{P} - \boldsymbol{P}\boldsymbol{B}\boldsymbol{R}^{-1}\boldsymbol{B}^T\boldsymbol{P} + \boldsymbol{Q}\right\}\boldsymbol{x} = \boldsymbol{0},$$

also, it brings the following differential Riccati equation

$$\dot{\boldsymbol{P}} + \boldsymbol{A}^T\boldsymbol{P} + \boldsymbol{P}\boldsymbol{A} - \boldsymbol{P}\boldsymbol{B}\boldsymbol{R}^{-1}\boldsymbol{B}^T\boldsymbol{P} + \boldsymbol{Q} = \boldsymbol{0} \tag{2.36}$$

because the HJB equation should hold for all $\boldsymbol{x}$.

As a matter of fact, for arbitrarily given weighting matrices $\boldsymbol{Q}(\boldsymbol{x}, t), \boldsymbol{R}(\boldsymbol{x}, t)$ in a quadratic PI (2.32), it is impossible for the Lyapunov matrix (2.35) to be a solution of the differential Riccati equation (2.36). However, the weighting matrices $\boldsymbol{Q}$ and $\boldsymbol{R}$ can be inversely found from the differential Riccati equation and Lyapunov function as suggested in following Theorem.

Theorem 1. *Assume that there exists a Lyapunov matrix $\boldsymbol{P}(\boldsymbol{x}, t)$ (2.35) for Lagrangian systems (2.31). If the control input weighting is defined as following diagonal constant matrix:*

$$\boldsymbol{R} = \boldsymbol{K}^{-1} > \boldsymbol{0}, \tag{2.37}$$

then the state weighting matrix can be inversely obtained from the differential Riccati equation (2.36) as follows:

$$\boldsymbol{Q} = \begin{bmatrix}\boldsymbol{K}_P^2\boldsymbol{K} & \boldsymbol{0}\\ \boldsymbol{0} & \boldsymbol{K}\end{bmatrix} > \boldsymbol{0}, \tag{2.38}$$

where $\boldsymbol{Q}$ is a positive definite and diagonal constant matrix.

Proof. Since the differential Riccati equation (2.36) can be rewritten as following form:

$$\dot{\boldsymbol{P}} + \boldsymbol{A}^T\boldsymbol{P} + \boldsymbol{P}\boldsymbol{A} - \boldsymbol{P}\boldsymbol{B}\boldsymbol{K}\boldsymbol{B}^T\boldsymbol{P} + \boldsymbol{Q} = \boldsymbol{0} \tag{2.39}$$

by definition of $\boldsymbol{R}$, we have only to obtain the matrix $\boldsymbol{Q}$ from above matrix equation. By using the characteristics $\dot{\boldsymbol{M}} - \boldsymbol{C}^T - \boldsymbol{C} = \boldsymbol{0}$ of Lagrangian system, the following can be firstly computed

$$\dot{\boldsymbol{P}} + \boldsymbol{A}^T\boldsymbol{P} + \boldsymbol{P}\boldsymbol{A} = \begin{bmatrix}\boldsymbol{0} & \boldsymbol{K}_P\boldsymbol{K}\\ \boldsymbol{K}_P\boldsymbol{K} & \boldsymbol{0}\end{bmatrix}.$$

Also, the remaining term is

$$\boldsymbol{PBKB}^T\boldsymbol{P} = \begin{bmatrix} \boldsymbol{K}_P^2\boldsymbol{K} & \boldsymbol{K}_P\boldsymbol{K} \\ \boldsymbol{K}_P\boldsymbol{K} & \boldsymbol{K} \end{bmatrix}.$$

Hence, the matrix $\boldsymbol{Q}$ (2.38) is derived from (2.39) and it is a positive definite and diagonal constant matrix. □

For constant and diagonal weighting matrices $\boldsymbol{Q}$ and $\boldsymbol{R}$ in above Theorem, the Lyapunov matrix satisfies the differential Riccati equation, hence, the auxiliary control (2.34) must be an optimal one for a PI (2.32). Also, we should notice that the auxiliary controller is the PD one. Finally, the modified computed-torque controller (2.29) has the following form:

$$\begin{aligned} \boldsymbol{\tau} = \boldsymbol{M}(\boldsymbol{q})(\ddot{\boldsymbol{q}}_d + \boldsymbol{K}_P\dot{\boldsymbol{e}}) + \boldsymbol{C}(\boldsymbol{q},\dot{\boldsymbol{q}})(\dot{\boldsymbol{q}}_d + \boldsymbol{K}_P\boldsymbol{e}) + \boldsymbol{g}(\boldsymbol{q}) \\ + \boldsymbol{K}\left(\dot{\boldsymbol{e}} + \boldsymbol{K}_P\boldsymbol{e}\right). \end{aligned} \tag{2.40}$$

To implement the optimal control of a modified-CTC, the dynamic parameters such as $\boldsymbol{M}(\boldsymbol{q}), \boldsymbol{C}(\boldsymbol{q},\dot{\boldsymbol{q}})$ and $\boldsymbol{g}(\boldsymbol{q})$ should be exactly identified in advance. If not, the optimality of controller can not be achieved for a given PI (2.32). Basically, the robust control such as $\mathcal{H}_\infty$ should be utilized to cope with these parameter uncertainties because the controller (2.40) does not assure the robustness for uncertain parameters. In [48, 49], Park and Chung suggested the $\mathcal{H}_\infty$ control of a modified-CTC against external disturbances and parameter uncertainties.

2.4.2 $\mathcal{H}_\infty$ Control of a Modified-CTC [Park and Chung]

The advent of linear $\mathcal{H}_\infty$ control in [67] brought increasing attention for nonlinear $\mathcal{H}_\infty$ control problem. In the meantime, the nonlinear $\mathcal{H}_\infty$ control for full state and output feedback cases were solved by Van der Schaft[64] and Isidori[29], respectively. To achieve the nonlinear $\mathcal{H}_\infty$ controller, the Hamilton-Jacobi-Isaacs (HJI) equation should be solved to assure the $\mathcal{H}_\infty$ optimality property. However, it is also a hard problem to solve HJI equation because the HJI equation is NPDE.

Similar to an optimal control of a modified-CTC in previous section, if we adopt the modified computed-torque control (Modified-CTC) input as following form:

$$\boldsymbol{\tau} = \widehat{\boldsymbol{M}}(\boldsymbol{q})(\ddot{\boldsymbol{q}}_d + \boldsymbol{K}_P\dot{\boldsymbol{e}} + \boldsymbol{K}_I\boldsymbol{e}) + \widehat{\boldsymbol{C}}(\boldsymbol{q},\dot{\boldsymbol{q}})(\dot{\boldsymbol{q}}_d + \boldsymbol{K}_P\boldsymbol{e} + \boldsymbol{K}_I\int\boldsymbol{e}) + \widehat{\boldsymbol{g}}(\boldsymbol{q}) - \boldsymbol{u}, \tag{2.41}$$

where $\boldsymbol{u}$ is the auxiliary control input and $(\widehat{\boldsymbol{M}}, \widehat{\boldsymbol{C}}, \widehat{\boldsymbol{g}})$ are the estimations for $(\boldsymbol{M}, \boldsymbol{C}, \boldsymbol{g})$, then the resultant system dynamics is given by

$$\boldsymbol{M}(\boldsymbol{q})(\ddot{\boldsymbol{e}} + \boldsymbol{K}_P\dot{\boldsymbol{e}} + \boldsymbol{K}_I\boldsymbol{e}) + \boldsymbol{C}(\boldsymbol{q},\dot{\boldsymbol{q}})(\dot{\boldsymbol{e}} + \boldsymbol{K}_P\boldsymbol{e} + \boldsymbol{K}_I\int\boldsymbol{e}) = \boldsymbol{u} + \boldsymbol{w}, \tag{2.42}$$

with

$$\boldsymbol{w} = \widetilde{\boldsymbol{M}}(\boldsymbol{q})(\ddot{\boldsymbol{q}}_d + \boldsymbol{K}_P\dot{\boldsymbol{e}} + \boldsymbol{K}_I\boldsymbol{e}) + \widetilde{\boldsymbol{C}}(\boldsymbol{q},\dot{\boldsymbol{q}})(\dot{\boldsymbol{q}}_d + \boldsymbol{K}_P\boldsymbol{e} + \boldsymbol{K}_I\int \boldsymbol{e}) + \widetilde{\boldsymbol{g}}(\boldsymbol{q}) + \boldsymbol{d}(t). \tag{2.43}$$

where $\widetilde{\boldsymbol{M}}(\boldsymbol{q}) = \boldsymbol{M}(\boldsymbol{q}) - \widehat{\boldsymbol{M}}(\boldsymbol{q})$, $\widetilde{\boldsymbol{C}}(\boldsymbol{q},\dot{\boldsymbol{q}}) = \boldsymbol{C}(\boldsymbol{q},\dot{\boldsymbol{q}}) - \widehat{\boldsymbol{C}}(\boldsymbol{q},\dot{\boldsymbol{q}})$ and $\widetilde{\boldsymbol{g}}(\boldsymbol{q}) = \boldsymbol{g}(\boldsymbol{q}) - \widehat{\boldsymbol{g}}(\boldsymbol{q})$. As a matter of fact, $\boldsymbol{w}$ of (2.43) is defined as a new disturbance including the model uncertainties and external disturbances. Here, if we define the state vector like this

$$\boldsymbol{x} \triangleq \begin{bmatrix} \boldsymbol{x}_1 \\ \boldsymbol{x}_2 \\ \boldsymbol{x}_3 \end{bmatrix} = \begin{bmatrix} \int \boldsymbol{e}dt \\ \boldsymbol{e} \\ \dot{\boldsymbol{e}} \end{bmatrix} \in \Re^{3n},$$

then the state space representation of the system (2.42) can be simply written by

$$\dot{\boldsymbol{x}} = \boldsymbol{A}(\boldsymbol{x},t)\boldsymbol{x} + \boldsymbol{B}(\boldsymbol{x},t)\boldsymbol{w} + \boldsymbol{B}(\boldsymbol{x},t)\boldsymbol{u} \tag{2.44}$$

where

$$\boldsymbol{A}(\boldsymbol{x},t) = \begin{bmatrix} \boldsymbol{0} & \boldsymbol{I} & \boldsymbol{0} \\ \boldsymbol{0} & \boldsymbol{0} & \boldsymbol{I} \\ -\boldsymbol{M}^{-1}\boldsymbol{C}\boldsymbol{K}_I & -\boldsymbol{M}^{-1}\boldsymbol{C}\boldsymbol{K}_P - \boldsymbol{K}_I & -\boldsymbol{M}^{-1}\boldsymbol{C} - \boldsymbol{K}_P \end{bmatrix}$$

$$\boldsymbol{B}(\boldsymbol{x},t) = \begin{bmatrix} \boldsymbol{0} \\ \boldsymbol{0} \\ \boldsymbol{M}^{-1} \end{bmatrix}.$$

Let us consider the typical $\mathcal{H}_\infty$ performance index (PI) as following form:

$$\int_0^\infty \left[\boldsymbol{x}^T\boldsymbol{Q}(\boldsymbol{x},t)\boldsymbol{x} + \boldsymbol{u}^T\boldsymbol{R}(\boldsymbol{x},t)\boldsymbol{u}\right] dt \le \gamma^2 \int_0^\infty \boldsymbol{w}^T\boldsymbol{w}dt. \tag{2.45}$$

The HJI equation for above PI can be found in the following Lemma, also in [47].

Lemma 4. *Let $\gamma > 0$, Suppose there exists a smooth function $V(\boldsymbol{x},t) > 0$ with $V(\boldsymbol{0},t) = 0$ that satisfies*

$$HJI = V_t + \boldsymbol{V}_x\boldsymbol{A}\boldsymbol{x} + \frac{1}{2\gamma^2}\boldsymbol{V}_x\boldsymbol{B}\boldsymbol{B}^T\boldsymbol{V}_x^T - \frac{1}{2}\boldsymbol{V}_x\boldsymbol{B}\boldsymbol{R}^{-1}\boldsymbol{B}^T\boldsymbol{V}_x^T + \frac{1}{2}\boldsymbol{x}^T\boldsymbol{Q}\boldsymbol{x} = 0, \tag{2.46}$$

where $V_t = \frac{\partial V}{\partial t}$ and $\boldsymbol{V}_x = \frac{\partial V}{\partial \boldsymbol{x}^T}$, then the auxiliary control

$$\boldsymbol{u} = -\boldsymbol{R}^{-1}\boldsymbol{B}^T\boldsymbol{V}_x^T \tag{2.47}$$

minimizes the $\mathcal{H}_\infty$ PI (2.45) with a given $\mathcal{L}_2$-gain γ.

Park and Chung [47] suggested a Lyapunov function $V(\boldsymbol{x},t) = \frac{1}{2}\boldsymbol{x}^T\boldsymbol{P}(\boldsymbol{x},t)\boldsymbol{x}$ for Lagrangian systems (2.44) as following form:

$$\boldsymbol{P}(\boldsymbol{x},t) = \begin{bmatrix} \boldsymbol{K}_I\boldsymbol{M}\boldsymbol{K}_I + \boldsymbol{K}_I\boldsymbol{K}_P\boldsymbol{K} & \boldsymbol{K}_I\boldsymbol{M}\boldsymbol{K}_P + \boldsymbol{K}_I\boldsymbol{K} & \boldsymbol{K}_I\boldsymbol{M} \\ \boldsymbol{K}_P\boldsymbol{M}\boldsymbol{K}_I + \boldsymbol{K}_I\boldsymbol{K} & \boldsymbol{K}_P\boldsymbol{M}\boldsymbol{K}_P + \boldsymbol{K}_P\boldsymbol{K} & \boldsymbol{K}_P\boldsymbol{M} \\ \boldsymbol{M}\boldsymbol{K}_I & \boldsymbol{M}\boldsymbol{K}_P & \boldsymbol{M} \end{bmatrix}, \quad (2.48)$$

where the positive definiteness of $\boldsymbol{P}(\boldsymbol{x},t)$ requires the following conditions

1. $\boldsymbol{K}, \boldsymbol{K}_P, \boldsymbol{K}_I > \boldsymbol{0}$ are constant diagonal matrices,
2. $\boldsymbol{K}_P^2 > 2\boldsymbol{K}_I$.

As a matter of fact, the Lagrangian system (2.44) and the Lyapunov matrix (2.48) were slightly changed in that $\boldsymbol{K}_P$ and $\boldsymbol{K}_I$ are diagonal matrices, not scalars k_v and k_p in [47], respectively. From now on, we are to obtain the differential Riccati equation from HJI one (2.46). First, we simplify the HJI equation to a matrix differential Riccati one. Note that

$$V_t = \frac{1}{2}\boldsymbol{x}^T\frac{\partial \boldsymbol{P}}{\partial t}\boldsymbol{x}, \quad \boldsymbol{V}_x = \frac{1}{2}\boldsymbol{x}^T\frac{\partial \boldsymbol{P}}{\partial \boldsymbol{x}^T}\boldsymbol{x} + \boldsymbol{x}^T\boldsymbol{P},$$

here, since $\boldsymbol{P}(\boldsymbol{x},t)$ is not a function of $\boldsymbol{x}_3 = \dot{\boldsymbol{e}}$, the following can be obtained:

$$\boldsymbol{V}_x = \frac{1}{2}\boldsymbol{x}^T\left[\frac{\partial \boldsymbol{P}}{\partial \boldsymbol{x}_1^T}\boldsymbol{x} \quad \frac{\partial \boldsymbol{P}}{\partial \boldsymbol{x}_2^T}\boldsymbol{x} \quad \boldsymbol{0}\right] + \boldsymbol{x}^T\boldsymbol{P}.$$

Then

$$\begin{aligned}\boldsymbol{V}_x\boldsymbol{A}\boldsymbol{x} &= \frac{1}{2}\boldsymbol{x}^T\boldsymbol{P}\boldsymbol{A}\boldsymbol{x} + \frac{1}{2}\boldsymbol{x}^T\boldsymbol{A}^T\boldsymbol{P}\boldsymbol{x} + \frac{1}{2}\boldsymbol{x}^T\left[\frac{\partial \boldsymbol{P}}{\partial \boldsymbol{x}_1^T}\boldsymbol{x} \quad \frac{\partial \boldsymbol{P}}{\partial \boldsymbol{x}_2^T}\boldsymbol{x} \quad \boldsymbol{0}\right]\begin{pmatrix}\boldsymbol{x}_2 \\ \boldsymbol{x}_3 \\ * \end{pmatrix} \\ &= \frac{1}{2}\boldsymbol{x}^T\left\{\boldsymbol{P}\boldsymbol{A} + \boldsymbol{A}^T\boldsymbol{P} + \sum_{k=1}^{2}\frac{\partial \boldsymbol{P}}{\partial \boldsymbol{x}_k^T}\dot{\boldsymbol{x}}_k\right\}\boldsymbol{x}\end{aligned}$$

and

$$\begin{aligned}V_t + \boldsymbol{V}_x\boldsymbol{A}\boldsymbol{x} &= \frac{1}{2}\boldsymbol{x}^T\left\{\frac{\partial \boldsymbol{P}}{\partial t} + \sum_{k=1}^{2}\frac{\partial \boldsymbol{P}}{\partial \boldsymbol{x}_k^T}\dot{\boldsymbol{x}}_k + \boldsymbol{P}\boldsymbol{A} + \boldsymbol{A}^T\boldsymbol{P}\right\}\boldsymbol{x} \\ &= \frac{1}{2}\boldsymbol{x}^T\left\{\dot{\boldsymbol{P}} + \boldsymbol{P}\boldsymbol{A} + \boldsymbol{A}^T\boldsymbol{P}\right\}\boldsymbol{x}.\end{aligned}$$

Also, $\boldsymbol{V}_x\boldsymbol{B}$ is simplified to

$$\boldsymbol{V}_x\boldsymbol{B} = \boldsymbol{x}^T\boldsymbol{P}\boldsymbol{B} + \frac{1}{2}\boldsymbol{x}^T\left[\frac{\partial \boldsymbol{P}}{\partial \boldsymbol{x}^T}\boldsymbol{x}\right]\boldsymbol{B} = \boldsymbol{x}^T\boldsymbol{P}\boldsymbol{B},$$

because

$$\left[\frac{\partial \boldsymbol{P}}{\partial \boldsymbol{x}^T}\boldsymbol{x}\right]\boldsymbol{B} = \left[\frac{\partial \boldsymbol{P}}{\partial \boldsymbol{x}_1^T}\boldsymbol{x} \;\; \frac{\partial \boldsymbol{P}}{\partial \boldsymbol{x}_2^T}\boldsymbol{x} \;\; \boldsymbol{0}\right]\begin{bmatrix}\boldsymbol{0}\\ \boldsymbol{0}\\ \boldsymbol{M}^{-1}\end{bmatrix} = \boldsymbol{0}.$$

Hence, the HJI equation (2.46) is arranged to:

$$\frac{1}{2}\boldsymbol{x}^T\left\{\dot{\boldsymbol{P}} + \boldsymbol{P}\boldsymbol{A} + \boldsymbol{A}^T\boldsymbol{P} - \boldsymbol{P}\boldsymbol{B}\boldsymbol{R}^{-1}\boldsymbol{B}^T\boldsymbol{P} + \frac{1}{\gamma^2}\boldsymbol{P}\boldsymbol{B}\boldsymbol{B}^T\boldsymbol{P} + \boldsymbol{Q}\right\}\boldsymbol{x} = \boldsymbol{0},$$

also, it brings the following differential Riccati equation

$$\dot{\boldsymbol{P}} + \boldsymbol{A}^T\boldsymbol{P} + \boldsymbol{P}\boldsymbol{A} - \boldsymbol{P}\boldsymbol{B}\boldsymbol{R}^{-1}\boldsymbol{B}^T\boldsymbol{P} + \frac{1}{\gamma^2}\boldsymbol{P}\boldsymbol{B}\boldsymbol{B}^T\boldsymbol{P} + \boldsymbol{Q} = \boldsymbol{0}, \tag{2.49}$$

because the HJI equation should hold for all $\boldsymbol{x}$.

For arbitrarily given weighting matrices $\boldsymbol{Q}(\boldsymbol{x}, t)$ and $\boldsymbol{R}(\boldsymbol{x}, t)$, the Lyapunov matrix (2.48) does not always satisfy the differential Riccati equation (2.49) as well. Similarly to Theorem 1 in previous section, the weighting matrices $\boldsymbol{Q}$ and $\boldsymbol{R}$ will be inversely found from the differential Riccati equation.

Theorem 2. *Assume that there exists a Lyapunov matrix $\boldsymbol{P}(\boldsymbol{x}, t)$ (2.48) for Lagrangian systems (2.44). If the control input weighting is defined as following matrix:*

$$\boldsymbol{R} = \left(\boldsymbol{K} + \frac{1}{\gamma^2}\boldsymbol{I}\right)^{-1}, \tag{2.50}$$

then the state weighting matrix can be inversely obtained from the differential Riccati equation (2.49) as follows:

$$\boldsymbol{Q} = \begin{bmatrix}\boldsymbol{K}_I^2\boldsymbol{K} & \boldsymbol{0} & \boldsymbol{0}\\ \boldsymbol{0} & (\boldsymbol{K}_P^2 - 2\boldsymbol{K}_I)\boldsymbol{K} & \boldsymbol{0}\\ \boldsymbol{0} & \boldsymbol{0} & \boldsymbol{K}\end{bmatrix} > \boldsymbol{0}, \tag{2.51}$$

where $\boldsymbol{Q}$ is a positive definite, diagonal and constant matrix.

Proof. Since the differential Riccati equation (2.49) can be simplified to

$$\dot{\boldsymbol{P}} + \boldsymbol{A}^T\boldsymbol{P} + \boldsymbol{P}\boldsymbol{A} - \boldsymbol{P}\boldsymbol{B}\boldsymbol{K}\boldsymbol{B}^T\boldsymbol{P} + \boldsymbol{Q} = \boldsymbol{0} \tag{2.52}$$

by definition of $\boldsymbol{R}$, we have only to obtain the matrix $\boldsymbol{Q}$ from above matrix equation. By using the characteristics $\dot{\boldsymbol{M}} - \boldsymbol{C}^T - \boldsymbol{C} = \boldsymbol{0}$ of Lagrangian system, the following can be firstly computed

$$\dot{\boldsymbol{P}} + \boldsymbol{A}^T\boldsymbol{P} + \boldsymbol{P}\boldsymbol{A} = \begin{bmatrix}\boldsymbol{0} & \boldsymbol{K}_I\boldsymbol{K}_P\boldsymbol{K} & \boldsymbol{K}_I\boldsymbol{K}\\ \boldsymbol{K}_I\boldsymbol{K}_P\boldsymbol{K} & 2\boldsymbol{K}_I\boldsymbol{K} & \boldsymbol{K}_P\boldsymbol{K}\\ \boldsymbol{K}_I\boldsymbol{K} & \boldsymbol{K}_P\boldsymbol{K} & \boldsymbol{0}\end{bmatrix}.$$

Also, the remaining term is

$$\boldsymbol{PBKB}^T\boldsymbol{P} = \begin{bmatrix} \boldsymbol{K}_I^2\boldsymbol{K} & \boldsymbol{K}_I\boldsymbol{K}_P\boldsymbol{K} & \boldsymbol{K}_I\boldsymbol{K} \\ \boldsymbol{K}_I\boldsymbol{K}_P\boldsymbol{K} & \boldsymbol{K}_P^2\boldsymbol{K} & \boldsymbol{K}_P\boldsymbol{K} \\ \boldsymbol{K}_I\boldsymbol{K} & \boldsymbol{K}_P\boldsymbol{K} & \boldsymbol{K} \end{bmatrix}.$$

Hence, the matrix $\boldsymbol{Q}$ found from (2.52) has the form of (2.51). Since $\boldsymbol{K}_P^2 > 2\boldsymbol{K}_I$, it is a positive definite, diagonal and constant matrix. □

For the constant weighting matrices $\boldsymbol{Q}$ and $\boldsymbol{R}$ given in above Theorem, since the Lyapunov matrix (2.48) satisfies the differential Riccati equation (2.49), hence, the auxiliary control input (2.47) is a $\mathcal{H}_\infty$ controller for a PI (2.45), also, the modified computed-torque controller of (2.41) has the following form:

$$\begin{aligned} \boldsymbol{\tau} = {} & \widehat{\boldsymbol{M}}(\boldsymbol{q})(\ddot{\boldsymbol{q}}_d + \boldsymbol{K}_P\dot{\boldsymbol{e}} + \boldsymbol{K}_I\boldsymbol{e}) + \widehat{\boldsymbol{C}}(\boldsymbol{q},\dot{\boldsymbol{q}})(\dot{\boldsymbol{q}}_d + \boldsymbol{K}_P\boldsymbol{e} + \boldsymbol{K}_I\int \boldsymbol{e}) + \widehat{\boldsymbol{g}}(\boldsymbol{q}) \\ & + \left(\boldsymbol{K} + \frac{1}{\gamma^2}\boldsymbol{I}\right)\left(\dot{\boldsymbol{e}} + \boldsymbol{K}_P\boldsymbol{e} + \boldsymbol{K}_I\int \boldsymbol{e}\right), \end{aligned} \tag{2.53}$$

where we should notice that the auxiliary controller (2.47) has the form of PID one.

2.5 Notes

One aspect of the classical Hamilton-Jacobi theory is concerned with finding the partial differential equation (HJ equation) satisfied by an optimal return function (a unique optimal value of the performance index: see chapter 4 in [8]). There is also a vector partial differential equation satisfied by an optimal return function. Bellman[1967] has generalized the Hamilton-Jacobi theory to include multi-variable systems and combinatorial problems and he calls this overall theory dynamic programming. Also, Bellman theory is associated with finding the first-order nonlinear partial differential equation (HJB equation).

In certain areas of game theory, one can find problems similar to our general control problem, but with the important exception that the behavior of the target as a function of time is not known to us in advance - there is an opponent capable of influencing the target, who is trying to keep us away from hitting the target. In other game theory problems, the opponent might be able to directly affect our state and control input (also, see [41]). Isaacs[1975] showed how differential game theory can be applied to control theory. Isaacs theory is also associated with finding the first-order nonlinear partial differential equation (HJI equation : for more detail, see [29, 65]) derived from the two player (one player corresponds to the control input, the other player to the exogenous disturbance input) differential game theory.

3

$\mathcal{H}_\infty$ Optimality of PID Control

3.1 Introduction

The conventional PID controller for automated machines is widely accepted by industry. According to a survey reported in [3, 66], more than 90% of control loops used in industry use PID. There are many types of PID controllers, *e.g.*, PID plus gravity compensator, PID plus friction compensator, PID plus disturbance observer, *etc.* The wide acceptance of the PID controller in industry is based on the following advantages: it is easy to use, each term in the PID controller has clear physical meanings (present, past and predictive), and it can be used irrespective of the system dynamics. A $\mathcal{H}_\infty$ optimal controller that is robust and performs well has been developed for nonlinear mechanical control systems; however, it has not been widely accepted in industry since it is not immediately clear which partial differential equations should be solved. To transfer $\mathcal{H}_\infty$ control theory to industry, it is worthwhile to describe the relationship between $\mathcal{H}_\infty$ control and PID. In this chapter, we analyze the $\mathcal{H}_\infty$ optimality of a PID controller, especially for Lagrangian systems.

Most industrial mechanical systems can be described by the Lagrangian equation of motion. Conventional PID trajectory tracking controllers are used because they provide very effective position control in Lagrangian systems. Unfortunately, they lack an asymptotic stability proof. Under some conditions with PID gains, the global (or semi-global) asymptotic stability of a PID set-point regulation controller was proved by [2, 32, 46, 51, 60] for robotic manipulator systems without external disturbances. However, they did not deal with a PID trajectory tracking controller, but set-point regulation one. Also they did not consider the effect of PID gains on the system performance from the standpoint of $\mathcal{H}_\infty$ optimality. On the other hand, the robust stability of decentralized (PID) control for mechanical systems have been tried to prove it by using either Kharitonov theorem or Lyapunov method in [43, 52, 61].

In optimal control theories, nonlinear $\mathcal{H}_\infty$ control methods that are robust and perform well have been proposed over the last decade. The basic control law theories are found in two papers[29, 64]: one describing the full state feed-

Y. Choi, W.K. Chung: PID Trajectory Tracking Control for Mechanical Systems, LNCIS 298, pp. 29–46, 2004.

back case, and the other considering the output feedback case. However, the partial differential Hamilton-Jacobi-Isaacs (HJI) equation must still be solved in a nonlinear $\mathcal{H}_\infty$ controller. This is not a trivial problem. There have been several attempts to solve the HJI equation. The approximation method was used by [12] to obtain an approximate solution to the Hamilton-Jacobi(HJ) equation for Lagrangian systems. The concept of extended disturbances, including system error dynamics, was developed by [18, 47, 48, 49] to solve the HJI equation. Finally, the Lyapunov equation was solved instead of the HJI equation by [59], who suggested that a nonlinear $\mathcal{H}_\infty$ controller can only be attained in this manner.

This chapter is organized as follows. Next section deals with the state-space representation used for trajectory tracking in a Lagrangian system. In section 3.3, $\mathcal{H}_\infty$ optimality of a PID controller is proved by inversely finding the $\mathcal{H}_\infty$ performance index from the PID control law. Also, an inverse optimal PID control law is suggested with the necessary and sufficient condition for its existence in section 3.4. Finally, performance estimation by using performance index show indirectly the validity of optimality for $\mathcal{H}_\infty$ performance index.

3.2 State-Space Description of Lagrangian Systems

In general, mechanical systems can be described by the Lagrangian equation of motion. If the mechanical system with n degrees of freedom is represented by n generalized configuration coordinates $\boldsymbol{q} = [q_1, q_2, \cdots, q_n]^T \in \Re^n$, then the Lagrangian system is described as

$$\boldsymbol{M}(\boldsymbol{q})\ddot{\boldsymbol{q}} + \boldsymbol{C}(\boldsymbol{q}, \dot{\boldsymbol{q}})\dot{\boldsymbol{q}} + \boldsymbol{g}(\boldsymbol{q}) + \boldsymbol{d}(t) = \boldsymbol{\tau}, \tag{3.1}$$

where $\boldsymbol{M}(\boldsymbol{q}) \in \Re^{n\times n}$ is Inertia matrix, $\boldsymbol{C}(\boldsymbol{q}, \dot{\boldsymbol{q}})\dot{\boldsymbol{q}} \in \Re^n$ Coriolis and centrifugal torque vector, $\boldsymbol{g}(\boldsymbol{q}) \in \Re^n$ gravitational torque vector, $\boldsymbol{\tau} \in \Re^n$ the control input torque vector and $\boldsymbol{d}(t)$ unknown external disturbances. Disturbances exerted on the system can be caused by the friction nonlinearity, parameter perturbation, *etc.* Also, the extended disturbance can be defined for the trajectory tracking control, including the external disturbance, as following form:

$$\begin{aligned}\boldsymbol{w}\left(t, \dot{\boldsymbol{e}}, \boldsymbol{e}, \int \boldsymbol{e}\right) &= \boldsymbol{M}(\boldsymbol{q})\left(\ddot{\boldsymbol{q}}_d + \boldsymbol{K}_P\dot{\boldsymbol{e}} + \boldsymbol{K}_I\boldsymbol{e}\right) \\ &\quad + \boldsymbol{C}(\boldsymbol{q}, \dot{\boldsymbol{q}})\left(\dot{\boldsymbol{q}}_d + \boldsymbol{K}_P\boldsymbol{e} + \boldsymbol{K}_I\int \boldsymbol{e}\right) + \boldsymbol{g}(\boldsymbol{q}) + \boldsymbol{d}(t),\end{aligned} \tag{3.2}$$

where $\boldsymbol{K}_P, \boldsymbol{K}_I$ are diagonal constant matrices, $\boldsymbol{e} = \boldsymbol{q}_d - \boldsymbol{q}$ is the configuration error and desired configurations $(\boldsymbol{q}_d, \dot{\boldsymbol{q}}_d, \ddot{\boldsymbol{q}}_d)$ are functions of time. Hence, the extended disturbance $\boldsymbol{w}$ is the function of time, configuration error, its derivative and integral because $\boldsymbol{q}(= \boldsymbol{q}_d - \boldsymbol{e})$ and $\dot{\boldsymbol{q}}(= \dot{\boldsymbol{q}}_d - \dot{\boldsymbol{e}})$ are the function of time, configuration error and its derivative. If the extended disturbance

defined above is used in the Lagrangian system of (3.1), then the trajectory tracking system model can be rewritten as

$$\boldsymbol{M}(\boldsymbol{q})\dot{\boldsymbol{s}} + \boldsymbol{C}(\boldsymbol{q}, \dot{\boldsymbol{q}})\boldsymbol{s} = \boldsymbol{w}\left(t, \dot{\boldsymbol{e}}, \boldsymbol{e}, \int \boldsymbol{e}\right) + \boldsymbol{u}, \tag{3.3}$$

where $\boldsymbol{u} = -\boldsymbol{\tau}$ and $\boldsymbol{s} = \dot{\boldsymbol{e}} + \boldsymbol{K}_P\boldsymbol{e} + \boldsymbol{K}_I \int \boldsymbol{e}dt$.

If the state vector is defined for the tracking system model (3.3) as follows:

$$\boldsymbol{x} \triangleq \begin{bmatrix} \boldsymbol{x}_1 \\ \boldsymbol{x}_2 \\ \boldsymbol{x}_3 \end{bmatrix} = \begin{bmatrix} \int \boldsymbol{e} \\ \boldsymbol{e} \\ \dot{\boldsymbol{e}} \end{bmatrix} \in \Re^{3n} \tag{3.4}$$

then the state space representation of Lagrangian system can be obtained as the following form:

$$\dot{\boldsymbol{x}} = \boldsymbol{A}(\boldsymbol{x}, t)\boldsymbol{x} + \boldsymbol{B}(\boldsymbol{x}, t)\boldsymbol{w} + \boldsymbol{B}(\boldsymbol{x}, t)\boldsymbol{u}, \tag{3.5}$$

where

$$\boldsymbol{A}(\boldsymbol{x}, t) = \begin{bmatrix} \boldsymbol{0} & \boldsymbol{I} & \boldsymbol{0} \\ \boldsymbol{0} & \boldsymbol{0} & \boldsymbol{I} \\ -\boldsymbol{M}^{-1}\boldsymbol{C}\boldsymbol{K}_I, & -\boldsymbol{M}^{-1}\boldsymbol{C}\boldsymbol{K}_P - \boldsymbol{K}_I, & -\boldsymbol{M}^{-1}\boldsymbol{C} - \boldsymbol{K}_P \end{bmatrix}$$

and

$$\boldsymbol{B}(\boldsymbol{x}, t) = \begin{bmatrix} \boldsymbol{0} \\ \boldsymbol{0} \\ \boldsymbol{M}^{-1} \end{bmatrix}.$$

This is one of generic forms defined by [49] for Lagrangian system. An available characteristics for Lagrangian system is that the equality ($\dot{\boldsymbol{M}} = \boldsymbol{C} + \boldsymbol{C}^T$) is always satisfied. This characteristics offers the clue to solve the inverse optimal problem for above Lagrangian system (3.5).

Remark 1. If the controller stabilizes the trajectory tracking system model (3.5), then it makes the original system (3.1) stable because the boundedness of a state vector $\boldsymbol{x}$ implies those of $\boldsymbol{q}$ and $\dot{\boldsymbol{q}}$. However, the converse is not true.

Remark 2. For the set-point regulation control, the system model (3.1) can be rewritten by using the state vector $\dot{\boldsymbol{q}}$ as follows:

$$\boldsymbol{M}(\boldsymbol{q})\ddot{\boldsymbol{q}} + \boldsymbol{C}(\boldsymbol{q}, \dot{\boldsymbol{q}})\dot{\boldsymbol{q}} = \boldsymbol{w}_1(t, \boldsymbol{q}) + \boldsymbol{\tau}, \tag{3.6}$$

where $\boldsymbol{w}_1(t, \boldsymbol{q}) = -\boldsymbol{g}(\boldsymbol{q}) - \boldsymbol{d}(t)$. On the other hand, for the trajectory tracking control, we obtained the system model (3.3) by using the state vector $\boldsymbol{s}$. Here, above two system models (3.3) and (3.6) show the same dynamic characteristics such as $\boldsymbol{M}(\boldsymbol{q})^{-1}\boldsymbol{C}(\boldsymbol{q}, \dot{\boldsymbol{q}})$.

3.3 ISS and $\mathcal{H}_\infty$ Optimality of PID Control

Among the stability theories for control systems, the notion of input-to-state stability (ISS) in [1, 10, 38, 57, 58] is more convenient to deal with the disturbance input than other theories. When there exist unknown bounded inputs such as perturbations and external disturbances acting on systems, the behavior of the system should remain bounded. Also, when the set of inputs including the control, perturbation and disturbance go to zero, the behavior of system tends toward the equilibrium point. This ISS notion is helpful to understand the effect of inputs on system states. Moreover, Krstic *et al.* showed in [36, 37] that the backstepping controller designed using the ISS notion is optimal for the performance index found inversely from the controller. This has offered a useful insight from which we can show the $\mathcal{H}_\infty$ optimality of PID control for Lagrangian systems. The basic characteristics and properties on the ISS are summarized in the followings.

The control system is said to be extended disturbance input-to-state stable(ISS) if there exist a class $\mathcal{KL}$ function β and a class $\mathcal{K}$ function γ such that the solution for (3.5) exists for all $t \geq 0$ and satisfies

$$|\boldsymbol{x}(t)| \leq \beta(|\boldsymbol{x}(0)|, t) + \gamma\left(\sup_{0\leq\tau\leq t} |\boldsymbol{w}(\tau)|\right), \tag{3.7}$$

for an initial state vector $\boldsymbol{x}(0)$ and for an extended disturbance vector $\boldsymbol{w}(\cdot)$ piecewise continuous and bounded on $[0, \infty)$. Especially, the ISS becomes available by using Lyapunov function. For the system (3.5), there exist a smooth positive definite radially unbounded function $V(\boldsymbol{x}, t)$, a class $\mathcal{K}_\infty$ function γ_1 and a class $\mathcal{K}$ function γ_2 such that the following dissipativity inequality is satisfied:

$$\dot{V} \leq -\gamma_1(|\boldsymbol{x}|) + \gamma_2(|\boldsymbol{w}|), \tag{3.8}$$

if and only if the system is ISS, where $\dot{V}$ represents the total derivative for Lyapunov function. Also, suppose that there exists a function $V(\boldsymbol{x}, t)$ such that for all $\boldsymbol{x}$ and $\boldsymbol{w}$:

$$|\boldsymbol{x}| \geq \rho(|\boldsymbol{w}|) \quad \Rightarrow \quad \dot{V} \leq -\gamma_3(|\boldsymbol{x}|), \tag{3.9}$$

where ρ and γ_3 are class $\mathcal{K}_\infty$ functions. Then, the system is ISS and even we can say the globally asymptotic stability(GAS) if the unknown disturbance input satisfies the condition $|\boldsymbol{x}| \geq \rho(|\boldsymbol{w}|)$ for an state vector. However, we do not know whether the extended disturbance $\boldsymbol{w}$ satisfies the condition or not, hence, only ISS is proved. Above properties on ISS will be utilized in following sections.

3.3.1 ISS-CLF for Lagrangian Systems

To show the ISS for Lagrangian system, we should find the Lyapunov function and control law. However, there can be many control laws satisfying the

ISS and the disturbance is basically unknown. Hence, we need the definition which can bring the Lyapunov function and a unique control input under the assumption on the unknown disturbance. Using the ISS, the input-to-state stabilizable control Lyapunov function, in short ISS-CLF, is defined by [36]. The regular definition for ISS-CLF is as follows: a smooth positive definite radially unbounded function $V(\boldsymbol{x},t) : \Re^{3n} \times \Re_+ \to \Re_+$ is called an ISS-CLF for (3.5) if there exists a class $\mathcal{K}_\infty$ function ρ such that the following implication holds for all $\boldsymbol{x} \neq \boldsymbol{0}$ and all $\boldsymbol{w}$:

$$|\boldsymbol{x}| \geq \rho(|\boldsymbol{w}|) \quad \Rightarrow \quad \inf_{\boldsymbol{u}} \dot{V} < 0. \tag{3.10}$$

The following Theorem suggests both the control law derived from ISS and an ISS-CLF for Lagrangian system. Here, we show that the modified form of Lyapunov function suggested by [49] is an ISS-CLF under two conditions.

Theorem 3. *Let* $\boldsymbol{s} \triangleq \dot{\boldsymbol{e}} + \boldsymbol{K}_P\boldsymbol{e} + \boldsymbol{K}_I \int \boldsymbol{e}dt \in \Re^n$. *If the Lagrangian system (3.5) is extended disturbance input-to-state stable(ISS), then the control law should have the following form with* $\alpha \geq \frac{1}{2}$*:*

$$\boldsymbol{u} = -\alpha \boldsymbol{K}\boldsymbol{s} - \rho^{-1}(|\boldsymbol{x}|)\frac{\boldsymbol{s}}{|\boldsymbol{s}|}, \tag{3.11}$$

and $V(\boldsymbol{x},t) = \frac{1}{2}\boldsymbol{x}^T\boldsymbol{P}(\boldsymbol{x},t)\boldsymbol{x}$ *is an ISS-CLF with* $\alpha = \frac{1}{2}$*, where*

$$\boldsymbol{P}(\boldsymbol{x},t) = \begin{bmatrix} \boldsymbol{K}_I\boldsymbol{M}\boldsymbol{K}_I + \boldsymbol{K}_I\boldsymbol{K}_P\boldsymbol{K} & \boldsymbol{K}_I\boldsymbol{M}\boldsymbol{K}_P + \boldsymbol{K}_I\boldsymbol{K} & \boldsymbol{K}_I\boldsymbol{M} \\ \boldsymbol{K}_P\boldsymbol{M}\boldsymbol{K}_I + \boldsymbol{K}_I\boldsymbol{K} & \boldsymbol{K}_P\boldsymbol{M}\boldsymbol{K}_P + \boldsymbol{K}_P\boldsymbol{K} & \boldsymbol{K}_P\boldsymbol{M} \\ \boldsymbol{M}\boldsymbol{K}_I & \boldsymbol{M}\boldsymbol{K}_P & \boldsymbol{M} \end{bmatrix} \tag{3.12}$$

under the following two conditions for $\boldsymbol{P}$*:*

1. $\boldsymbol{K}, \boldsymbol{K}_P, \boldsymbol{K}_I > \boldsymbol{0}$ *constant diagonal matrices*
2. $\boldsymbol{K}_P^2 > 2\boldsymbol{K}_I$.

Proof. First, we show that the Lyapunov matrix $\boldsymbol{P}$ (3.12) is positive definite. If we manipulate the Lyapunov function as following form:

$$\begin{aligned} V(\boldsymbol{x},t) &= \frac{1}{2}\boldsymbol{x}^T\boldsymbol{P}(\boldsymbol{x},t)\boldsymbol{x} \\ &= \frac{1}{2}\boldsymbol{s}^T\boldsymbol{M}\boldsymbol{s} + \frac{1}{2}\begin{bmatrix} \int \boldsymbol{e} \\ \boldsymbol{e} \end{bmatrix}^T \begin{bmatrix} \boldsymbol{K}_I\boldsymbol{K}_P\boldsymbol{K} & \boldsymbol{K}_I\boldsymbol{K} \\ \boldsymbol{K}_I\boldsymbol{K} & \boldsymbol{K}_P\boldsymbol{K} \end{bmatrix} \begin{bmatrix} \int \boldsymbol{e} \\ \boldsymbol{e} \end{bmatrix}, \end{aligned}$$

then we can see that the Lyapunov function is positive definite under conditions 1 and 2 except $\boldsymbol{x} = \boldsymbol{0}$ because the Inertia matrix $\boldsymbol{M}$ is positive definite. Second, the total derivative of Lyapunov function is given by

$$\dot{V} = V_t + \boldsymbol{V}_x\boldsymbol{A}\boldsymbol{x} + \boldsymbol{V}_x\boldsymbol{B}\boldsymbol{w} + \boldsymbol{V}_x\boldsymbol{B}\boldsymbol{u},$$

and its components can be calculated using $\dot{\boldsymbol{M}} - \boldsymbol{C}^T - \boldsymbol{C} = \boldsymbol{0}$ as follows:

$$
\begin{aligned}
V_t + \boldsymbol{V}_x \boldsymbol{A}\boldsymbol{x} &= \frac{1}{2}\boldsymbol{x}^T \left(\dot{\boldsymbol{P}} + \boldsymbol{P}\boldsymbol{A} + \boldsymbol{A}^T\boldsymbol{P}\right)\boldsymbol{x} \\
&= \frac{1}{2}\boldsymbol{x}^T \begin{bmatrix} \boldsymbol{0} & \boldsymbol{K}_I\boldsymbol{K}_P\boldsymbol{K} & \boldsymbol{K}_I\boldsymbol{K} \\ \boldsymbol{K}_I\boldsymbol{K}_P\boldsymbol{K} & 2\boldsymbol{K}_I\boldsymbol{K} & \boldsymbol{K}_P\boldsymbol{K} \\ \boldsymbol{K}_I\boldsymbol{K} & \boldsymbol{K}_P\boldsymbol{K} & \boldsymbol{0} \end{bmatrix}\boldsymbol{x} \\
&= \frac{1}{2}\left(\boldsymbol{s}^T\boldsymbol{K}\boldsymbol{s} - \int \boldsymbol{e}^T\boldsymbol{K}_I^2\boldsymbol{K}\int \boldsymbol{e} - \boldsymbol{e}^T(\boldsymbol{K}_P^2 - 2\boldsymbol{K}_I)\boldsymbol{K}\boldsymbol{e} - \dot{\boldsymbol{e}}^T\boldsymbol{K}\dot{\boldsymbol{e}}\right)
\end{aligned} \tag{3.13}
$$

and

$$
\boldsymbol{V}_x\boldsymbol{B} = \boldsymbol{x}^T\boldsymbol{P}\boldsymbol{B} = \boldsymbol{x}^T\left[\ \boldsymbol{K}_I\ ,\ \boldsymbol{K}_P\ ,\ \boldsymbol{I}\ \right]^T = \boldsymbol{s}^T. \tag{3.14}
$$

Now, the total derivative of Lyapunov function is calculated by using (3.13) and (3.14) as follows:

$$
\begin{aligned}
\dot{V} = \frac{1}{2}&\left(\boldsymbol{s}^T\boldsymbol{K}\boldsymbol{s} - \int \boldsymbol{e}^T\boldsymbol{K}_I^2\boldsymbol{K}\int \boldsymbol{e} - \boldsymbol{e}^T(\boldsymbol{K}_P^2 - 2\boldsymbol{K}_I)\boldsymbol{K}\boldsymbol{e} - \dot{\boldsymbol{e}}^T\boldsymbol{K}\dot{\boldsymbol{e}}\right) \\
&+\boldsymbol{s}^T\boldsymbol{w} + \boldsymbol{s}^T\boldsymbol{u} < 0,
\end{aligned}
$$

hence,

$$
\frac{1}{2}\boldsymbol{s}^T\boldsymbol{K}\boldsymbol{s} + \boldsymbol{s}^T\boldsymbol{w} + \boldsymbol{s}^T\boldsymbol{u} < \frac{1}{2}\left(\int \boldsymbol{e}^T(\boldsymbol{K}_I^2\boldsymbol{K})\int \boldsymbol{e} + \boldsymbol{e}^T(\boldsymbol{K}_P^2 - 2\boldsymbol{K}_I)\boldsymbol{K}\boldsymbol{e} + \dot{\boldsymbol{e}}^T\boldsymbol{K}\dot{\boldsymbol{e}}\right). \tag{3.15}
$$

Let us consider only the right hand side of (3.15). Then we can see that it is always positive definite except $\boldsymbol{x} = \boldsymbol{0}$ under conditions 1 and 2. Also, if the condition $|\boldsymbol{x}| \geq \rho(|\boldsymbol{w}|)$ of (3.9) is utilized, then the left hand side of (3.15) has the following form:

$$
\begin{aligned}
\frac{1}{2}\boldsymbol{s}^T\boldsymbol{K}\boldsymbol{s} + \boldsymbol{s}^T\boldsymbol{w} + \boldsymbol{s}^T\boldsymbol{u} &\leq \frac{1}{2}\boldsymbol{s}^T\boldsymbol{K}\boldsymbol{s} + |\boldsymbol{s}||\boldsymbol{w}| + \boldsymbol{s}^T\boldsymbol{u} \\
&\leq \frac{1}{2}\boldsymbol{s}^T\boldsymbol{K}\boldsymbol{s} + |\boldsymbol{s}|\rho^{-1}(|\boldsymbol{x}|) + \boldsymbol{s}^T\boldsymbol{u}.
\end{aligned}
$$

Here, above equation should at least be negative semi-definite to satisfy the ISS of (3.9). Hence, we obtain the control law (3.11) with the condition $\alpha \geq \frac{1}{2}$. Also, since the infimum among the control inputs that satisfy (3.15) is achieved at $\alpha = \frac{1}{2}$, we can know that the definition (3.10) is always satisfied with $\alpha = \frac{1}{2}$ for all $\boldsymbol{x} \neq \boldsymbol{0}$. Third, the $V(\boldsymbol{x}, t)$ is a differentiable and radially unbounded function because $V(\boldsymbol{x}, t) \to \infty$ as $\boldsymbol{x} \to \infty$. Therefore, we conclude that $V(\boldsymbol{x}, t)$ is an ISS-CLF with $\alpha = \frac{1}{2}$ for the Lagrangian system. □

An important characteristics of controller (3.11) is that it has the PID control type as follows:

$$
\boldsymbol{u} = -\left(\alpha\boldsymbol{K} + \frac{\rho^{-1}(|\boldsymbol{x}|)}{|\boldsymbol{s}|}\boldsymbol{I}\right)\left(\dot{\boldsymbol{e}} + \boldsymbol{K}_P\boldsymbol{e} + \boldsymbol{K}_I\int \boldsymbol{e}dt\right). \tag{3.16}
$$

Another characteristics of above controller is that it can be rewritten as the optimal control type of $\boldsymbol{u} = -\boldsymbol{R}^{-1}\boldsymbol{B}^T\boldsymbol{P}\boldsymbol{x}$ by letting

$$\boldsymbol{R}(\boldsymbol{x}) = \left(\alpha\boldsymbol{K} + \frac{\rho^{-1}(|\boldsymbol{x}|)}{|\boldsymbol{s}|}\boldsymbol{I}\right)^{-1},$$

because $\boldsymbol{B}^T\boldsymbol{P}\boldsymbol{x} = \dot{\boldsymbol{e}} + \boldsymbol{K}_P\boldsymbol{e} + \boldsymbol{K}_I\int \boldsymbol{e}dt$ as shown in (3.14). Strictly speaking, the controller (3.16) is not a conventional PID one since it includes the unknown function $\rho^{-1}(|\boldsymbol{x}|)$. In the following section, we will find the bounds and meaning of $\rho^{-1}(|\boldsymbol{x}|)$ in a viewpoint of the optimality of $\mathcal{H}_\infty$ control.

3.3.2 $\mathcal{H}_\infty$ Optimality of PID Control Law

To state the optimality of nonlinear $\mathcal{H}_\infty$ control system suggested in [29, 64, 65], the Hamilton-Jacobi-Isaacs (HJI) equation which is derived from the direct optimization for the performance index should be solved, but the solution of HJI equation is too hard to obtain for general systems, including Lagrangian system, because it is the multi-variable partial differential equation. To overcome this difficulty of a direct optimization, Krstic *et al* showed in [36] that the inverse optimal problem is solvable if the system is disturbance input-to-state stable. Also, Park *et al* showed in [49] that the nonlinear $\mathcal{H}_\infty$ control problem for robotic manipulators can be solved using the characteristics of Lagrangian system. The HJI equation for the Lagrangian system and its analytic solution were suggested by [47], but it dealt with the modified computed torque controller form, not a PID controller type.

Now, we are to show the $\mathcal{H}_\infty$ optimality of PID control type for Lagrangian systems by using the control law in Theorem 3. Consider a general $\mathcal{H}_\infty$ performance index(PI) as following form:

$$PI(t,\boldsymbol{x},\boldsymbol{u},\boldsymbol{w}) = \lim_{t\to\infty}\left[2V(\boldsymbol{x}(t),t) + \int_0^t \left(\boldsymbol{x}^T\boldsymbol{Q}(\boldsymbol{x})\boldsymbol{x} + \boldsymbol{u}^T\boldsymbol{R}(\boldsymbol{x})\boldsymbol{u} - \gamma^2\boldsymbol{w}^T\boldsymbol{w}\right)d\sigma\right], \tag{3.17}$$

where $\boldsymbol{Q}(\boldsymbol{x})$ is a state weighting matrix, $\boldsymbol{R}(\boldsymbol{x})$ control input weighting and γ means $\mathcal{L}_2$-gain. Also, the HJI equation is derived from the optimization for $\mathcal{H}_\infty$ performance index, with Lagrangian system constraint of (3.5), as following form:

$$HJI = \dot{\boldsymbol{P}} + \boldsymbol{A}^T\boldsymbol{P} + \boldsymbol{P}\boldsymbol{A} - \boldsymbol{P}\boldsymbol{B}\boldsymbol{R}^{-1}\boldsymbol{B}^T\boldsymbol{P} + \frac{1}{\gamma^2}\boldsymbol{P}\boldsymbol{B}\boldsymbol{B}^T\boldsymbol{P} + \boldsymbol{Q} = \boldsymbol{0}. \tag{3.18}$$

As a matter of fact, above HJI equation is equal to the differential Riccati equation for a linear multi-variable time varying system. Above HJI equation (3.18) plays important roles which give the $\mathcal{H}_\infty$ optimality and stability to the control system. In the next Theorem, we show that the PID control law can be a minimum solution of $\mathcal{H}_\infty$ performance index. And it is inverse optimal in that the state weighting matrix $\boldsymbol{Q}(\boldsymbol{x})$ and control input one $\boldsymbol{R}(\boldsymbol{x})$ can be

found from the gains of controller and even the HJI equation can be obtained from $\boldsymbol{Q}(\boldsymbol{x})$.

Theorem 4. *For a given Lagrangian system (3.5), suppose that there exists an ISS-CLF in Theorem 3. If the PID control law (3.16) as following form:*

$$\boldsymbol{u} = -\boldsymbol{R}^{-1}\boldsymbol{B}^T\boldsymbol{P}\boldsymbol{x} \tag{3.19}$$

is utilized with conditions

1. $\alpha = 1$
2. $\rho^{-1}(|\boldsymbol{x}|) \geq \frac{1}{\gamma^2}|\boldsymbol{s}|$,

then the controller (3.19) is a solution of the minimization problem for $\mathcal{H}_\infty$ performance index (3.17) using

$$\boldsymbol{Q}(\boldsymbol{x}) = -\left(\dot{\boldsymbol{P}} + \boldsymbol{A}^T\boldsymbol{P} + \boldsymbol{P}\boldsymbol{A} - \boldsymbol{P}\boldsymbol{B}\boldsymbol{K}\boldsymbol{B}^T\boldsymbol{P}\right) \tag{3.20}$$

$$\boldsymbol{R}(\boldsymbol{x}) = \left(\boldsymbol{K} + \frac{\rho^{-1}(|\boldsymbol{x}|)}{|\boldsymbol{s}|}\boldsymbol{I}\right)^{-1}. \tag{3.21}$$

Proof. First, we show that the matrix $\boldsymbol{Q}(\boldsymbol{x})$ of (3.20) is positive definite and constant matrix. Let us obtain the state weighting matrix $\boldsymbol{Q}(\boldsymbol{x})$ using (3.13) and (3.14) in proof of Theorem 3, then $\boldsymbol{Q}(\boldsymbol{x})$ is acquired as following constant matrix:

$$\boldsymbol{Q} = \begin{bmatrix} \boldsymbol{K}_I^2\boldsymbol{K} & \boldsymbol{0} & \boldsymbol{0} \\ \boldsymbol{0} & (\boldsymbol{K}_P^2 - 2\boldsymbol{K}_I)\boldsymbol{K} & \boldsymbol{0} \\ \boldsymbol{0} & \boldsymbol{0} & \boldsymbol{K} \end{bmatrix}. \tag{3.22}$$

Hence, $\boldsymbol{Q}$ is a positive definite and constant matrix. This was proved by [48] for the first time. Second, we prove the $\mathcal{H}_\infty$ optimality inversely by showing that a PID control type (3.19) achieves the minimum of the $\mathcal{H}_\infty$ performance index. The first condition of $\alpha = 1$, not $\frac{1}{2}$, makes it possible to solve the optimization problem, in other words, the optimal α is two times the value obtained by the definition of ISS-CLF in Theorem 3. This fact was proved by [36] for the first time. If we put $\boldsymbol{Q}$ into the performance index and use $\boldsymbol{K} = \boldsymbol{R}^{-1}(\boldsymbol{x}) - \frac{\rho^{-1}(|\boldsymbol{x}|)}{|\boldsymbol{s}|}\boldsymbol{I}$ of (3.21), then we can manipulate the performance index as follows:

$$
\begin{aligned}
PI(t,\boldsymbol{x},\boldsymbol{u},\boldsymbol{w}) &= \lim_{t\to\infty}\Big[2V(\boldsymbol{x}(t),t) \\
&\quad - \int_0^t \boldsymbol{x}^T\left[\dot{\boldsymbol{P}}+\boldsymbol{A}^T\boldsymbol{P}+\boldsymbol{P}\boldsymbol{A}-\boldsymbol{P}\boldsymbol{B}\boldsymbol{K}\boldsymbol{B}^T\boldsymbol{P}\right]\boldsymbol{x}d\tau \\
&\quad + \int_0^t \left(\boldsymbol{u}^T\boldsymbol{R}(\boldsymbol{x})\boldsymbol{u}-\gamma^2\boldsymbol{w}^T\boldsymbol{w}\right)d\tau\Big] \\
&= \lim_{t\to\infty}\Big[2V(\boldsymbol{x}(t),t) \\
&\quad - \int_0^t \left(\boldsymbol{x}^T\left[\dot{\boldsymbol{P}}+\boldsymbol{A}^T\boldsymbol{P}+\boldsymbol{P}\boldsymbol{A}\right]\boldsymbol{x}+2\boldsymbol{x}^T\boldsymbol{P}\boldsymbol{B}\boldsymbol{u}+2\boldsymbol{x}^T\boldsymbol{P}\boldsymbol{B}\boldsymbol{w}\right)d\tau \\
&\quad + \int_0^t \left(\boldsymbol{u}^T\boldsymbol{R}(\boldsymbol{x})\boldsymbol{u}+2\boldsymbol{x}^T\boldsymbol{P}\boldsymbol{B}\boldsymbol{u}+\boldsymbol{x}^T\boldsymbol{P}\boldsymbol{B}\boldsymbol{K}\boldsymbol{B}^T\boldsymbol{P}\boldsymbol{x}\right)d\tau \\
&\quad + \int_0^t \left(2\boldsymbol{x}^T\boldsymbol{P}\boldsymbol{B}\boldsymbol{w}-\gamma^2\boldsymbol{w}^T\boldsymbol{w}\right)d\tau\Big] \\
&= \lim_{t\to\infty}\Big[2V(\boldsymbol{x}(t),t)-2\int_0^t \dot{V}d\tau \\
&\quad + \int_0^t (\boldsymbol{u}+\boldsymbol{R}^{-1}\boldsymbol{B}^T\boldsymbol{P}\boldsymbol{x})^T\boldsymbol{R}(\boldsymbol{u}+\boldsymbol{R}^{-1}\boldsymbol{B}^T\boldsymbol{P}\boldsymbol{x})d\tau \\
&\quad -\gamma^2\int_0^t \left(\boldsymbol{w}-\frac{1}{\gamma^2}\boldsymbol{B}^T\boldsymbol{P}\boldsymbol{x}\right)^T\left(\boldsymbol{w}-\frac{1}{\gamma^2}\boldsymbol{B}^T\boldsymbol{P}\boldsymbol{x}\right)d\tau \\
&\quad - \int_0^t \left(\frac{\rho^{-1}(|\boldsymbol{x}|)}{|\boldsymbol{s}|}-\frac{1}{\gamma^2}\right)\boldsymbol{x}^T\boldsymbol{P}\boldsymbol{B}\boldsymbol{B}^T\boldsymbol{P}\boldsymbol{x}d\tau\Big] \\
&= 2V(\boldsymbol{x}(0),0)+\int_0^\infty (\boldsymbol{u}+\boldsymbol{R}^{-1}\boldsymbol{B}^T\boldsymbol{P}\boldsymbol{x})^T\boldsymbol{R}(\boldsymbol{u}+\boldsymbol{R}^{-1}\boldsymbol{B}^T\boldsymbol{P}\boldsymbol{x})d\tau \\
&\quad -\gamma^2\int_0^\infty \left|\boldsymbol{w}-\frac{1}{\gamma^2}\boldsymbol{B}^T\boldsymbol{P}\boldsymbol{x}\right|^2 d\tau \\
&\quad - \int_0^\infty \left(\frac{\rho^{-1}(|\boldsymbol{x}|)}{|\boldsymbol{s}|}-\frac{1}{\gamma^2}\right)|\boldsymbol{s}|^2 d\tau. \qquad (3.23)
\end{aligned}
$$

From (3.23), we can see that the minimum for $\mathcal{H}_\infty$ performance index is achieved in the case that the control law is (3.19). Also, the worst case disturbance is given by

$$\boldsymbol{w}^* = \frac{1}{\gamma^2}\boldsymbol{B}^T\boldsymbol{P}\boldsymbol{x}$$

and $|\boldsymbol{w}^*| = \frac{1}{\gamma^2}|\boldsymbol{s}|$. The second condition of $\rho^{-1}(|\boldsymbol{x}|) \geq \frac{1}{\gamma^2}|\boldsymbol{s}|$ should be satisfied for the minimization of (3.23). Therefore, we conclude that the PID control law (3.19) minimizes $\mathcal{H}_\infty$ performance index (3.17) using the given $\boldsymbol{Q}$ and $\boldsymbol{R}(\boldsymbol{x})$. □

Remark 3. The condition 2 in Theorem 4 is the design guideline of function $\rho^{-1}(|\boldsymbol{x}|)$ to be $\mathcal{H}_\infty$ optimal controller. As a matter of fact, it implies that

$\rho^{-1}(|\boldsymbol{x}|)$ should not be smaller than at least the magnitude of worst case disturbance. Here, if we choose the magnitude of worst case disturbance for the function $\rho^{-1}(|\boldsymbol{x}|)$, in other words, $\rho^{-1}(|\boldsymbol{x}|) = |\boldsymbol{w}^*| = \frac{1}{\gamma^2}|\boldsymbol{s}|$, then the PID control law (3.19) recovers fortunately the static gain PID one because the matrix $\boldsymbol{R}(\boldsymbol{x})$ of (3.21) becomes a constant matrix as follows:

$$\boldsymbol{R} = \left(\boldsymbol{K} + \frac{1}{\gamma^2}\boldsymbol{I}\right)^{-1}. \tag{3.24}$$

Also, the matrix $\boldsymbol{Q}$ of (3.20) implies the HJI equation of (3.18), though the HJI is not explicitly utilized to show the $\mathcal{H}_\infty$ optimality of a PID control law in Theorem 4.

In a viewpoint of an optimal control theory, the magnitude of a state weighting $\boldsymbol{Q}$ has the relation with system errors, *e.g.*, if we enlarge the magnitude of a state weighting matrix by four times, then the control performance will be approximately enhanced by two times, in other words, the error will be approximately reduced by half. This property will be shown through experimental results later. Therefore, if we are to reduce the error of system, we should enlarge the magnitude of a matrix $\boldsymbol{K}$ in the state weighting. However, it reduces the magnitude of a control input weighting matrix $\boldsymbol{R}$ and produces the bigger control effort. Conversely, if we reduce the magnitude of $\boldsymbol{K}$, then the smaller control effort is required and the bigger error is generated. The common $\boldsymbol{K}$ in the state weighting and the control input weighting has the trade-off characteristics between the system performance and control effort. Also, it seems that the $\mathcal{L}_2$-gain γ has no the effect on state weighting and affects only the control input weighting, but it does affect the control performance by increasing the robustness for disturbances.

3.4 Inverse Optimal PID Control

In the previous section, the $\mathcal{H}_\infty$ optimality of PID controller for the performance index was shown through Theorem 3, 4 and Remark 3. Here, we define the inverse optimal PID controller using the static gain one in Remark 3 and summarize its design conditions in following Theorem.

Theorem 5. *If the inverse optimal PID controller:*

$$\boldsymbol{\tau} = \left(\boldsymbol{K} + \frac{1}{\gamma^2}\boldsymbol{I}\right)\left(\dot{\boldsymbol{e}} + \boldsymbol{K}_P\boldsymbol{e} + \boldsymbol{K}_I\int \boldsymbol{e}\right) \tag{3.25}$$

satisfying next conditions:

1. $\boldsymbol{K}, \boldsymbol{K}_P, \boldsymbol{K}_I > \boldsymbol{0}$, *constant diagonal matrices*
2. $\boldsymbol{K}_P^2 > 2\boldsymbol{K}_I$,
3. $\gamma > 0$

is applied to the Lagrangian system (3.5), then the closed-loop control system is extended disturbance input-to-state stable(ISS).

Proof. The conditions 1 and 2 assure the existence of Lyapunov matrix $\boldsymbol{P} > \boldsymbol{0}$ by Theorem 3 and the condition 3 means $\mathcal{L}_2$-gain in the $\mathcal{H}_\infty$ performance index. If the inverse optimal PID controller (3.25) is applied to the Lagrangian system (3.5), then we know that the HJI equation of (3.18) is satisfied by Remark 3. Therefore, along the solution trajectory of (3.5) with the inverse optimal PID control law, we get the time derivative of Lyapunov function:

$$\begin{aligned}\dot{V} &= V_t + \boldsymbol{V}_x\boldsymbol{A}\boldsymbol{x} + \boldsymbol{V}_x\boldsymbol{B}\boldsymbol{u} + \boldsymbol{V}_x\boldsymbol{B}\boldsymbol{w} \\ &= \frac{1}{2}\boldsymbol{x}^T\left(\dot{\boldsymbol{P}} + \boldsymbol{A}^T\boldsymbol{P} + \boldsymbol{P}\boldsymbol{A}\right)\boldsymbol{x} \\ &\quad -\boldsymbol{x}^T\boldsymbol{P}\boldsymbol{B}\boldsymbol{R}^{-1}\boldsymbol{B}^T\boldsymbol{P}\boldsymbol{x} + \boldsymbol{x}^T\boldsymbol{P}\boldsymbol{B}\boldsymbol{w},\end{aligned}$$

where $\boldsymbol{u} = -\boldsymbol{\tau} = -\boldsymbol{R}^{-1}\boldsymbol{B}^T\boldsymbol{P}\boldsymbol{x}$. Here, if above equation is rearranged by using the HJI (3.18) and Young's inequality $\boldsymbol{x}^T\boldsymbol{P}\boldsymbol{B}\boldsymbol{w} \le \frac{1}{\gamma^2}|\boldsymbol{x}^T\boldsymbol{P}\boldsymbol{B}|^2 + \gamma^2|\boldsymbol{w}|^2$, then we get the following similar to (3.8):

$$\dot{V} \le -\frac{1}{2}\boldsymbol{x}^T\left(\boldsymbol{Q} + \boldsymbol{P}\boldsymbol{B}\boldsymbol{K}\boldsymbol{B}^T\boldsymbol{P}\right)\boldsymbol{x} + \gamma^2|\boldsymbol{w}|^2. \tag{3.26}$$

Since the right hand side of above inequality (3.26) is unbounded function for $\boldsymbol{x}$ and $\boldsymbol{w}$ respectively, hence, the Lagrangian system with an inverse optimal PID controller is extended disturbance input-to-state stable(ISS). □

Corollary 1. *The inverse optimal PID controller of (3.25) exists if and only if the Lagrangian system (3.5) is extended disturbance input-to-state stable(ISS).*

Proof. The proof consists of Theorem 3, 4, 5 and Remark 3 as follows:

$$\begin{array}{ccc} \text{ISS} & \xrightarrow{\text{Th.3}} & \text{Control Law (3.11)} \\ \text{Th.5}\uparrow & & \downarrow\text{Th.4} \\ \text{Inverse Optimal PID (3.25)} & \xleftarrow[\text{Re.3}]{} & \mathcal{H}_\infty \text{ Optimality} \end{array}$$

□

By Corollary 1, we showed the necessary and sufficient condition for the existence of an inverse optimal PID controller. Though the inverse optimal PID controller guarantees the ISS, it does not give the global asymptotic stability(GAS). This fact brings the selection guidelines for gains of an inverse optimal PID control.

3.4.1 Selection Guidelines for Gains

There are four parameters to adjust the control performance in an inverse optimal PID control: $\boldsymbol{K}, \boldsymbol{K}_P, \boldsymbol{K}_I$ and γ. The selection conditions of gains are suggested using the time derivative of Lyapunov function. First of all, let us reconsider the extended disturbance of (3.2) as follows:

$$\begin{aligned}|\boldsymbol{w}|^2 &= \left|\boldsymbol{M}\left(\ddot{\boldsymbol{q}}_d + \boldsymbol{K}_P\dot{\boldsymbol{e}} + \boldsymbol{K}_I\boldsymbol{e}\right) + \boldsymbol{C}\left(\dot{\boldsymbol{q}}_d + \boldsymbol{K}_P\boldsymbol{e} + \boldsymbol{K}_I\int \boldsymbol{e}\right) + \boldsymbol{g} + \boldsymbol{d}\right|^2 \\ &= \left|\boldsymbol{M}\boldsymbol{K}_P\dot{\boldsymbol{e}} - \boldsymbol{C}\dot{\boldsymbol{e}} + \boldsymbol{M}\boldsymbol{K}_I\boldsymbol{e} + \boldsymbol{C}\boldsymbol{s} + \boldsymbol{h}\right|^2 \quad \text{(by Schwarz inequality)} \\ &\le 5\left|\boldsymbol{M}\boldsymbol{K}_P\dot{\boldsymbol{e}}\right|^2 + 5\left|\boldsymbol{C}\dot{\boldsymbol{e}}\right|^2 + 5\left|\boldsymbol{M}\boldsymbol{K}_I\boldsymbol{e}\right|^2 + 5\left|\boldsymbol{C}\boldsymbol{s}\right|^2 + 5\left|\boldsymbol{h}\right|^2, \end{aligned} \tag{3.27}$$

where $\boldsymbol{h} = \boldsymbol{M}(\boldsymbol{q})\ddot{\boldsymbol{q}}_d + \boldsymbol{C}(\boldsymbol{q},\dot{\boldsymbol{q}})\dot{\boldsymbol{q}}_d + \boldsymbol{g}(\boldsymbol{q}) + \boldsymbol{d}(t)$. The following Theorem proposes the selection guidelines for gains using (3.26) and (3.27).

Theorem 6. *Let* $|\boldsymbol{M}(\boldsymbol{q})| \le m$, $|\boldsymbol{C}(\boldsymbol{q},\dot{\boldsymbol{q}})| \le c_0|\dot{\boldsymbol{q}}|$, $\boldsymbol{K} = k\boldsymbol{I}, \boldsymbol{K}_P = k_P\boldsymbol{I}$ *and* $\boldsymbol{K}_I = k_I\boldsymbol{I} \in \Re^{n\times n}$. *Suppose that the tuning variables*[1] (γ, k) *satisfy following condition*

$$\sqrt{k}/\gamma > \sqrt{10}c_0|\dot{\boldsymbol{q}}|, \tag{3.28}$$

then the gain k_P *should be confined to the following constraint:*

$$k_P < \frac{\sqrt{(k/\gamma^2) - 10c_0^2|\dot{\boldsymbol{q}}|^2}}{\sqrt{10}m}, \tag{3.29}$$

and the gain k_I *should be confined to the following constraint:*

$$k_I < \frac{\sqrt{(k/\gamma^2)^2 + 10m^2k_P^2(k/\gamma^2)} - k/\gamma^2}{10m^2}. \tag{3.30}$$

Proof. First, if we apply $|\boldsymbol{M}(\boldsymbol{q})| \le m$, $|\boldsymbol{C}(\boldsymbol{q},\dot{\boldsymbol{q}})| \le c_0|\dot{\boldsymbol{q}}|$, $\boldsymbol{K} = k\boldsymbol{I}, \boldsymbol{K}_P = k_P\boldsymbol{I}, \boldsymbol{K}_I = k_I\boldsymbol{I}$ to the extended disturbance (3.27), then it is simplified as follows:

$$|\boldsymbol{w}|^2 \le 5(m^2k_P^2 + c_0^2|\dot{\boldsymbol{q}}|^2)|\dot{\boldsymbol{e}}|^2 + 5m^2k_I^2|\boldsymbol{e}|^2 + 5c_0^2|\dot{\boldsymbol{q}}|^2\left|\boldsymbol{s}\right|^2 + 5\left|\boldsymbol{h}\right|^2. \tag{3.31}$$

Second, if we rewrite the time derivative of Lyapunov function (3.26) using (3.14) and (3.31), then $\dot{V}$ is obtained as follows:

[1] The tuning variables will be used for performance tuning in next chapter.

$$
\begin{aligned}
\dot{V} &\leq -\frac{1}{2}\boldsymbol{x}^T\boldsymbol{Q}\boldsymbol{x} - \frac{1}{2}\boldsymbol{s}^T\boldsymbol{K}\boldsymbol{s} + \gamma^2|\boldsymbol{w}|^2 \\
&= -\frac{1}{2}\left(k|\dot{\boldsymbol{e}}|^2 + k(k_P^2 - 2k_I)|\boldsymbol{e}|^2 + kk_I^2\left|\int \boldsymbol{e}\right|^2\right) - \frac{1}{2}k|\boldsymbol{s}|^2 + \gamma^2|\boldsymbol{w}|^2 \\
&\leq -\frac{1}{2}\left(k - 10\gamma^2(m^2k_P^2 + c_0^2|\dot{\boldsymbol{q}}|^2)\right)|\dot{\boldsymbol{e}}|^2 \\
&\quad -\frac{1}{2}\left(k(k_P^2 - 2k_I) - 10\gamma^2m^2k_I^2\right)|\boldsymbol{e}|^2 \\
&\quad -\frac{1}{2}kk_I^2\left|\int \boldsymbol{e}\right|^2 \\
&\quad -\frac{1}{2}\left(k - 10\gamma^2c_0^2|\dot{\boldsymbol{q}}|^2\right)|\boldsymbol{s}|^2 \\
&\quad +5\gamma^2|\boldsymbol{h}|^2 .
\end{aligned} \tag{3.32}
$$

If the condition (3.28) for tuning variables is satisfied, then the negative definiteness of a term $|\boldsymbol{s}|^2$ in (3.32) is assured. Also, we can obtain the upper bounds of gains k_P of (3.29) and k_I of (3.30) using the negative definiteness of each term $|\dot{\boldsymbol{e}}|^2$ and $|\boldsymbol{e}|^2$, respectively. □

The condition (3.28) in Theorem 6 means that the relation between tuning variables should be chosen proportional to $|\dot{\boldsymbol{q}}|$, but we can not know $\dot{\boldsymbol{q}}$ before the experiment. However, the desired configuration derivative $\dot{\boldsymbol{q}}_d$ can be approximately utilized instead of $\dot{\boldsymbol{q}}$. As the maximum $\dot{\boldsymbol{q}}_d$ is faster, the following relation should hold:

$$\sqrt{k}/\gamma \propto \max\{|\dot{\boldsymbol{q}}_d|\}. \tag{3.33}$$

Also, the condition (3.29) says that the value of k_P should be determined inversely proportional to the maximum eigenvalue of Inertia matrix. Hence, the large k_P can be used for small Inertia systems and *vice versa*. In general, since the relation $(\sqrt{k}/\gamma)$ will be chosen large according to (3.28), we can notice the proportional relation of

$$k_P \propto (1/m)(\sqrt{k}/\gamma) \tag{3.34}$$

from the condition (3.29). Also the proportional relation for k_I can be found from (3.30). If we manipulate (3.30) using $\sqrt{a^2+b^2} \leq |a| + |b|$ as following forms:

$$
\begin{aligned}
k_I &< \frac{\sqrt{(k/\gamma^2)^2 + 10m^2k_P^2(k/\gamma^2)} - k/\gamma^2}{10m^2} \\
&< \frac{(k/\gamma^2) + \sqrt{10}mk_P(\sqrt{k}/\gamma) - (k/\gamma^2)}{10m^2} \\
&= \frac{k_P(\sqrt{k}/\gamma)}{\sqrt{10}m}, \\
k_I &\propto (k_P/m)(\sqrt{k}/\gamma),
\end{aligned} \tag{3.35}
$$

then the proportional relation of (3.35) can be found. Hence, the value of k_I should be chosen inversely proportional to m and directly proportional to k_P.

Remark 4. Assume that the Lagrangian system (3.5) is extended disturbance input-to-state stable (ISS) and the configuration velocity is bounded by applying an inverse optimal PID controller, *e.g.*, $|\dot{\boldsymbol{q}}| < c_q$. If there exists no gravity torque ($\boldsymbol{g}(\boldsymbol{q}) = \boldsymbol{0}$), then the term $|\boldsymbol{h}|^2$ in (3.32) can be upper bounded using Schwarz inequality as follows:

$$\begin{aligned} |\boldsymbol{h}|^2 &= |\boldsymbol{M}(\boldsymbol{q})\ddot{\boldsymbol{q}}_d + \boldsymbol{C}(\boldsymbol{q},\dot{\boldsymbol{q}})\dot{\boldsymbol{q}}_d + \boldsymbol{d}|^2 \\ &\le 3m^2|\ddot{\boldsymbol{q}}_d|^2 + 3c_0^2c_q^2|\dot{\boldsymbol{q}}_d|^2 + 3|\boldsymbol{d}|^2. \end{aligned}$$

Here, if above inequality is inserted in (3.32), then it is modified to:

$$\begin{aligned} \dot{V} \le & -\frac{1}{2}\left(k - 10\gamma^2(2m^2k_P^2 + c_0^2c_q^2)\right)|\dot{\boldsymbol{e}}|^2 \\ & -\frac{1}{2}\left(k(k_P^2 - 2k_I) - 10\gamma^2m^2k_I^2\right)|\boldsymbol{e}|^2 \\ & -\frac{1}{2}kk_I^2\left|\int \boldsymbol{e}\right|^2 \\ & -\frac{1}{2}\left(k - 10\gamma^2c_0^2c_q^2\right)|\boldsymbol{s}|^2 \\ & +15\gamma^2m^2|\ddot{\boldsymbol{q}}_d|^2 \\ & +15\gamma^2c_0^2c_q^2|\dot{\boldsymbol{q}}_d|^2 \\ & +15\gamma^2|\boldsymbol{d}|^2. \end{aligned} \tag{3.36}$$

Hence, we can mention that it is the reference and external disturbance input$(\dot{\boldsymbol{q}}_d, \ddot{\boldsymbol{q}}_d, \boldsymbol{d})$-to-state$(\boldsymbol{e}, \dot{\boldsymbol{e}}, \int \boldsymbol{e}, \boldsymbol{s})$ stable from (3.36), additionally.

3.4.2 Performance Estimation by Optimality

The optimal controller was obtained from the minimization for a performance index as proved in Theorem 4, hence, the performance index (3.17) can be rearranged using an inverse optimal PID control (3.25) as follows:

$$PI(t,\boldsymbol{x},\boldsymbol{w}) = \lim_{t\to\infty}\left[2V(\boldsymbol{x}(t),t) + \int_0^t \left(\boldsymbol{x}^T\left(\boldsymbol{Q} + \boldsymbol{PBR}^{-1}\boldsymbol{B}^T\boldsymbol{P}\right)\boldsymbol{x} - \gamma^2\boldsymbol{w}^T\boldsymbol{w}\right)d\sigma\right]. \tag{3.37}$$

As a matter of fact, the magnitude of performance index remains nearly unchanged when the controller obtained from optimization is used. Also, if the applied controller stabilizes the closed system, then the magnitude of extended disturbance is mainly affected by that of inverse dynamics $\boldsymbol{h}$ in (3.27) according to desired configurations, because the errors in (3.27) will be small. Also, since the extended disturbance will show nearly same magnitude for the same

desired configurations, the following term dependent on state vector remains also nearly unchanged in above performance index:

$$\int_0^t \boldsymbol{x}^T(\sigma)\left(\boldsymbol{Q}+\boldsymbol{PBR}^{-1}\boldsymbol{B}^T\boldsymbol{P}\right)\boldsymbol{x}(\sigma)d\sigma \approx a\ constant. \tag{3.38}$$

In above equation, the matrix can be defined and decomposed as follows:

$$\boldsymbol{Q}+\boldsymbol{PBR}^{-1}\boldsymbol{B}^T\boldsymbol{P} \triangleq \boldsymbol{K}_{PI}\boldsymbol{K}_\gamma\boldsymbol{K}_{PI}, \tag{3.39}$$

where

$$\boldsymbol{K}_{PI}=\begin{bmatrix} k_I\boldsymbol{I} & \boldsymbol{0} & \boldsymbol{0} \\ \boldsymbol{0} & k_P\boldsymbol{I} & \boldsymbol{0} \\ \boldsymbol{0} & \boldsymbol{0} & \boldsymbol{I} \end{bmatrix}$$

$$\boldsymbol{K}_\gamma=\begin{bmatrix} \left(k+\frac{\gamma^2}{k\gamma^2+1}\right)\boldsymbol{I} & \frac{\gamma^2}{k\gamma^2+1}\boldsymbol{I} & \frac{\gamma^2}{k\gamma^2+1}\boldsymbol{I} \\ \frac{\gamma^2}{k\gamma^2+1}\boldsymbol{I} & \left(k+\frac{\gamma^2}{k\gamma^2+1}-\frac{2k_Ik}{k_P^2}\right)\boldsymbol{I} & \frac{\gamma^2}{k\gamma^2+1}\boldsymbol{I} \\ \frac{\gamma^2}{k\gamma^2+1}\boldsymbol{I} & \frac{\gamma^2}{k\gamma^2+1}\boldsymbol{I} & \left(k+\frac{\gamma^2}{k\gamma^2+1}\right)\boldsymbol{I} \end{bmatrix}.$$

Since $k_P^2 > 2k_I$ by the second condition in Theorem 5, the mid matrix $\boldsymbol{K}_\gamma$ of (3.39) is hardly affected by gains k_P, k_I, but by gains k and γ. Therefore, for a constant k and γ, the following relation can be approximately obtained from (3.38):

$$\|\boldsymbol{K}_{PI}\boldsymbol{x}\| \approx\ a\ constant \rightarrow \|\boldsymbol{x}\| \propto \frac{1}{|\boldsymbol{K}_{PI}|}, \tag{3.40}$$

where $\|.\|$ means $\mathcal{L}_2$-norm. For example, if we increase the proportional gain k_P by two times, then the integral gain k_I should be increased by two times according to (3.35), also, the size of $\boldsymbol{K}_{PI}$ is increased approximately by two times. Therefore, the $\mathcal{L}_2$-norm performance of state vector is approximately reduced to a half according to (3.40).

3.4.3 Illustrative Example

To show the validity of performance estimation by optimality in previous section, we perform a simple simulation for pendulum system as shown in Fig. 3.1. Since Lagrangian equation of motion for pendulum system is described as follow:

$$ml^2\ddot{q}+mgl\sin(q)=\tau, \tag{3.41}$$

the trajectory tracking system model can be obtained as follow:

$$ml^2\dot{s}=w(t,e,\dot{e})+u,$$

by defining the extended disturbance and composite error as follows:

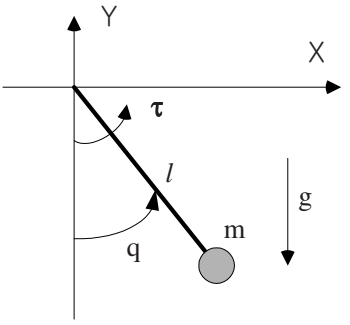

Fig. 3.1. Simple pendulum system

$$
\begin{aligned}
w(t, e, \dot{e}) &= ml^2(\ddot{q}_d + k_P\dot{e} + k_I e) + mgl\sin(q), \\
s &= \dot{e} + k_P e + k_I \int e dt \\
u &= -\tau.
\end{aligned}
$$

First, since the desired trajectory is determined as following fifth-order polynomial function:

$$
q_d(t) = \begin{cases} 5\pi t^3 - 7.5\pi t^4 + 3\pi t^5, & \text{for } 0 \le t \le 1 \\ 0.5\pi - 5\pi(t-1)^3 + 7.5\pi(t-1)^4 - 3\pi(t-1)^5, & \text{for } 1 \le t \le 2 \end{cases}
$$

the profiles for desired trajectory and its derivative are given smoothly as shown in Fig. 3.2. Second, the plant parameters and part of gains are deter-

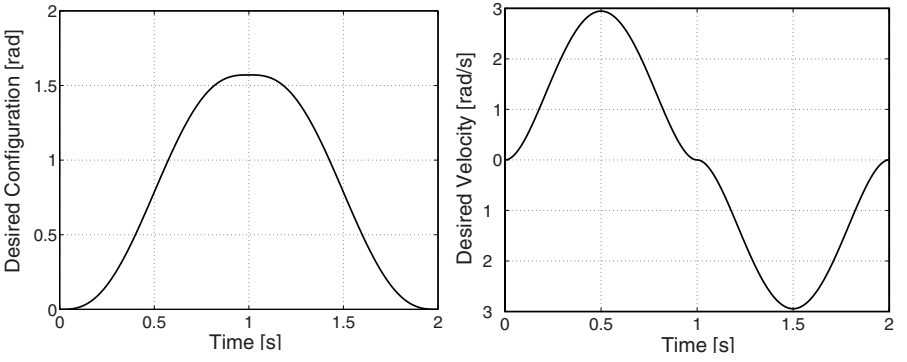

(a) Desired configuration : q_d (b) Desired velocity : $\dot{q}_d$

Fig. 3.2. Desired trajectory for pendulum system

mined as: $m = 1kg,\ l = 1m,\ g = 9.806m/s^2,\ k = 10,\ \gamma = 0.2$. Third, if the PID controller as following form is applied to above pendulum system (3.41):

$$\tau = \left(k + \frac{1}{\gamma^2}\right)\left(\dot{e} + k_P e + k_I \int e dt\right), \tag{3.42}$$

then simulation results are shown in Fig. 3.3 according to the changes of gains k_P and k_I. First of all, we should remember the tuning rule (3.35), in other words, the increment ratios of k_P and k_I should be identical each other. Therefore, if the increment ratio of gain k_P is one and half times, *e.g.*, $20 \rightarrow 30 \rightarrow 40$, then the gain k_I should be increased by one and half times like $100 \rightarrow 150 \rightarrow 200$.

Whenever k_P and k_I gains are increased by one and half times like $20|100 \rightarrow 30|150 \rightarrow 40|200$ for $k = 10$ and $\gamma = 0.2$ as shown in Table 3.1, the $\mathcal{L}_2$ norms of state vector are reduced to an approximate two thirds times (1/1.5) according to (3.40) because $|\boldsymbol{K}_{PI}|$ is increased by one and half times. The simulation results show that $\mathcal{L}_2$ norm of state vector is changed as $0.676 \rightarrow 0.471 \rightarrow 0.361$ as shown in Table 3.1. The maximum deviation between the real performance enhancement and the expected is 13% in Table 3.1. Also, even maximum configuration errors follow the rule (3.40) as shown in Fig. 3.3 and Table 3.2. The maximum deviation between the real performance enhancement for configuration error and the expected is 8.3% in Table 3.2. Additionally, experiment will be performed to show the validity of the performance estimation by optimality in section 4.4.2.

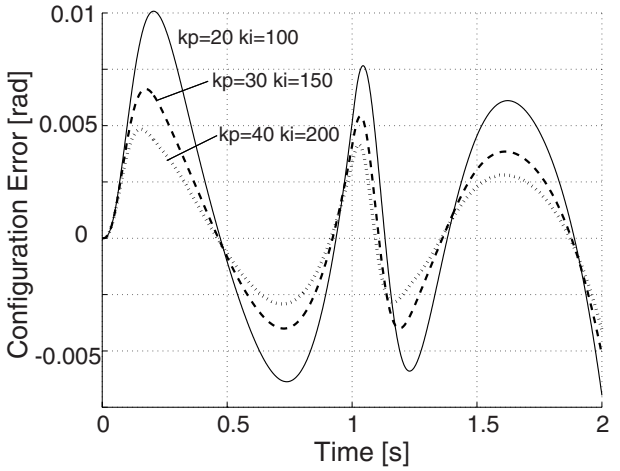

Fig. 3.3. Simulation results for pendulum system when $k = 10, \gamma = 0.2$

Table 3.1. The $\mathcal{L}_2$-norm of state vector for various k_P and k_I when $k = 10$ and $\gamma = 0.2$, where the subscript u or l means the corresponding value of either upper or lower data

$k_P \vert k_I$	$\Vert x\Vert$	$\Vert x\Vert_u / \Vert x\Vert_l$	Expected
20|100	0.0676	1.435	1.5
30|150	0.0471	1.305	1.5
40|200	0.0361		

Table 3.2. The maximum configuration error for various k_P and k_I when $k = 10$ and $\gamma = 0.2$, where data were obtained from Fig. 3.3

$k_P \vert k_I$	$\Vert e\Vert_\infty$	$\Vert e\Vert_{\infty,u} / \Vert e\Vert_{\infty,l}$	Expected
20|100	0.0101	1.530	1.5
30|150	0.0066	1.375	1.5
40|200	0.0048		

3.5 Summary

This chapter suggested an inverse optimal PID control to track trajectories in Lagrangian systems. The inverse optimal PID controller exists if and only if the Lagrangian system is extended disturbance input-to-state stable. First, we found the Lyapunov function and the control law that satisfy the extended disturbance input-to-state stability (ISS) by using the characteristics of the Lagrangian system. Fortunately, the control law has a PID control form and satisfies the Hamilton-Jacobi-Isaacs (HJI) equation. Hence, the $\mathcal{H}_\infty$ inverse optimality of the closed-loop system dynamics was acquired through the PID controller if several conditions for the control law could be satisfied.

4

Performance Limitation and Tuning

4.1 Introduction

Most mechanical systems are described by Lagrangian equation of motion and their controllers consist of the conventional PID one. In the previous chapter and [10, 14], the inverse $\mathcal{H}_\infty$ optimality of PID control was proved for mechanical control systems, inspired by the extended disturbance input-to-state stability(ISS) of PID control under some conditions for gains. Also, it was proved that an inverse optimal PID controller exists if and only if the mechanical control system is extended disturbance input-to-state stable(ISS). However, an inverse optimal PID controller brings the performance limitation for trajectory tracking mechanical systems. In this chapter, we derive several performance tuning methods of an inverse optimal PID control from its performance limitation.

There have been many PID gain tuning methods. For the first time, the PID gain tuning method was suggested by Ziegler and Nichols in [68] based on the response characteristics of control system. Second, the PID gain tuning methods using the relay feedback were proposed for process control systems in [3, 66]. Third, it was shown in [40] that the PID gain tuning using Taguchi method developed for process control systems could be also applied to mechanical systems. Fourth, PID tuning guidelines for robot manipulators were suggested in [31, 51], however, most existing performance tuning methods are for just actuators in mechanical system, not for mechanical system itself. In this chapter, we propose a performance tuning method of an inverse optimal PID controller for mechanical control systems.

This chapter is organized as follows. First, square/linear performance tuning laws are proposed in section 4.2. Second, compound performance tuning method unifying square and linear tuning laws is suggested in section 4.3. Finally, experimental results show the validity of suggested performance tuning laws in section 4.4.

Y. Choi, W.K. Chung: PID Trajectory Tracking Control for Mechanical Systems, LNCIS 298, pp. 47–70, 2004.

4.2 Square and Linear Performance Tunings

In this section, we are to derive simple tuning rules from the performance limitation of an inverse optimal PID controller for trajectory tracking mechanical systems. First of all, an inverse optimal PID controller has the following form:

$$\boldsymbol{\tau} = \left(\boldsymbol{K} + \frac{1}{\gamma^2}\boldsymbol{I}\right)\left(\dot{\boldsymbol{e}} + \boldsymbol{K}_P\boldsymbol{e} + \boldsymbol{K}_I\int \boldsymbol{e}dt\right), \tag{4.1}$$

and its design conditions are as follows:

(C1) $\boldsymbol{K}, \boldsymbol{K}_P, \boldsymbol{K}_I > \boldsymbol{0}$, constant diagonal matrices
(C2) $\boldsymbol{K}_P^2 > 2\boldsymbol{K}_I$,
(C3) $\mathcal{L}_2$-gain $\gamma > 0$.

From now on, we will omit terms 'inverse optimal' in an inverse optimal PID controller. If a PID controller (4.1) is applied to trajectory tracking mechanical system (3.5) as shown in Theorem 5, then the closed-loop has the following form:

$$\dot{V} \leq -\frac{1}{2}\boldsymbol{x}^T\left(\boldsymbol{Q} + \boldsymbol{PBKB}^T\boldsymbol{P}\right)\boldsymbol{x} + \gamma^2|\boldsymbol{w}|^2. \tag{4.2}$$

To find very simple performance tuning rules: 'square' and 'linear' laws, first of all, the performance limitation is suggested using above equation (4.2) and extended disturbance in following section.

4.2.1 Performance Limitation for State Vector

The extended disturbance of (3.2) can be expressed as a function of time and state vector as following form:

$$\boldsymbol{w}(\boldsymbol{x}, t) = \boldsymbol{H}(\boldsymbol{x}, t)\boldsymbol{x} + \boldsymbol{h}(\boldsymbol{x}, t) \tag{4.3}$$

where

$$\begin{aligned}\boldsymbol{H}(\boldsymbol{x}, t) &= [\ \boldsymbol{CK}_I\ ,\ \boldsymbol{MK}_I + \boldsymbol{CK}_P\ ,\ \boldsymbol{MK}_P\ ]\\ \boldsymbol{h}(\boldsymbol{x}, t) &= \boldsymbol{M}\ddot{\boldsymbol{q}}_d + \boldsymbol{C}\dot{\boldsymbol{q}}_d + \boldsymbol{g} + \boldsymbol{d}.\end{aligned}$$

Now, consider the Euclidian norm of extended disturbance of (4.3). Then we get the insight such that the extended disturbance can be bounded by the function of Euclidian norm of a state vector under the following two assumptions:

(A1) : the configuration derivative $\dot{\boldsymbol{q}}$ is bounded
(A2) : the external disturbance $\boldsymbol{d}(t)$ is bounded.

The first assumption is not a hard condition to be satisfied if the applied controller can stabilize the system. Also, we think that the second assumption is a minimal information for the unknown external disturbance. By the

bounds of $\dot{\boldsymbol{q}}$, the Coriolis and centrifugal matrix $\boldsymbol{C}(\boldsymbol{q}, \dot{\boldsymbol{q}})$ can be bounded, *e.g.*, $|\boldsymbol{C}(\boldsymbol{q}, \dot{\boldsymbol{q}})| \leq c_0|\dot{\boldsymbol{q}}|$ with a positive constant c_0. Additionally, we know that the gravitational torque $\boldsymbol{g}(\boldsymbol{q})$ is bounded if the system stays at the earth, and the Inertia matrix $\boldsymbol{M}(\boldsymbol{q})$ is bounded by its own maximum eigenvalue m, *e.g.*, $|\boldsymbol{M}(\boldsymbol{q})| \leq m$. Also, the desired configurations $(\boldsymbol{q}_d, \dot{\boldsymbol{q}}_d, \ddot{\boldsymbol{q}}_d)$ are specified as the bounded values. Therefore, we can derive the following relationship from above assumptions:

$$\begin{aligned} |\boldsymbol{w}|^2 &= \boldsymbol{x}^T(\boldsymbol{H}^T\boldsymbol{H})\boldsymbol{x} + 2(\boldsymbol{h}^T\boldsymbol{H})\boldsymbol{x} + (\boldsymbol{h}^T\boldsymbol{h}) \\ &\leq c_1|\boldsymbol{x}|^2 + c_2|\boldsymbol{x}| + c_3 \end{aligned} \tag{4.4}$$

where c_1, c_2 and c_3 are some positive constants. Under above assumptions, we know that the Euclidian norm of an extended disturbance can be upper bounded by the function of that of a state vector, conversely, the Euclidian norm of a state vector can be lower bounded by the inverse function of that of an extended disturbance:

$$|\boldsymbol{w}| \leq \rho_o^{-1}(|\boldsymbol{x}|) \quad \leftrightarrows \quad \rho_o(|\boldsymbol{w}|) \leq |\boldsymbol{x}|,$$

where $\rho_o(|\boldsymbol{w}|) = 0$ for $0 \leq |\boldsymbol{w}| \leq \sqrt{c_3}$ because when $0 \leq |\boldsymbol{w}| \leq \sqrt{c_3}$, necessarily $\boldsymbol{x} = \boldsymbol{0}$. Also, the constant c_3 of (4.4) can not be zero either in the case of a trajectory tracking control or in the presence of the external disturbances and the gravitational torques. Though the function ρ_o must be a continuous, unbounded and increasing function, ρ_o is not a class $\mathcal{K}_\infty$ function because it is not strictly increasing as shown in Fig. 4.1.

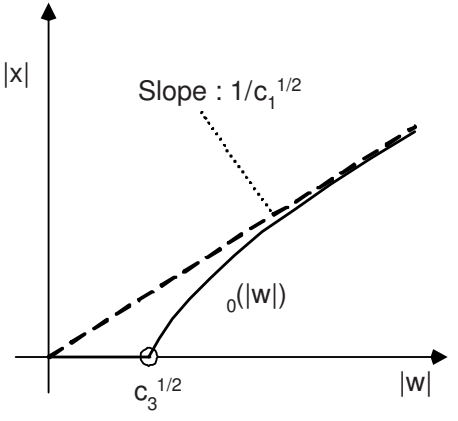

Fig. 4.1. Function $\rho_o(|\boldsymbol{w}|)$

On the other hand, if there exist no external disturbances ($\boldsymbol{d}(t) = \boldsymbol{0}$) and the gravity torques ($\boldsymbol{g}(\boldsymbol{q}) = \boldsymbol{0}$), then the GAS can be proved for the set-point

regulation control ($\ddot{\boldsymbol{q}}_d = \boldsymbol{0}, \dot{\boldsymbol{q}}_d = \boldsymbol{0}$) because $c_2 = 0, c_3 = 0$ and the function ρ_o becomes a class $\mathcal{K}_\infty$. For the first time, the GAS of the set-point regulation PD/PID controller was proved for mechanical systems by [2, 60]. However, either in the trajectory tracking or in the existence of external disturbance, the static PID controller can not ensure the GAS without using a dynamic model compensator. This fact brings a performance limitation of the PID controller.

The control performance is determined by the gain values of a controller. Hence, it is important to perceive the relation between the gain values and the errors. This relationship can be found by examining the point that the time derivative of Lyapunov function is equal to zero. The following Theorem suggests a mathematical expression for the performance limitation measure.

Theorem 7. *Let* $\boldsymbol{K} = k\boldsymbol{I}, \boldsymbol{K}_P = k_P\boldsymbol{I}$ *and* $\boldsymbol{K}_I = k_I\boldsymbol{I} \in \Re^{n\times n}$. *Suppose that* λ_{min} *is the minimum eigenvalue of following matrix*

$$\boldsymbol{Q}_K = \boldsymbol{Q} + \boldsymbol{P}\boldsymbol{B}\boldsymbol{K}\boldsymbol{B}^T\boldsymbol{P}, \tag{4.5}$$

and that the performance limitation $|\boldsymbol{x}|_{P.L}$ *is defined as the Euclidian norm of a state vector that satisfies* $\dot{V} = 0$. *If a PID controller in Theorem 5 is applied to the Lagrangian system of (3.5) and* λ_{min} *is chosen sufficiently large and* γ *sufficiently small in order that* $\lambda_{min} - 2\gamma^2 c_1 > 0$ *is satisfied, then its performance limitation is upper bounded by*

$$|\boldsymbol{x}|_{P.L} \leq \left(\frac{\gamma^2}{\lambda_\gamma}\right)\left[c_2 + \sqrt{c_2^2 + 2c_3\left(\frac{\lambda_\gamma}{\gamma^2}\right)}\right] \tag{4.6}$$

where c_1, c_2, c_3 *are coefficients for the upper bound of extended disturbance (4.4),* $\lambda_\gamma = \lambda_{min} - 2\gamma^2 c_1$ *and the minimum eigenvalue of* $\boldsymbol{Q}_K$ *is determined by*

$$\lambda_{min} \geq \min\left\{k, (k_P^2 - 2k_I)k, k_I^2 k\right\}. \tag{4.7}$$

This equation (4.6) can be regarded as the performance prediction equation which can predict the performance of the closed-loop system as gain changes.

Proof. First, we examine the point that the time derivative of Lyapunov function (3.26) stays at zero:

$$\begin{aligned}\dot{V}(\boldsymbol{x}, t) &\leq -\frac{1}{2}\boldsymbol{x}^T\boldsymbol{Q}_K\boldsymbol{x} + \gamma^2|\boldsymbol{w}|^2 \\ &\leq -\frac{1}{2}\lambda_\gamma|\boldsymbol{x}|^2 + c_2\gamma^2|\boldsymbol{x}| + c_3\gamma^2. \end{aligned}\tag{4.8}$$

where $\lambda_\gamma = \lambda_{min} - 2\gamma^2 c_1$ and the state vector can not be further reduced at the point satisfying $\dot{V} = 0$. By definition of the performance limitation, the inequality (4.8) brings the performance limitation of (4.6). Second, let us consider the minimum eigenvalue λ_{min} of the matrix $\boldsymbol{Q}_K$:

$$\begin{aligned}\boldsymbol{Q}_K &= \begin{bmatrix} kk_I^2\boldsymbol{I} & 0 & 0 \\ 0 & k(k_P^2-2k_I)\boldsymbol{I} & 0 \\ 0 & 0 & k\boldsymbol{I} \end{bmatrix} + k \begin{bmatrix} k_I\boldsymbol{I} \\ k_P\boldsymbol{I} \\ \boldsymbol{I} \end{bmatrix} [k_I\boldsymbol{I}, k_P\boldsymbol{I}, \boldsymbol{I}] \\ &= \boldsymbol{Q} + k\boldsymbol{Z}\boldsymbol{Z}^T\end{aligned}$$

where $\boldsymbol{Q}$ is the diagonal positive definite matrix and $\boldsymbol{Z}\boldsymbol{Z}^T$ is a symmetric positive semi-definite matrix. Therefore, the following inequality is always satisfied by Weyl's Theorem in [22, 27]

$$\lambda_{min}(\boldsymbol{Q}) + \lambda_{min}(k\boldsymbol{Z}\boldsymbol{Z}^T) \leq \lambda_{min} \triangleq \lambda_{min}(\boldsymbol{Q}_K). \tag{4.9}$$

Since $\lambda_{min}(k\boldsymbol{Z}\boldsymbol{Z}^T)$ is zero, the minimum eigenvalue of $\boldsymbol{Q}_K$ is not smaller than the minimum value among diagonal entries of $\boldsymbol{Q}$. □

Remark 5. If we choose k_P and k_I satisfying $k_P^2 - 2k_I > 1$ and $k_I > k_P > 1$ in Theorem 7, then the eigenvalues of $\boldsymbol{Q}_K$ (4.5) satisfy the following interlacing property:

$$k < \lambda_3 < (k_P^2 - 2k_I)k < \lambda_2 < k_I^2 k < \lambda_1, \tag{4.10}$$

where $\lambda_1, \lambda_2, \lambda_3$ are the block diagonal eigenvalues of $\boldsymbol{Q}_K$ with the descending order.

Proof. Although the $\boldsymbol{Q}_K$ has $3n$ eigenvalues, it is sufficient to show only 3 eigenvalues because it shares each n same eigenvalues. Let us define the reduced matrix for $\boldsymbol{Q}_K$ as following form:

$$\begin{aligned}\boldsymbol{D}_K &= \begin{bmatrix} kk_I^2 & 0 & 0 \\ 0 & k(k_P^2-2k_I) & 0 \\ 0 & 0 & k \end{bmatrix} + k \begin{bmatrix} k_I \\ k_P \\ 1 \end{bmatrix} [k_I, k_P, 1] \\ &= \boldsymbol{D} + k\boldsymbol{z}\boldsymbol{z}^T\end{aligned}$$

where $\boldsymbol{D}$ is the diagonal matrix with descending order. To begin with, we consider the eigenvalue computation

$$(\boldsymbol{D} + k\boldsymbol{z}\boldsymbol{z}^T)\boldsymbol{v} = \lambda\boldsymbol{v}, \qquad \boldsymbol{v} \neq \boldsymbol{0} \tag{4.11}$$

where $\boldsymbol{D}$ and $\boldsymbol{D}_K$ do not have common eigenvalues and $\boldsymbol{z}^T\boldsymbol{v} \neq 0$ because $\boldsymbol{z}$ has no zero components as explained in [22, 42]. Since $(\boldsymbol{D}-\lambda\boldsymbol{I})$ is nonsingular, if we apply $\boldsymbol{z}^T(\boldsymbol{D}-\lambda\boldsymbol{I})^{-1}$ to both sides of (4.11), then we obtain the following:

$$\boldsymbol{z}^T\boldsymbol{v}(1 + k\boldsymbol{z}^T(\boldsymbol{D} - \lambda\boldsymbol{I})^{-1}\boldsymbol{z}) = 0.$$

Since $\boldsymbol{z}^T\boldsymbol{v} \neq 0$, the following function should be zero:

$$\begin{aligned}f(\lambda) &= 1 + k\boldsymbol{z}^T(\boldsymbol{D} - \lambda\boldsymbol{I})^{-1}\boldsymbol{z} \\ &= 1 + k\left(\frac{k_I^2}{kk_I^2 - \lambda} + \frac{k_P^2}{k(k_P^2-2k_I) - \lambda} + \frac{1}{k-\lambda}\right) \\ &= 0.\end{aligned}$$

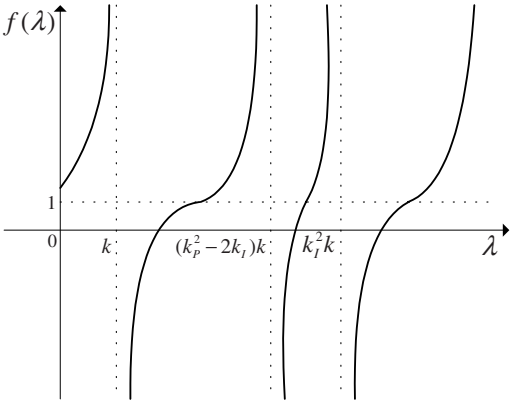

Fig. 4.2. Function $f(\lambda)$

If we obtain the differentiation of $f(\lambda)$, then we can know that $f'(\lambda) > 0$. Therefore, the function $f(\lambda)$ is monotone in between its poles as shown in Fig. 4.2. This allows us to conclude that $f(\lambda)$ has precisely 3 roots($\lambda_3 < \lambda_2 < \lambda_1$), one in each of the intervals

$$[k \sim (k_P^2 - 2k_I)k] < [(k_P^2 - 2k_I)k \sim k_I^2 k] < [k_I^2 k \sim \infty].$$

Therefore, it follows that the block diagonal eigenvalues of $\boldsymbol{Q}_K$ satisfy the interlacing property of (4.10). □

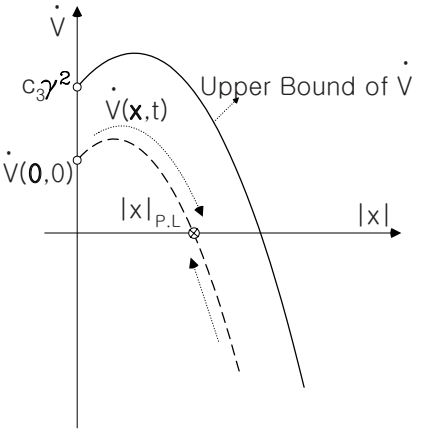

Fig. 4.3. Relation b/w $|\boldsymbol{x}|_{P.L}$ and the upper bound of $\dot{V}$

For the set-point regulation control, the value of Lyapunov function is large at the start time and it is gradually reduced to zero because the controller is designed so that the time derivative of Lyapunov function remains negative definite. On the other hand, for the trajectory tracking control, we start the simulation/experiment with zero error $\boldsymbol{x} = \mathbf{0}$ after adjusting initial conditions. The value of Lyapunov function is zero at the start time, however, the error increases to some extent because $\dot{V}(\mathbf{0}, 0)$ may have any positive constant smaller than $c_3\gamma^2$ as shown in Fig. 4.3. This figure depicts the upper bound of $\dot{V}$ vs. $|\boldsymbol{x}|$ of the equation (4.8). Since the performance limitation $|\boldsymbol{x}|_{P.L}$ upper bounded by the inequality (4.6) is the convergent point as we can see in Fig. 4.3, the Euclidian norm of a state vector tends to stay at this point. This analysis can naturally illustrate the performance tuning.

4.2.2 Square and Linear Rules

The PID gain tuning has been an important subject, however, it has not been much investigated till now. Recently, the noticeable tuning method was suggested as the name of "square law" in [48]. They showed that the square law is a good tuning method by their experiments for a industrial robot manipulator. Theoretically, we can confirm once more that the square law is a good tuning method by showing that the performance limitation of (4.6) can be written approximately as following form:

$$|\boldsymbol{x}|_{P.L} \propto \gamma^2,$$

where the square law means that the error is approximately reduced to the square times of the reduction ratio for γ values. Though the square law must be a good performance tuning method, it is not always exact or applicable. The exact performance tuning measure is the performance limitation of (4.6) in Theorem 7, however, the coefficients c_1, c_2, c_3 are unknowns. To develop an available and more exact tuning method, we rewrite the performance limitation (4.6) as follows:

$$\begin{aligned} |\boldsymbol{x}|_{P.L} &\leq \left(\frac{\gamma}{\sqrt{\lambda_\gamma}}\right)^2 \left[c_2 + \sqrt{c_2^2 + 2c_3\left(\frac{\sqrt{\lambda_\gamma}}{\gamma}\right)^2}\right] \\ &\leq \left(\frac{\gamma}{\sqrt{\lambda_\gamma}}\right)^2 \left[2c_2 + \sqrt{2c_3}\left(\frac{\sqrt{\lambda_\gamma}}{\gamma}\right)\right] \\ &= 2c_2\left(\frac{\gamma}{\sqrt{\lambda_\gamma}}\right)^2 + \sqrt{2c_3}\left(\frac{\gamma}{\sqrt{\lambda_\gamma}}\right) \end{aligned} \tag{4.12}$$

where $\lambda_\gamma = \lambda_{min} - 2\gamma^2 c_1$. Since the γ value can be chosen sufficiently small, we assume that $\lambda_\gamma \approx \lambda_{min}$. If the values of k_P and k_I satisfying $k_P^2 - 2k_I > 1$

and $k_I > k_P > 1$, then the value of λ_{min} is lower bounded by k as shown in Remark 5, *i.e.*, $\lambda_{min} \geq k$. By letting $\lambda_\gamma \approx k$ and defining the tuning variable as $(\gamma/\sqrt{k})$, the performance limitation of (4.12) can be expressed by the function of tuning variable $(\gamma/\sqrt{k})$ as following form:

$$|\boldsymbol{x}|_{P.L} \propto 2c_2 \left(\frac{\gamma}{\sqrt{k}}\right)^2 + \sqrt{2c_3}\left(\frac{\gamma}{\sqrt{k}}\right). \tag{4.13}$$

For a large tuning variable, since the second order term governs the inequality (4.13), the following square tuning law is approximately obtained from (4.13):

$$|\boldsymbol{x}|_{P.L} \propto \gamma^2, \quad \text{for a small } \sqrt{k}. \tag{4.14}$$

Also, if the tuning variable $(\gamma/\sqrt{k})$ is small, then we can perceive another linear tuning law:

$$|\boldsymbol{x}|_{P.L} \propto \gamma, \quad \text{for a large } \sqrt{k}, \tag{4.15}$$

because the first order term of (4.13) becomes dominant. Here, we propose two tuning methods; one is the coarse tuning which brings the square relation of (4.14) and the other is the fine tuning which brings the linear relation of (4.15). Roughly speaking, the coarse tuning is achieved for a small k value and the fine tuning for a large k. As a matter of fact, the criterion between small k and large k is dependent on coefficients c_1, c_2 and c_3, in other words, what k value can be a criterion for a given system should be determined through experiments/simulations.

4.2.3 Illustrative Example

To show the effectiveness of square and linear rules, we perform some simulations for pendulum system as shown in Fig. 3.1. The desired trajectory and plant parameters ($m = 1kg,\ l = 1m,\ g = 9.806m/s^2$) are determined identically with the example in section 3.4.3. Here, if the PID controller (3.42) using $k_P = 20$ and $k_I = 100$ is applied to pendulum system in Fig. 3.1, then the simulation results are obtained as shown in Fig. 4.4 according to the changes of γ when $k = 5$. The maximum values of Fig. 4.4.(a) are rearranged in Table 4.1. In figure and table, $|\boldsymbol{x}|$ and $\|\boldsymbol{x}\|_\infty$ mean Euclidean norm and $\mathcal{L}_\infty$ norm of state vector, respectively.

Whenever γ values are halved like $0.4 \rightarrow 0.2 \rightarrow 0.1$ for $k = 5$ as shown in Table 4.1, the maximum magnitude of state vector are reduced to an approximate quarter like $0.4606 \rightarrow 0.1456 \rightarrow 0.0312$. In Fig. 4.4 and Table 4.1, we can see that the control performances comply with the square tuning rule (4.14) for a relatively small $k = 5$. The maximum deviation between the real performance enhancement and expected one is 21% in Table 4.1. Also, the configuration errors comply well with the square tuning rule as shown in Fig. 4.4.(b) and Table 4.2. The maximum deviation is 20% in Table 4.2.

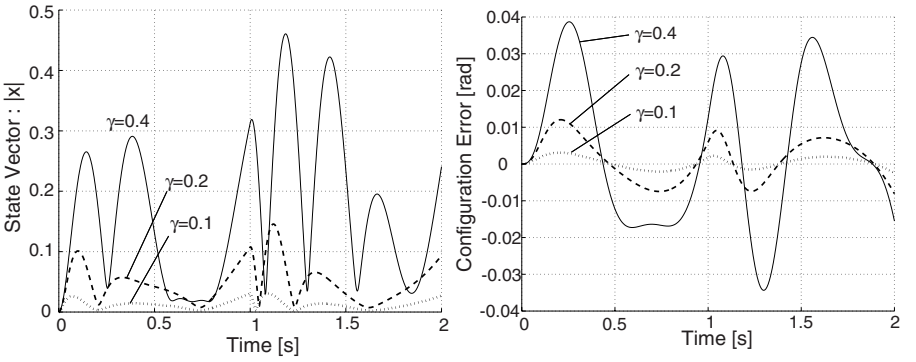

(a) State Vector : $|\boldsymbol{x}|$ (b) Configuration error : e

Fig. 4.4. Simulation results for pendulum system when $k = 5$

Table 4.1. The maximum magnitude of state vector for various γ when $k = 5$, where the subscript u or l means the corresponding value of either upper or lower data

γ	$\|x\|_\infty$	$\|x\|_{\infty,u}/\|x\|_{\infty,l}$	Expected, γ_u^2/γ_l^2
0.4	0.4606	3.163	4.0
0.2	0.1456	4.667	4.0
0.1	0.0312		

Table 4.2. The maximum configuration error for various γ when $k = 5$

γ	$\|e\|_\infty$	$\|e\|_{\infty,u}/\|e\|_{\infty,l}$	Expected, γ_u^2/γ_l^2
0.4	0.0387	3.198	4.0
0.2	0.0121	3.903	4.0
0.1	0.0031		

For a relatively large $k = 30$, the simulation brings the results of Fig. 4.5 and Table 4.3 and 4.4. Whenever γ values are halved like $0.4 \rightarrow 0.2 \rightarrow 0.1$ for $k = 30$ as shown in Table 4.3, the maximum magnitude of state vector are reduced to an approximate half like $0.1153 \rightarrow 0.0685 \rightarrow 0.0245$. In Fig. 4.5.(a) and Table 4.3, we can see that the control performances comply with the linear tuning rule (4.15) for a relatively large $k = 30$. The maximum deviation between the real performance enhancement and expected one is 40% in Table 4.3. Also, the configuration errors comply well with the linear tuning rule as shown in Fig. 4.5.(b) and Table 4.4. The maximum deviation is 22% in Table 4.4.

Though the square and linear tuning rules are very simple in applying them to mechanical systems, the deviation between the real performance enhancement and expected one by tuning rules is a little large. Also, the cri-

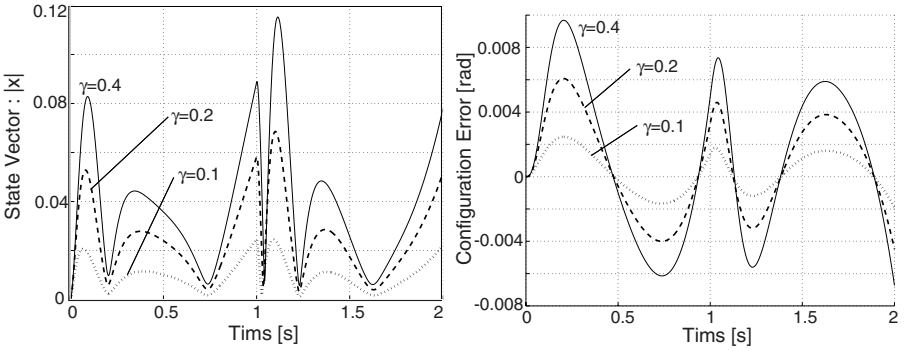

(a) State Vector : $|\boldsymbol{x}|$ (b) Configuration error : e

Fig. 4.5. Simulation results for pendulum system when $k = 30$

Table 4.3. The maximum magnitude of state vector for various γ when $k = 30$

γ	$\|x\|_\infty$	$\|x\|_{\infty,u}/\|x\|_{\infty,l}$	Expected, γ_u/γ_l
0.4	0.1153	1.683	2.0
0.2	0.0685	2.796	2.0
0.1	0.0245		

Table 4.4. The maximum configuration error for various γ when $k = 30$

γ	$\|e\|_\infty$	$\|e\|_{\infty,u}/\|e\|_{\infty,l}$	Expected, γ_u/γ_l
0.4	0.0097	1.590	2.0
0.2	0.0061	2.440	2.0
0.1	0.0025		

terion between small k and large k is unclear in applying either square or linear tuning rule because it depends on uncertain coefficients c_1, c_2 and c_3. In following section, more exact performance tuning rule is developed for a composite error, not for a state vector.

4.3 Compound Performance Tuning

In this section, we are to develop more exact tuning rule than the linear and square tuning rules suggested in previous sections, from the performance limitation imposed by applying a PID controller to Lagrangian systems. If the PID controller (4.1) is expressed by using a composite error vector, then the PID controller has the following compact form:

$$\boldsymbol{\tau} = \left(\boldsymbol{K} + \frac{1}{\gamma^2} \boldsymbol{I} \right) \boldsymbol{s}, \tag{4.16}$$

where three design conditions for (4.1) should be satisfied. To find a useful tuning rule for PID control systems, first of all, we are to obtain the performance limitation for a composite error in following section.

4.3.1 Performance Limitation for Composite Error

If above PID controller (4.16) is applied to the trajectory tracking system (3.3), then the composite error vector of closed-loop system is upper bounded by the extended disturbance as suggested in following Theorem. As a matter of fact, the bound of composite error in following Theorem means the performance limitation of PID controller for n-dimensional trajectory tracking system.

Theorem 8. *Let $\boldsymbol{s} = \dot{\boldsymbol{e}} + \boldsymbol{K}_P\boldsymbol{e} + \boldsymbol{K}_I \int \boldsymbol{e}dt \in \Re^n$. If the PID controller (4.16) is applied to the trajectory tracking system (3.3), then the composite error is upper bounded as following form:*

$$|\boldsymbol{s}(t)| \leq |\boldsymbol{s}(0)|e^{-\frac{k\gamma^2+0.5}{\lambda\gamma^2}t} + \frac{\gamma^2}{\sqrt{2k\gamma^2+1}}\|\boldsymbol{w}\|_\infty, \tag{4.17}$$

where $\boldsymbol{s}(0)$ is the initial composite error vector, λ is a maximum eigenvalue of Inertia matrix $\boldsymbol{M}$, and k is a minimum diagonal element of $\boldsymbol{K}$.

Proof. If the PID controller of (4.16) is applied to (3.3), then the closed-loop control system becomes as follows:

$$\boldsymbol{M}\dot{\boldsymbol{s}} + \boldsymbol{C}\boldsymbol{s} = \boldsymbol{w} - \left(\boldsymbol{K} + \frac{1}{\gamma^2}\boldsymbol{I}\right)\boldsymbol{s}. \tag{4.18}$$

Since above closed-loop system is also Lagrangian system, the characteristics of Lagrangian system can be used for above system. An useful characteristics is that the equality ($\dot{\boldsymbol{M}} = \boldsymbol{C}^T + \boldsymbol{C}$) is always satisfied. Now, let us differentiate the positive real-valued function $\left(\frac{1}{2}\boldsymbol{s}^T\boldsymbol{M}\boldsymbol{s}\right)$ along (4.18) as follows:

$$\begin{aligned}
\frac{d}{dt}\left(\frac{1}{2}\boldsymbol{s}^T\boldsymbol{M}\boldsymbol{s}\right) &= \frac{1}{2}\dot{\boldsymbol{s}}^T\boldsymbol{M}\boldsymbol{s} + \frac{1}{2}\boldsymbol{s}^T\dot{\boldsymbol{M}}\boldsymbol{s} + \frac{1}{2}\boldsymbol{s}^T\boldsymbol{M}\dot{\boldsymbol{s}}, \\
&= -\boldsymbol{s}^T\left(\boldsymbol{K} + \frac{1}{\gamma^2}\boldsymbol{I}\right)\boldsymbol{s} + \boldsymbol{s}^T\boldsymbol{w}, \qquad \text{by using } \dot{\boldsymbol{M}} = \boldsymbol{C} + \boldsymbol{C}^T \\
&= -\boldsymbol{s}^T\left(\boldsymbol{K} + \frac{1}{2\gamma^2}\boldsymbol{I}\right)\boldsymbol{s} - \frac{\gamma^2}{2}\left|\frac{1}{\gamma^2}\boldsymbol{s} - \boldsymbol{w}\right|^2 + \frac{\gamma^2}{2}|\boldsymbol{w}|^2, \\
&\leq -\boldsymbol{s}^T\left(\boldsymbol{K} + \frac{1}{2\gamma^2}\boldsymbol{I}\right)\boldsymbol{s} + \frac{\gamma^2}{2}|\boldsymbol{w}|^2.
\end{aligned}$$

Using the maximum eigenvalue of Inertia matrix $\boldsymbol{M}$ and the minimum diagonal element of gain matrix $\boldsymbol{K}$, above inequality can be simplified to:

$$\frac{d}{dt}\left(\frac{\lambda}{2}|\boldsymbol{s}|^2\right) \leq -\left(k+\frac{1}{2\gamma^2}\right)|\boldsymbol{s}|^2+\frac{\gamma^2}{2}|\boldsymbol{w}|^2.$$

If we multiply above inequality by $\boldsymbol{e}^{\frac{2k\gamma^2+1}{\lambda\gamma^2}t}$, then it becomes

$$\frac{d}{dt}\left(\lambda|\boldsymbol{s}|^2\boldsymbol{e}^{\frac{2k\gamma^2+1}{\lambda\gamma^2}t}\right) \leq \gamma^2|\boldsymbol{w}|^2\boldsymbol{e}^{\frac{2k\gamma^2+1}{\lambda\gamma^2}t}. \tag{4.19}$$

Integrating (4.19) over [0,t], we arrive at the following form:

$$\begin{aligned}
|\boldsymbol{s}(t)|^2 &\leq |\boldsymbol{s}(0)|^2\boldsymbol{e}^{-\frac{2k\gamma^2+1}{\lambda\gamma^2}t}+\frac{\gamma^2}{\lambda}\int_0^t \boldsymbol{e}^{-\frac{2k\gamma^2+1}{\lambda\gamma^2}(t-\tau)}|\boldsymbol{w}(\tau)|^2d\tau \\
&\leq |\boldsymbol{s}(0)|^2\boldsymbol{e}^{-\frac{2k\gamma^2+1}{\lambda\gamma^2}t}+\frac{\gamma^2}{\lambda}\sup_{\tau\in[0,t]}\left\{|\boldsymbol{w}(\tau)|^2\right\}\int_0^t \boldsymbol{e}^{-\frac{2k\gamma^2+1}{\lambda\gamma^2}(t-\tau)}d\tau \\
&= |\boldsymbol{s}(0)|^2\boldsymbol{e}^{-\frac{2k\gamma^2+1}{\lambda\gamma^2}t}+\frac{\gamma^2}{\lambda}\|\boldsymbol{w}\|_\infty^2\frac{\lambda\gamma^2}{2k\gamma^2+1}(\boldsymbol{e}^{-\frac{2k\gamma^2+1}{\lambda\gamma^2}t}-1).
\end{aligned}$$

By applying the property of $\sqrt{a^2+b^2} \leq |a|+|b|$ to right hand side of above inequality, an explicit upper bound of composite error vector is obtained as follow:

$$\begin{aligned}
|\boldsymbol{s}(t)| &\leq |\boldsymbol{s}(0)|\boldsymbol{e}^{-\frac{k\gamma^2+0.5}{\lambda\gamma^2}t}+\frac{\gamma^2}{\sqrt{2k\gamma^2+1}}\|\boldsymbol{w}\|_\infty\sqrt{(1-\boldsymbol{e}^{-\frac{2k\gamma^2+1}{\lambda\gamma^2}t})} \\
&\leq |\boldsymbol{s}(0)|\boldsymbol{e}^{-\frac{k\gamma^2+0.5}{\lambda\gamma^2}t}+\frac{\gamma^2}{\sqrt{2k\gamma^2+1}}\|\boldsymbol{w}\|_\infty.
\end{aligned}$$

□

The first term of right hand side of (4.17) is a class $\mathcal{KL}$ function because it is an increasing function for $|\boldsymbol{s}(0)|$ and decreasing one for time t. Also, the second term is a class $\mathcal{K}$ function since it is an increasing one for $\|\boldsymbol{w}\|_\infty$. Hence, the extended disturbance input-to-state stability (ISS) can be also proved from Theorem 8 because the upper bound (4.17) follows the ISS characteristics of (3.7). Though the exponential term of (4.17) goes to zero as $t \to \infty$, the composite error can not be zero because the extended disturbance of (3.2) includes the inverse dynamics according to desired configurations $(\boldsymbol{q}_d, \dot{\boldsymbol{q}}_d, \ddot{\boldsymbol{q}}_d)$ and gravity force $\boldsymbol{g}(\boldsymbol{q})$, moreover, $\boldsymbol{w} \neq \boldsymbol{0}$ as shown in following equation even when $\boldsymbol{e}=\boldsymbol{0}, \dot{\boldsymbol{e}}=\boldsymbol{0}, \int \boldsymbol{e}dt=\boldsymbol{0}$:

$$\begin{aligned}
\boldsymbol{w}(t,\dot{\boldsymbol{e}},\boldsymbol{e},\int \boldsymbol{e}dt) &= \boldsymbol{M}\ddot{\boldsymbol{q}}_d+\boldsymbol{C}\dot{\boldsymbol{q}}_d+\boldsymbol{g}+\boldsymbol{d} \\
&\quad +\boldsymbol{M}\boldsymbol{K}_P\dot{\boldsymbol{e}}+(\boldsymbol{M}\boldsymbol{K}_I+\boldsymbol{C}\boldsymbol{K}_P)\boldsymbol{e}+\boldsymbol{C}\boldsymbol{K}_I\int \boldsymbol{e}dt.
\end{aligned} \tag{4.20}$$

Also, the size of composite error is affected by the size of extended disturbance as shown in equation (4.17). As a matter of fact, the boundedness of (4.17)

expresses the performance limitation imposed by using a PID trajectory tracking controller. Although the PID trajectory tracking controller guarantees the extended disturbance input-to-state stability(ISS) for Lagrangian systems, it does not bring the globally asymptotic stability(GAS). This was proved for the first time in [14]. Also, the upper bound of composite error naturally suggests a new performance tuning rule.

4.3.2 Compound Rule

The performance tuning method can be perceived from the relation between gain and error. In the trajectory tracking control, since the initial composite error $\boldsymbol{s}(0)$ of (4.17) can be set to zero vector by the initialization of control system, the composite error can be bounded only by $\mathcal{L}_\infty$ norm of the extended disturbance as follows:

$$|\boldsymbol{s}(t)| \leq \frac{\gamma^2}{\sqrt{2k\gamma^2+1}}\|\boldsymbol{w}\|_\infty. \tag{4.21}$$

As a matter of fact, the boundedness of (4.21) includes the performance tuning law representing the relation between the composite error ($\boldsymbol{s}$) and gains (k, γ) of PID controller. If the PID controller stabilizes the trajectory tracking system, then error vectors will be smaller than desired configurations in the extended disturbance (4.20). Then, the extended disturbance shows almost same magnitude for same trajectory because it is largely affected by inverse dynamics according to desired configurations. Therefore, if the utilized PID controller can stabilize the system, then we can find the following proportional relation from (4.21):

$$|\boldsymbol{s}| \propto \frac{\gamma^2}{\sqrt{2k\gamma^2+1}}. \tag{4.22}$$

Above is the 'compound tuning rule' unifying both square and linear tuning rules suggested in previous sections. Also, this is a passive performance tuning method in that above tuning rule can be applied after we performed experiment once at least.

Remark 6. In previous sections, the square and linear tuning rules were proposed and proved through experiments. For a composite error, these square and linear tuning rules can be also found by approximating (4.22) according to the size of gain k as follows:

$$\begin{aligned} \text{Square Tuning} &: |\boldsymbol{s}| \propto \gamma^2, \text{ for a small } \quad k, \\ \text{Linear Tuning} &: |\boldsymbol{s}| \propto \gamma, \text{ for a large } \quad k. \end{aligned}$$

Although above rules are very useful in tuning the control performance, they can be utilized only by repetitive experiments for same trajectory because the tuning rules consist of proportional relations. Hence, these also correspond to passive performance tuning methods.

4.3.3 Illustrative Example

To show the validity of compound tuning rule, we implemented same simulations with the desired trajectory of Fig. 3.2 for a pendulum system as shown in Fig. 3.1. The simulation results were obtained as shown in Fig. 4.6 according to the change of γ when $k = 10$, $k_P = 20$ and $k_I = 100$. In that figure, we can see that the control performances comply with the compound tuning rule (4.22). For instance, the maximum values of composite errors in Fig. 4.6.(a) were rearranged in Table 4.5, here, the proportional constant determined by gains of (4.22) are calculated as 0.0781 for $\gamma = 0.4$ and 0.0298 for $\gamma = 0.2$, hence, the performance will be enhanced by 2.621 times since $(0.0781 \rightarrow 0.0298)$, in other words, the composite error will be reduced by 1/2.621 times. As we can see in Table. 4.5, the real composite errors comply well with the compound tuning rule. The maximum deviation between the real performance enhancement and expected one is 5.1% in Table 4.5. Since the configuration error has the proportional relation with the composite error, the configuration errors comply also well with the compound tuning rule as shown in Fig. 4.6.(b) and Table 4.6. The maximum deviation is 5.9% in Table 4.6 . The compound tuning rule brings smaller deviation than square and linear tuning rules in previous sections.

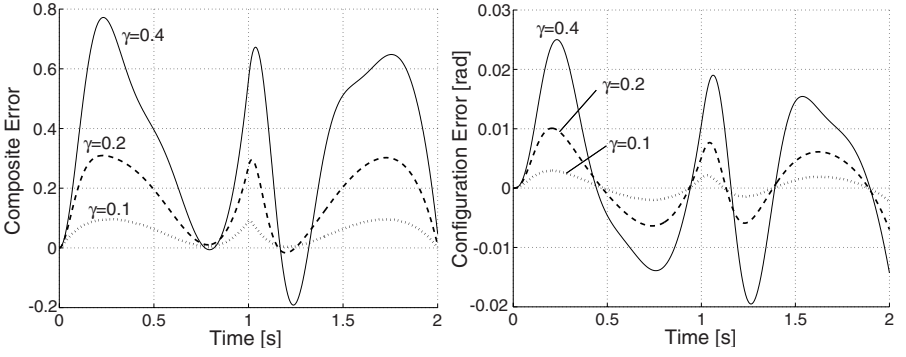

(a) Composite error : s (b) Configuration error : e

Fig. 4.6. Simulation results for pendulum system when $k = 10$

Another advantage of compound tuning rule is that it unifies both the square tuning rule and linear one explained in Remark 6 as one tuning rule. Though it must be a more exact tuning rule than the square and linear tuning rules, however, it loses the advantage of simplicity of square and linear rules as we can see in the compound rule (4.22).

Remark 7. Till now, we suggested three performance tuning rules: square rule, linear one and compound one. Since these can be applied after we perform the

Table 4.5. The maximum composite error for various γ when $k = 10$

γ	$\|s\|_\infty$	$\|s\|_{\infty,u}/\|s\|_{\infty,l}$	Expected, $\left(\frac{\gamma^2}{\sqrt{2k\gamma^2+1}}\right)_u / \left(\frac{\gamma^2}{\sqrt{2k\gamma^2+1}}\right)_l$
0.4	0.7720	2.495	2.621
0.2	0.3094	3.230	3.275
0.1	0.0958		

Table 4.6. The maximum configuration error for various γ when $k = 10$

γ	$\|e\|_\infty$	$\|e\|_{\infty,u}/\|e\|_{\infty,l}$	Expected, $\left(\frac{\gamma^2}{\sqrt{2k\gamma^2+1}}\right)_u / \left(\frac{\gamma^2}{\sqrt{2k\gamma^2+1}}\right)_l$
0.4	0.0250	2.475	2.621
0.2	0.0101	3.483	3.275
0.1	0.0029		

experiment at least once, however, these are all passive performance tuning methods. To overcome this disadvantage of passive tuning rule, we will devise an automatic performance tuning method in next chapter.

4.4 Experimental Results

To show the validity of optimality of PID control experimentally, we utilize the planar three link robot manipulator (POSTECH DDARM II in Fig. 4.7). This mechanical robot system interfaces with the 400MHz computer CPU via the interface boards such as the encoder counting S626 PCI board (S626 manufactured by Sensoray Co.) and D/A converting PCL726 ISA board (PCL726 manufactured by Advantech Co.). The RTLinux V2.2 is utilized as the real time operating system of a computer. We can raise the control frequency up to 5kHz thanks to RTLinux. And the desired trajectory consists of the fifth order polynomial functions of time so that the initial/final velocity and acceleration can be set to zero and the execution time is 5 seconds. The utilized inverse optimal PID controller has the following form:

$$\boldsymbol{\tau} = \left(k + \frac{1}{\gamma^2}\right)\left(\dot{\boldsymbol{e}} + k_P\boldsymbol{e} + k_I\int \boldsymbol{e}dt\right).$$

As proved in Theorem 4 and Remark 3, the controller is optimal for $\mathcal{H}_\infty$ performance index of (3.17) using

$$\boldsymbol{Q} = \begin{bmatrix} k_I^2 k\boldsymbol{I} & \boldsymbol{0} & \boldsymbol{0} \\ \boldsymbol{0} & (k_P^2 - 2k_I)k\boldsymbol{I} & \boldsymbol{0} \\ \boldsymbol{0} & \boldsymbol{0} & k\boldsymbol{I} \end{bmatrix}$$

$$\boldsymbol{R} = \left(k + \frac{1}{\gamma^2}\right)^{-1}\boldsymbol{I}.$$

First of all, the Euclidian norm and the $\mathcal{L}_2$ norm performances for the state vector $\boldsymbol{x}$ are evaluated, respectively. The Euclidian norm performance means the instant performance at time t and $\mathcal{L}_2$ norm performance represents the average performance for the total execution time.

Additionally, we inclined the planar robot in Fig. 4.7 about 10° to give the gravity effect. This mechanical manipulator is composed of three direct drive motors: the base motor has the 200[Nm] capability, the second one 55[Nm] and the third one 18[Nm]. To make use of the unified control scheme, we scaled up the applied torque according to the capacity of motor, *e.g.*, the scaling factor of base motor is 8.0, that of second one 3.0, that of third one 1.0. The desired trajectories are the fifth order polynomial functions of time so that the initial/final velocity and acceleration can be set to zeros. As shown in Fig. 4.7, they are composed of 3 forward line segments and 3 backward ones, also, the execution time per each line segment is 2 seconds and total one is 12 seconds.

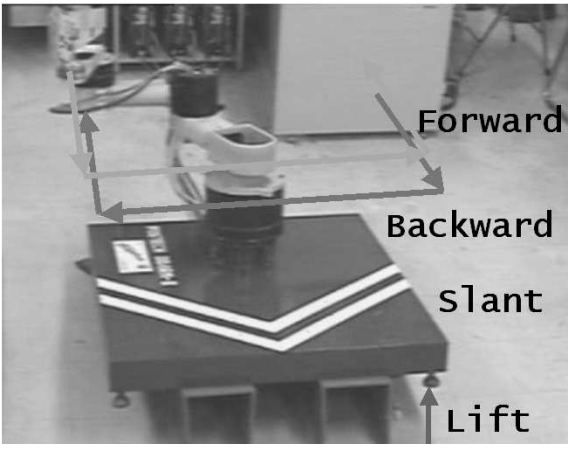

Fig. 4.7. Desired Trajectory of Robot Manipulator System

4.4.1 Experiment: Square and Linear Rules

At first, we determined initial gains $k_P = 20$ and $k_I = 100$ that satisfy conditions (C1) and (C2) of (4.1. After fixing $k = 0.05$ and $\gamma = 1.0$, we obtained the configuration error ($\boldsymbol{e}$) profile of Fig. 4.8.(a) and the applied torque ($\boldsymbol{\tau}$) profile of Fig. 4.8.(b). Also, we obtained Fig. 4.8.(c),(d) for $\gamma = 0.5$ and Fig. 4.8.(e),(f) for $\gamma = 0.25$. In Fig. 4.8, whenever the γ values are halved like $1.0 \rightarrow 0.5 \rightarrow 0.25$, the maximum range of y-axis expressing configuration errors are approximately reduced to a quarter like $0.4 \rightarrow 0.1 \rightarrow 0.02$. Hence, it complied with the "square(coarse) tuning rule" of (4.14). Second, we increased

the k value gradually and, at $k = 3$, Fig. 4.9 was obtained for the same condition. Whenever the γ values are halved for $k = 3$, the maximum range of y-axis expressing configuration errors are approximately reduced to a half like $0.1 \rightarrow 0.05 \rightarrow 0.015$. Hence, it corresponded to the "linear(fine) tuning rule". The torques were not changed much as we can see in Fig. 4.8 and 4.9.

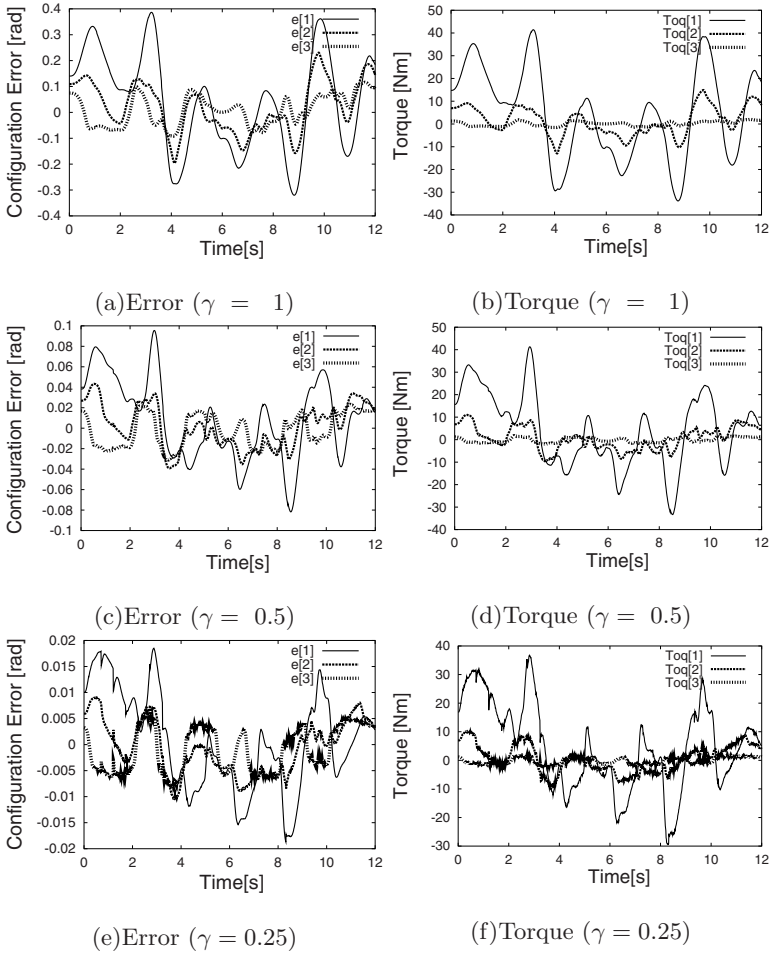

(a)Error ($\gamma = 1$) (b)Torque ($\gamma = 1$)

(c)Error ($\gamma = 0.5$) (d)Torque ($\gamma = 0.5$)

(e)Error ($\gamma = 0.25$) (f)Torque ($\gamma = 0.25$)

Fig. 4.8. The control performance for $k = 0.05$, $k_P = 20$ and $k_I = 100$ according to γ change : [square(coarse) tuning rule]

In above experiments, we showed the validity of tuning laws for fixed k_P and k_I. As a matter of fact, the change of gains k_P and k_I also affects on the performance of control system. To begin with, we should remember two proportional relations of (3.34) and (3.35). If the gain k_P is increased

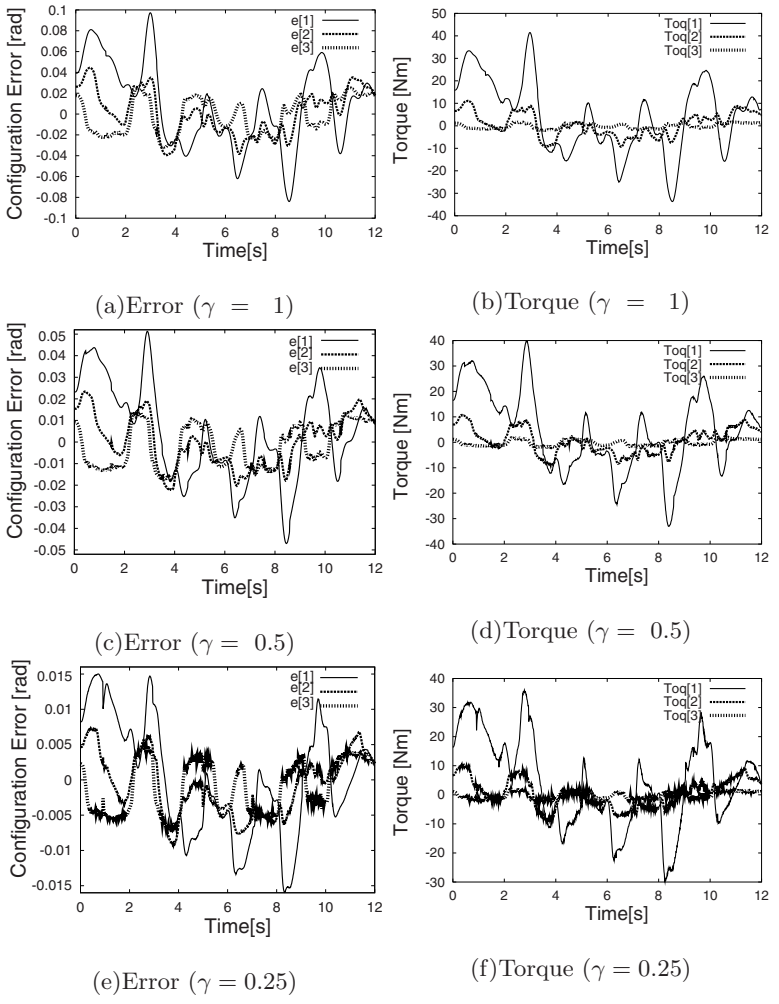

(a)Error ($\gamma = 1$) (b)Torque ($\gamma = 1$)

(c)Error ($\gamma = 0.5$) (d)Torque ($\gamma = 0.5$)

(e)Error ($\gamma = 0.25$) (f)Torque ($\gamma = 0.25$)

Fig. 4.9. The control performance for $k = 3$, $k_P = 20$ and $k_I = 100$ according to γ change : [linear(fine) tuning rule]

to one and half times ($k_P : 20 \rightarrow 30$), then the gain k_I should be increased by the same increment ratio ($k_I : 100 \rightarrow 150$) according to a proportional relation (3.35). Although we had changed gains to $k_P = 30$ and $k_I = 150$, the experimental results for $k = 0.05$ complied with the square tuning rule, *e.g.*, $0.25 \rightarrow 0.06 \rightarrow 0.015$ as shown in Fig. 4.10 and those of $k = 3$ complied with the linear tuning rule, *e.g.*, $0.06 \rightarrow 0.03 \rightarrow 0.01$ as shown in Fig. 4.11.

We showed through experiments that the maximum configuration errors complied with the square/linear tuning rules. However, it does not imply that the average control performances comply with the tuning rules. Now, we

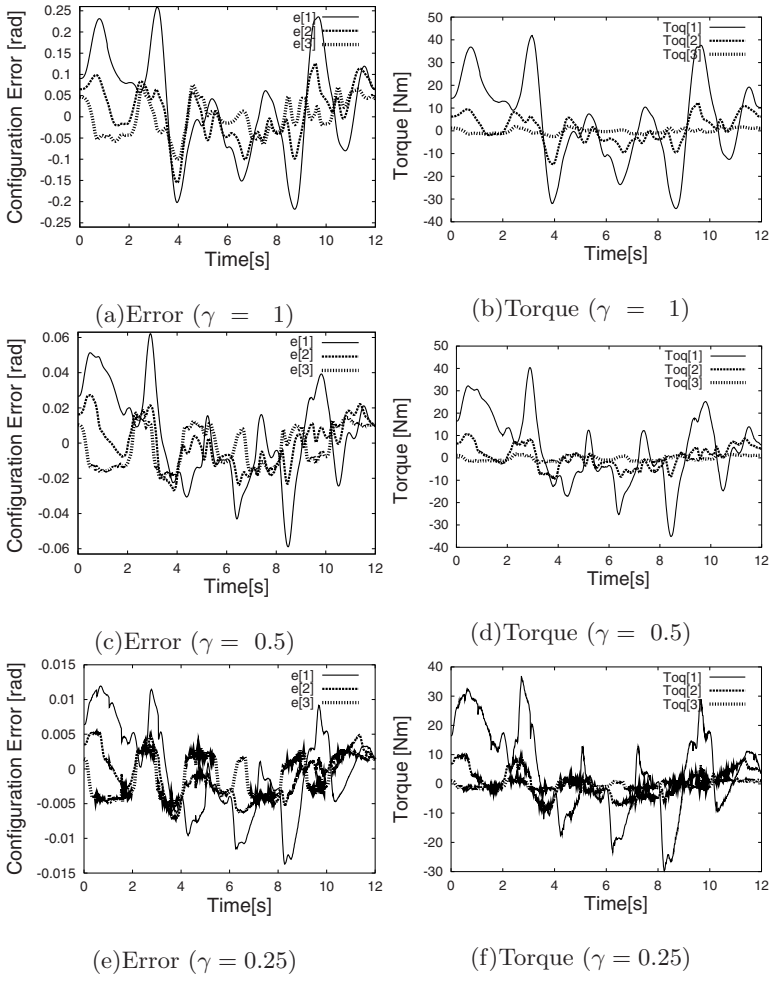

(a)Error ($\gamma = 1$) (b)Torque ($\gamma = 1$)

(c)Error ($\gamma = 0.5$) (d)Torque ($\gamma = 0.5$)

(e)Error ($\gamma = 0.25$) (f)Torque ($\gamma = 0.25$)

Fig. 4.10. The control performance for $k = 0.05$, $k_P = 30$ and $k_I = 150$ according to γ change : [square(coarse) tuning rule]

consider the $\mathcal{L}_2$ norm performance for a state vector. In Table 4.7, the $\mathcal{L}_2$ norm performances were evaluated by

$$\|\boldsymbol{x}\| = \sqrt{\int_0^{12} \left[\dot{\boldsymbol{e}}^T \dot{\boldsymbol{e}} + \boldsymbol{e}^T \boldsymbol{e} + \int \boldsymbol{e}^T \int \boldsymbol{e} \right] \, dt}.$$

The average performance for the $k = 0.05$ complied with the square tuning rule and for the $k = 3$ the linear one as shown in Table 4.7. For the $k_P = 20, k_I = 100$, the maximum deviation for the square/linear tuning rules between the experimental and the expected value was 22.5% in the upper

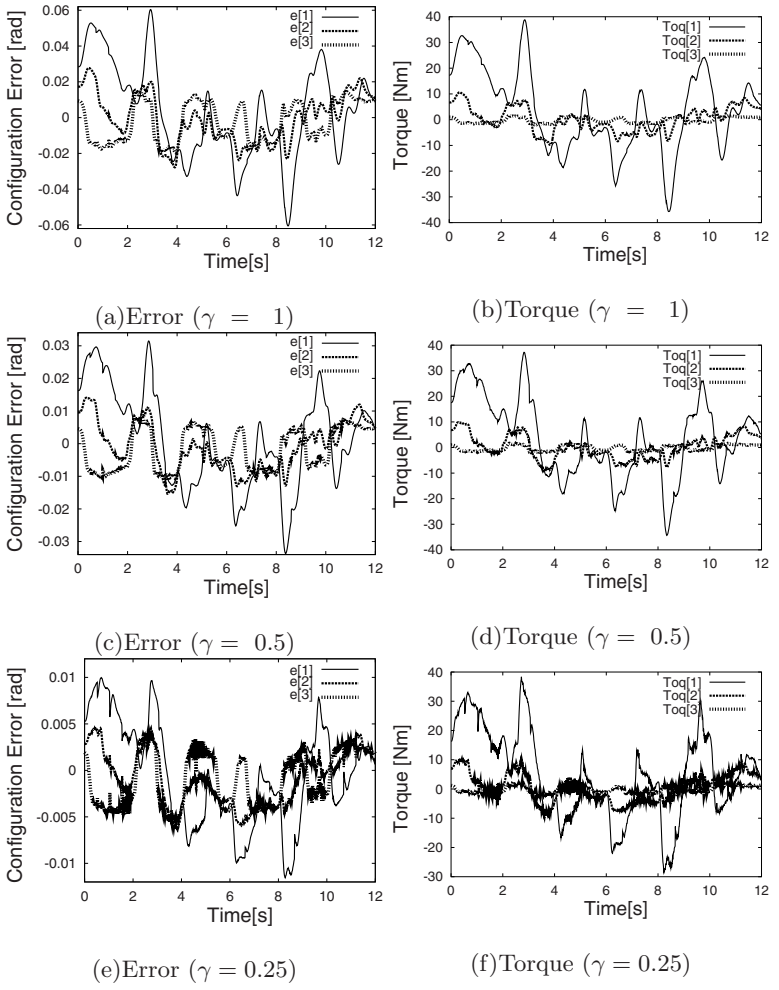

(a)Error ($\gamma = 1$) (b)Torque ($\gamma = 1$)

(c)Error ($\gamma = 0.5$) (d)Torque ($\gamma = 0.5$)

(e)Error ($\gamma = 0.25$) (f)Torque ($\gamma = 0.25$)

Fig. 4.11. The control performance for $k = 3$, $k_P = 30$ and $k_I = 150$ according to γ change : [linear(fine) tuning rule]

part of Table 4.7. Also, for $k_P = 30, k_I = 150$, the maximum deviation became 35.6% in the lower part of Table 4.7.

4.4.2 Experiment: Performance Estimation by Optimality

As shown in previous chapter, the performance change by the increment of k_P and k_I can be estimated by (3.40). For example, if we increase gains k_P and k_I by two times, then the magnitude of $\boldsymbol{K}_{PI}$ in (3.40) is increased approximately by two times. Therefore, the state vector $\boldsymbol{x}$ will be reduced to a

Table 4.7. The $\mathcal{L}_2$-norm performances for various γ and k, where Expected are calculated by either γ_u^2/γ_l^2 for $k = 0.05$ or γ_u/γ_l for $k = 3$, and the subscript u or l means the corresponding value of either upper or lower data

k_P/k_I	k	γ	$\|\boldsymbol{x}\|$	$\|\boldsymbol{x}\|_u/\|\boldsymbol{x}\|_l$	Expected
20/100	0.05	1	2.147	3.890 3.101	4.0
		0.5	0.552		
		0.25	0.178		
	3	1	0.562	1.698 2.006	2.0
		0.5	0.331		
		0.25	0.165		
30/150	0.05	1	1.545	3.796 2.576	4.0
		0.5	0.407		
		0.25	0.158		
	3	1	0.409	1.623 1.565	2.0
		0.5	0.252		
		0.25	0.161		

half, in other words, the control performance becomes better by two times. In our experiments, since the increment ratio was one and half times, we could see the performance enhancement by one and half times. Compare the Fig. 4.8 and 4.10, then the performances for the error were enhanced by one and half times, *e.g.*, $0.4 \to 0.25$ in (a), $0.1 \to 0.06$ in (c) and $0.02 \to 0.015$ in (e). Also, we could see the same performance enhancement in the Fig. 4.9 and 4.11. From these experimental results, we could confirm experimentally that a PID controller is optimal for the $\mathcal{H}_\infty$ performance index of (3.17). Finally, since the increment ratio was one and half times, the $\mathcal{L}_2$ norm performances were also enhanced approximately by one and half times as shown in Table 4.8. The maximum deviation between the experimental and expected data was 31.7%. Actually, when $k = 3$ and $\gamma = 0.25$ in Table 4.8, the performance enhancement is little because the third motor of robotic manipulator reaches the hardware limitation as we can see in Fig. 4.9.(e),(f) and 4.11.(e),(f).

4.4.3 Experiment: Compound Rule

Though the square and linear tuning rules must be good ones, they can not be applied to the intermediate value between $k = 0.05$ and $k = 3$. For instance, the experimental results in Fig. 4.12 and 4.13 obtained by using an intermediate $k = 1$ do not comply with either square or linear tuning rule, but the compound tuning rule (4.22).

As a matter of fact, the compound tuning rule can be also applied to experimental results obtained by using $k = 0.05$ and $k = 3$ in previous section. To show this, if we arrange the maximum value among configuration errors of 1st base motor $e[1]$ from experimental results of Fig. 4.8 – 4.13, then we can get Table 4.9. In that table, we can see that the compound tuning rule (4.22)

Table 4.8. $\mathcal{L}_2$-norm performance changes by increments of gains k_P and k_I

k	γ	k_P/k_I	$\|\boldsymbol{x}\|$	$\|\boldsymbol{x}\|_u/\|\boldsymbol{x}\|_l$	Expected
0.05	1	20/100	2.147	1.390	1.5
		30/150	1.545		
	0.5	20/100	0.522	1.283	
		30/150	0.407		
	0.25	20/100	0.178	1.127	
		30/150	0.158		
3	1	20/100	0.562	1.374	
		30/150	0.409		
	0.5	20/100	0.331	1.313	
		30/150	0.252		
	0.25	20/100	0.165	1.025	
		30/150	0.161		

performs well for entire experimental results, though it is somewhat difficult to calculate the expected value for performance enhancement in Table 4.9. The maximum deviation is 28.6%. Also, maximum values among configuration errors of 2nd motor $e[2]$ and 3rd motor $e[3]$ show similar tendency.

Table 4.9. The maximum configuration error $e[1]$ for various γ and k, where Expected is calculated by $\left(\frac{\gamma^2}{\sqrt{2k\gamma^2+1}}\right)_u / \left(\frac{\gamma^2}{\sqrt{2k\gamma^2+1}}\right)_l$

k_P/k_I	k	γ	$\|e[1]\|_\infty$	$\|e[1]\|_{\infty,u}/\|e[1]\|_{\infty,l}$	Expected
20/100	0.05	1	0.387	4.1	3.9
		0.5	0.095	5.0	4.0
		0.25	0.019		
	1	1	0.204	2.7	2.8
		0.5	0.076	4.5	3.5
		0.25	0.017		
	3	1	0.097	1.9	2.4
		0.5	0.051	3.2	3.0
		0.25	0.016		
30/150	0.05	1	0.260	4.2	3.9
		0.5	0.062	4.4	4.0
		0.25	0.014		
	1	1	0.131	2.7	2.8
		0.5	0.049	3.8	3.5
		0.25	0.013		
	3	1	0.061	1.8	2.4
		0.5	0.034	2.8	3.0
		0.25	0.012		

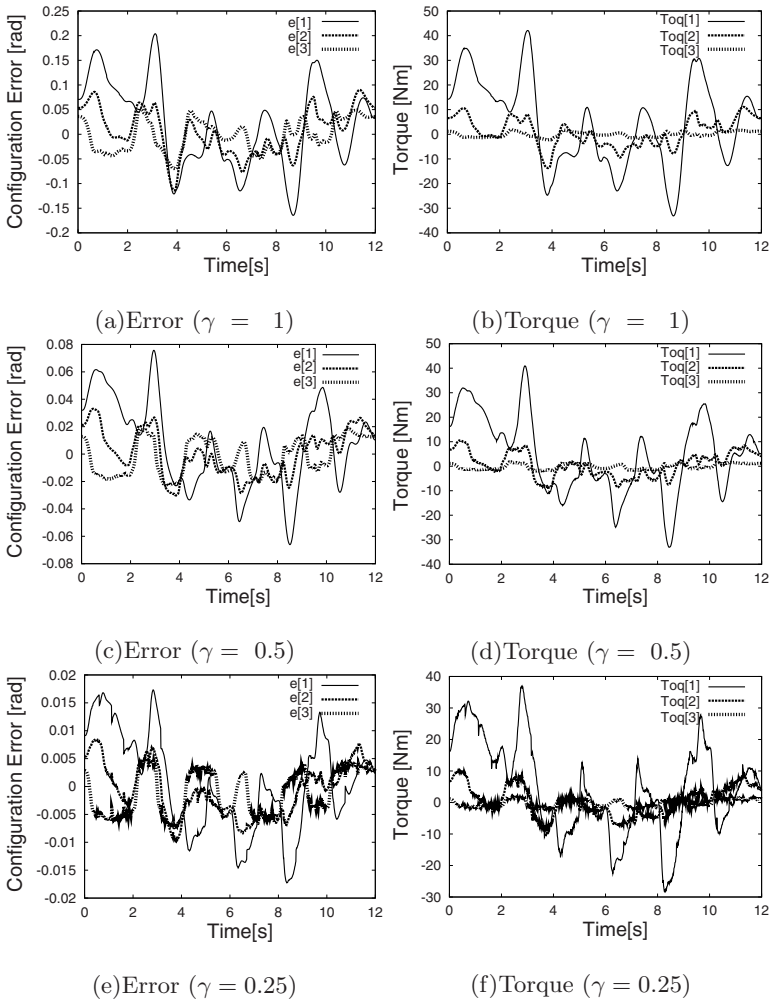

(a)Error ($\gamma = 1$) (b)Torque ($\gamma = 1$)

(c)Error ($\gamma = 0.5$) (d)Torque ($\gamma = 0.5$)

(e)Error ($\gamma = 0.25$) (f)Torque ($\gamma = 0.25$)

Fig. 4.12. The control performance for $k = 1$, $k_P = 20$ and $k_I = 100$ according to γ change : [compound tuning rule]

4.5 Summary

A performance analysis of the inverse optimal PID controller was provided in view of the performance limitation and tuning. The simple square/linear (coarse/fine) performance tuning rules were derived from the performance limitation for state vector. Also, the compound performance tuning rule was suggested as more exact tuning rule. Also, experimental results demonstrated the validity of three performance tuning laws.

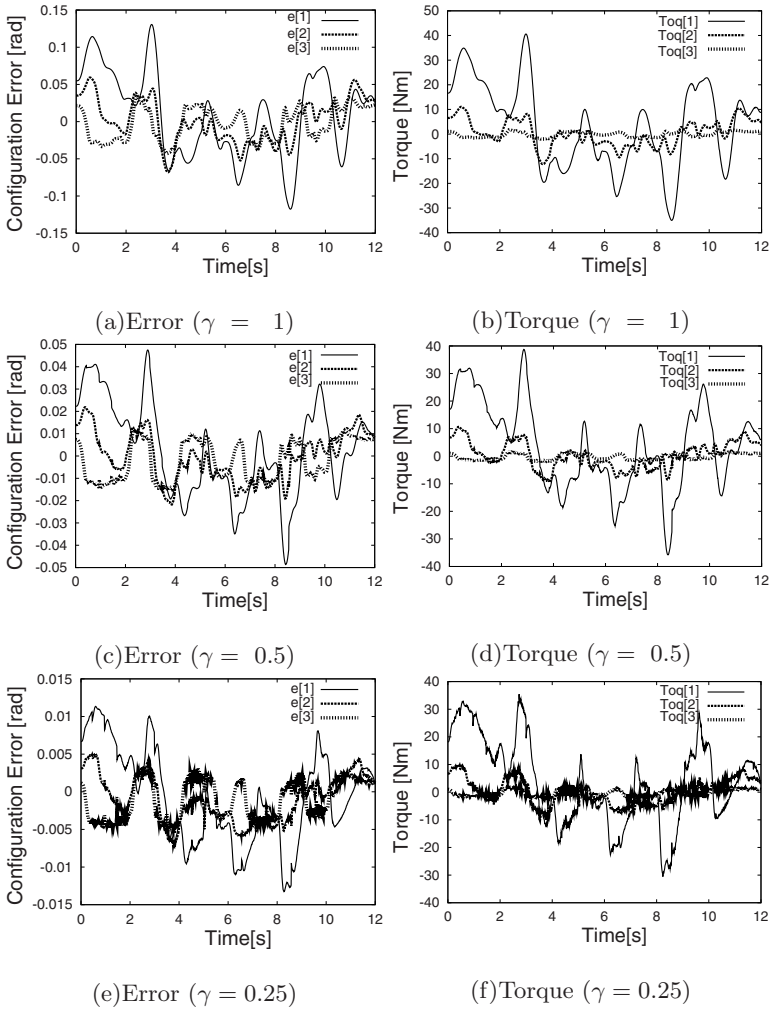

(a)Error ($\gamma = 1$) (b)Torque ($\gamma = 1$)

(c)Error ($\gamma = 0.5$) (d)Torque ($\gamma = 0.5$)

(e)Error ($\gamma = 0.25$) (f)Torque ($\gamma = 0.25$)

Fig. 4.13. The control performance for $k = 1$, $k_P = 30$ and $k_I = 150$ according to γ change : [compound tuning rule]

5

Automatic Performance Tuning

5.1 Introduction

The PID controller for mechanical systems has been widely used with various usages. In previous chapter 4 and [11, 13, 14], the noticeable 'square tuning' and 'linear tuning' rules have been proposed using an inverse optimal PID controller suggested in chapter 3. Also, the 'compound tuning' rule unifying both square tuning and linear rules has been proposed using the performance limitation expressed by composite error. However, these tuning methods are all passive in that the control performance can not be estimated or adjusted by tuning rules themselves, because they are composed of all proportional relations.

Many automatic performance tuning methods of PID controller were proposed in [3, 26, 66], however, they are all about the chemical process control systems. Since most process systems show very slow responses with time-delay effect, the auto-tuning algorithms developed for process control systems can not be directly applied to mechanical systems. Though the performance tuning by gain changes has brought one's interest with wide acceptance, there still exist no generally applicable auto-tuning laws of PID controller for mechanical systems. In this chapter, an automatic performance tuning method of a PID controller[1] will be proposed by making use of the direct adaptive control scheme, based on the extended disturbance input-to-state stability in chapter 3 and an analysis result of performance limitation in chapter 4.

Recently, the direct adaptive control scheme for nonlinear systems was developed in [9, 24, 25, 53]. Especially in [24], Haddad and Hayakawa suggested the direct adaptive control method with $\mathcal{L}_2$-gain disturbance attenuation for nonlinear systems. The direct adaptive control is different from the indirect adaptive control in that the control parameters are estimated directly without intermediate calculations involving plant parameter estimates. Strictly speak-

[1] In this chapter, the PID controller stands for an inverse optimal PID trajectory tracking controller suggested in chapter 3.

Y. Choi, W.K. Chung: PID Trajectory Tracking Control for Mechanical Systems, LNCIS 298, pp. 71–85, 2004.

ing, the conventional adaptive motion (trajectory tracking) control methods given in [16, 23, 30, 45, 55, 56] can be classified as the indirect adaptive control for mechanical system, especially a robotic manipulator, because the parameters of mechanical system are estimated to construct a dynamical model compensator. As far as we know, the direct adaptive control for nonlinear dynamical system similar to Lagrangian system was investigated for the first time in [9]. In a viewpoint of direct adaptive control, an auto-tuning law of PID controller will be proposed in this chapter.

This chapter is organized as follows: a quasi-equilibrium region is newly defined in section 5.2, an automatic performance tuning law of PID controller will be derived from the direct adaptive control scheme for trajectory tracking system in section 5.3, the performance enhancement obtained by using the model adaptation is optionally suggested in section 5.4 and experimental results to show the effectiveness of auto-tuning law are given in section 5.5.

5.2 Quasi-equilibrium Region

The state space representation for mechanical system, especially Lagrangian system, was given in previous section 3.2. For $3n$-dimensional state space description (3.5), the extended disturbance defined as (3.2) conceals a number of characteristics of trajectory tracking mechanical system. As a matter of fact, the extended disturbance $\boldsymbol{w}$ can be divided into the linear parameterization part and external disturbances as following form:

$$\boldsymbol{w}(\boldsymbol{x},t) = \boldsymbol{Y}(\boldsymbol{x},t)\boldsymbol{\theta} + \boldsymbol{d}(t), \tag{5.1}$$

where the regressor matrix $\boldsymbol{Y}(\boldsymbol{x},t)$ can be found by separating a real parameter vector $\boldsymbol{\theta}$ from

$$\boldsymbol{Y}(\boldsymbol{x},t)\boldsymbol{\theta} = \boldsymbol{M}(\boldsymbol{q})(\ddot{\boldsymbol{q}}_d + \boldsymbol{K}_P\dot{\boldsymbol{e}} + \boldsymbol{K}_I\boldsymbol{e}) + \boldsymbol{C}(\boldsymbol{q},\dot{\boldsymbol{q}})(\dot{\boldsymbol{q}}_d + \boldsymbol{K}_P\boldsymbol{e} + \boldsymbol{K}_I\int \boldsymbol{e}) + \boldsymbol{g}(\boldsymbol{q}),$$

and the real parameters consist of constant masses and moments of Inertia of each link, *etc.* Using the extended disturbance of (5.1), the state-space representation of (3.5) can be modified to

$$\dot{\boldsymbol{x}} = \boldsymbol{A}(\boldsymbol{x},t)\boldsymbol{x} + \boldsymbol{B}(\boldsymbol{x},t)\boldsymbol{Y}(\boldsymbol{x},t)\boldsymbol{\theta} + \boldsymbol{B}(\boldsymbol{x},t)\boldsymbol{d} + \boldsymbol{B}(\boldsymbol{x},t)\boldsymbol{u}, \tag{5.2}$$

where $\boldsymbol{\theta}$ is not an input vector, but a positive constant one obtained from Lagrangian system itself. Also, the regressor $\boldsymbol{Y}(\boldsymbol{x},t)$ is not a zero matrix at $\boldsymbol{x} = \boldsymbol{0}$ except the case of set-point regulation control and gravity free motion. In other words, if $\boldsymbol{g}(\boldsymbol{q}) \neq \boldsymbol{0}$ or $\ddot{\boldsymbol{q}}_d \neq \boldsymbol{0}, \dot{\boldsymbol{q}}_d \neq \boldsymbol{0}$, then $\boldsymbol{Y}(\boldsymbol{x},t) \neq \boldsymbol{0}$ at $\boldsymbol{x} = \boldsymbol{0}$. Hence, $\boldsymbol{x} = \boldsymbol{0}$ can not be an equilibrium point of (5.2) even when $\boldsymbol{d}(t) = \boldsymbol{0}$, because one term $\boldsymbol{B}(\boldsymbol{0},t)\boldsymbol{Y}(\boldsymbol{0},t)\boldsymbol{\theta}$ has the time-varying characteristics according to desired trajectories. Actually, since the equilibrium point can not be

found for system model (5.2), the concept of quasi-equilibrium region will be introduced in following section.

To begin with, we assume that there exist no external disturbances for system model (5.2), namely, $\boldsymbol{d} = \boldsymbol{0}$. If the PID controller (4.1) using $3n$-dimensional state vector as following form:

$$\boldsymbol{u} = -\left(\boldsymbol{K} + \gamma^{-2}\boldsymbol{I}\right)\left[\boldsymbol{K}_I, \boldsymbol{K}_P, \boldsymbol{I}\right]\boldsymbol{x}$$

is applied to (5.2), then the closed-loop control system is obtained as follows:

$$\dot{\boldsymbol{x}} = \boldsymbol{A}_c(\boldsymbol{x}, t)\boldsymbol{x} + \boldsymbol{B}(\boldsymbol{x}, t)\boldsymbol{Y}(\boldsymbol{x}, t)\boldsymbol{\theta} \tag{5.3}$$

where

$$\boldsymbol{A}_c = \boldsymbol{A} - \boldsymbol{B}\left(\boldsymbol{K} + \gamma^{-2}\boldsymbol{I}\right)\left[\boldsymbol{K}_I, \boldsymbol{K}_P, \boldsymbol{I}\right].$$

Since above closed-loop system has no equilibrium points as explained before, we will define the quasi-equilibrium region and find it for above closed-loop system in following Theorem.

Theorem 9. *If the quasi-equilibrium region is defined as the interior region of ball with the largest radius among state vectors satisfying* $\dot{\boldsymbol{x}} = \boldsymbol{0}$*, then it is obtained as following form:*

$$|\boldsymbol{x}| \leq \|\boldsymbol{x}_e\|_\infty = \sup_{0 \leq t \leq t_f} |\boldsymbol{x}_e(t)|,$$

where $\boldsymbol{x}_e(t)$ *means the state vector satisfying* $\dot{\boldsymbol{x}} = \boldsymbol{0}$ *in (5.3) and its Euclidian norm is as follows:*

$$|\boldsymbol{x}_e(t)| = \left|\boldsymbol{K}_I^{-1}\left[\boldsymbol{K} + \gamma^{-2}\boldsymbol{I}\right]^{-1}\boldsymbol{Y}_e(t)\boldsymbol{\theta}\right|, \tag{5.4}$$

and $\boldsymbol{Y}_e(t)\boldsymbol{\theta} = \boldsymbol{M}(\boldsymbol{q}_d)\ddot{\boldsymbol{q}}_d + \boldsymbol{C}(\boldsymbol{q}_d, \dot{\boldsymbol{q}}_d)\dot{\boldsymbol{q}}_d + \boldsymbol{g}(\boldsymbol{q}_d)$.

Proof. First, since $\dot{\boldsymbol{x}} = \boldsymbol{0}$ means $\dot{\boldsymbol{x}}_1 = \boldsymbol{x}_2 = \boldsymbol{e} = \boldsymbol{0}$ and $\dot{\boldsymbol{x}}_2 = \boldsymbol{x}_3 = \dot{\boldsymbol{e}} = \boldsymbol{0}$, we can easily know that

$$\boldsymbol{x}_e = \begin{bmatrix} \boldsymbol{x}_{e1} \\ \boldsymbol{x}_{e2} = \boldsymbol{0} \\ \boldsymbol{x}_{e3} = \boldsymbol{0} \end{bmatrix} \quad \rightarrow \quad |\boldsymbol{x}_e| = |\boldsymbol{x}_{e1}|$$

and $\boldsymbol{q} = \boldsymbol{q}_d$, $\dot{\boldsymbol{q}} = \dot{\boldsymbol{q}}_d$ from $\boldsymbol{e} = \dot{\boldsymbol{e}} = \boldsymbol{0}$. Second, to determine $\boldsymbol{x}_{e1}$, we should solve the following equation:

$$\boldsymbol{0} = \boldsymbol{A}_c(\boldsymbol{x}_e, t)\boldsymbol{x}_e + \boldsymbol{B}(\boldsymbol{x}_e, t)\boldsymbol{Y}(\boldsymbol{x}_e, t)\boldsymbol{\theta}. \tag{5.5}$$

Here, $\boldsymbol{A}_c$ has the following form:

$$
\begin{aligned}
\boldsymbol{A}_c(\boldsymbol{x}_e,t) &= \begin{bmatrix} \boldsymbol{0} & \boldsymbol{I} & \boldsymbol{0} \\ \boldsymbol{0} & \boldsymbol{0} & \boldsymbol{I} \\ \boldsymbol{A}_{c31} & \boldsymbol{A}_{c32} & \boldsymbol{A}_{c33} \end{bmatrix} \\
\boldsymbol{A}_{c31} &= -\boldsymbol{M}^{-1}(\boldsymbol{q}_d)\left[\boldsymbol{C}(\boldsymbol{q}_d,\dot{\boldsymbol{q}}_d)+\boldsymbol{K}+\gamma^{-2}\boldsymbol{I}\right]\boldsymbol{K}_I \\
\boldsymbol{A}_{c32} &= -\boldsymbol{M}^{-1}(\boldsymbol{q}_d)\left[\boldsymbol{C}(\boldsymbol{q}_d,\dot{\boldsymbol{q}}_d)+\boldsymbol{K}+\gamma^{-2}\boldsymbol{I}\right]\boldsymbol{K}_P-\boldsymbol{K}_I \\
\boldsymbol{A}_{c33} &= -\boldsymbol{M}^{-1}(\boldsymbol{q}_d)\left[\boldsymbol{C}(\boldsymbol{q}_d,\dot{\boldsymbol{q}}_d)+\boldsymbol{K}+\gamma^{-2}\boldsymbol{I}\right]-\boldsymbol{K}_P.
\end{aligned}
$$

Also, $\boldsymbol{B}(\boldsymbol{x}_e,t)$ and $\boldsymbol{Y}(\boldsymbol{x}_e,t)\boldsymbol{\theta}$ have the following forms:

$$
\begin{aligned}
\boldsymbol{B}(\boldsymbol{x}_e,t) &= \left[\boldsymbol{0},\boldsymbol{0},\boldsymbol{M}^{-1}(\boldsymbol{q}_d)\right]^T, \\
\boldsymbol{Y}(\boldsymbol{x}_e,t)\boldsymbol{\theta} &= \boldsymbol{M}(\boldsymbol{q}_d)\ddot{\boldsymbol{q}}_d+\boldsymbol{C}(\boldsymbol{q}_d,\dot{\boldsymbol{q}}_d)(\dot{\boldsymbol{q}}_d+\boldsymbol{K}_I\int \boldsymbol{e})+\boldsymbol{g}(\boldsymbol{q}_d) \\
&= \boldsymbol{Y}_e(t)\boldsymbol{\theta}+\boldsymbol{C}(\boldsymbol{q}_d,\dot{\boldsymbol{q}}_d)\boldsymbol{K}_I\boldsymbol{x}_{e1},
\end{aligned}
$$

where $\boldsymbol{Y}_e(t)\boldsymbol{\theta}$ is the inverse dynamics according to desired configurations $(\boldsymbol{q}_d,\dot{\boldsymbol{q}}_d,\ddot{\boldsymbol{q}}_d)$. Hence, above equation (5.5) can be simplified to the following form:

$$
\begin{aligned}
\boldsymbol{0} = &-\boldsymbol{M}^{-1}(\boldsymbol{q}_d)\left[\boldsymbol{C}(\boldsymbol{q}_d,\dot{\boldsymbol{q}}_d)+\boldsymbol{K}+\gamma^{-2}\boldsymbol{I}\right]\boldsymbol{K}_I\boldsymbol{x}_{e1} \\
&+\boldsymbol{M}^{-1}(\boldsymbol{q}_d)\left[\boldsymbol{Y}_e(t)\boldsymbol{\theta}+\boldsymbol{C}(\boldsymbol{q}_d,\dot{\boldsymbol{q}}_d)\boldsymbol{K}_I\boldsymbol{x}_{e1}\right],
\end{aligned}
$$

hence, $\boldsymbol{x}_{e1}$ is determined as follows:

$$
\boldsymbol{x}_{e1}(t) = \boldsymbol{K}_I^{-1}\left[\boldsymbol{K}+\gamma^{-2}\boldsymbol{I}\right]^{-1}\boldsymbol{Y}_e(t)\boldsymbol{\theta}.
$$

Finally, the quasi-equilibrium region is obtained by its definition as follows:

$$
|\boldsymbol{x}| \le \|\boldsymbol{x}_e\|_\infty = \sup_{0\le t\le t_f}|\boldsymbol{x}_e(t)|,
$$

where $|\boldsymbol{x}_e(t)| = \left|\boldsymbol{K}_I^{-1}\left[\boldsymbol{K}+\gamma^{-2}\boldsymbol{I}\right]^{-1}\boldsymbol{Y}_e(t)\boldsymbol{\theta}\right|$. □

The size of quasi-equilibrium region is inversely proportional to the integral gain $\boldsymbol{K}_I$ as we can see in an equation (5.4). Also, large $\boldsymbol{K}$ and small γ make the quasi-equilibrium region small. If we are to approach the quasi-equilibrium region to the point $\boldsymbol{x}_e = \boldsymbol{0}$ using PID controller, irrespective of the constant parameter vector $\boldsymbol{\theta}$ and desired configurations $(\boldsymbol{q}_d,\dot{\boldsymbol{q}}_d,\ddot{\boldsymbol{q}}_d)$, then one of three conditions should be satisfied: the one is that $\boldsymbol{K}_I$ gain matrix goes to infinity, another is that $\mathcal{L}_2$-gain γ to zero and the other is that the gain $\boldsymbol{K}$ to infinity. This explains indirectly the reason why the PID controller for trajectory tracking model of Lagrangian system can not bring the global asymptotic stability(GAS). In fact, the quasi-equilibrium region of Theorem 9 has very close relation with performance limitation of PID controller. Till now, the quasi-equilibrium region was obtained using $3n$-dimensional state vector in Theorem 9. Another expression for quasi-equilibrium region will be suggested using n-dimensional composite error in following Remark.

Remark 8. Let $\boldsymbol{s} = \dot{\boldsymbol{e}} + \boldsymbol{K}_P\boldsymbol{e} + \boldsymbol{K}_I \int \boldsymbol{e}dt$. If we multiply $[\boldsymbol{K}_I, \boldsymbol{K}_P, \boldsymbol{I}]$ by $\boldsymbol{x}_e$ in Theorem 9:

$$\begin{aligned} \boldsymbol{s}_e(t) &\triangleq [\boldsymbol{K}_I, \boldsymbol{K}_P, \boldsymbol{I}]\boldsymbol{x}_e(t) \\ &= \left[\boldsymbol{K} + \gamma^{-2}\boldsymbol{I}\right]^{-1} \boldsymbol{Y}_e(t)\boldsymbol{\theta}, \end{aligned} \tag{5.6}$$

then the quasi-equilibrium region expressed by composite error vector is obtained as follows:

$$|\boldsymbol{s}| \leq \|\boldsymbol{s}_e\|_\infty = \sup_{0\leq t\leq t_f} |\boldsymbol{s}_e(t)|.$$

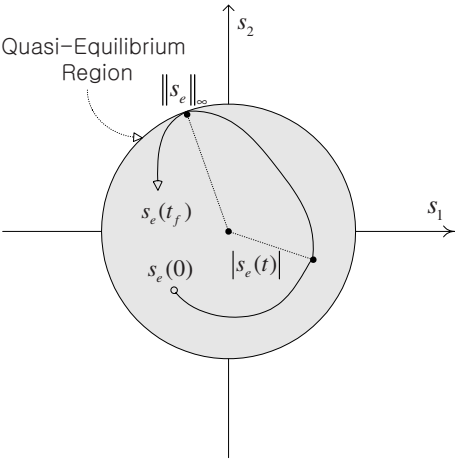

Fig. 5.1. Quasi-equilibrium region

In above Remark, the quasi-equilibrium region was defined using the composite error as shown in Fig. 5.1. Its size is dependent upon the gain $\boldsymbol{K}$ matrix, $\mathcal{L}_2$-gain γ and the inverse dynamics $\boldsymbol{Y}_e(t)\boldsymbol{\theta}$ according to desired configurations. In a practical respect, the quasi-equilibrium region can be used as a criterion for target performance chosen by user. Also, it indirectly proves the existence of gains which can achieve the target performance. In following section, we will propose an automatic performance tuning method of PID controller assisting to accomplish the target performance.

5.3 Automatic Performance Tuning

In this section, the automatic performance tuning method of PID controller for Lagrangian systems will be proposed using the concept of direct adaptive

control. Since the PID controller shows the performance limitation for trajectory tracking model of Lagrangian system as shown in previous section, the automatic performance tuning method is devised so that it can accomplish the target performance of PID control system. The target performance implies that the composite error should stay within ball boundary (Ω) chosen by user, in other words, $|\boldsymbol{s}(t)| \leq \Omega$ for all t.

5.3.1 Auto-tuning Law

Since the quasi-equilibrium region is determined by the size of gains of PID controller and the inverse dynamics $\boldsymbol{Y}_e(t)\boldsymbol{\theta}$ depending on desired configurations $(\boldsymbol{q}_d, \dot{\boldsymbol{q}}_d, \ddot{\boldsymbol{q}}_d)$, we should know the regressor matrix $\boldsymbol{Y}_e(t)$ and plant parameter vector $\boldsymbol{\theta}$ to calculate the quasi-equilibrium region. Since it is difficult to exactly identify the parameters of Lagrangian systems, conversely, we will use the quasi-equilibrium region as a criterion of target performance. For example, if the target performance is determined, then the size of quasi-equilibrium region should be adjusted so that it can achieve the target performance. Therefore, the auto-tuning law for gains of PID controller is required to adjust it. In this respect, we choose the gain matrix $\boldsymbol{K}$ in (5.6) as an auto-tuning parameter. Finally, the auto-tuning law is derived from the direct adaptive control scheme, based on ISS characteristics of trajectory tracking system, in following Theorem.

Theorem 10. *Let $\boldsymbol{s} = \dot{\boldsymbol{e}} + \boldsymbol{K}_P\boldsymbol{e} + \boldsymbol{K}_I \int \boldsymbol{e}dt$. Assume that there exists the smallest constant diagonal gain matrix $\boldsymbol{K}_\Omega > \boldsymbol{0}$ accomplishing the target performance (Ω) as follows:*

$$\sup_{0 \leq t \leq t_f} |\boldsymbol{s}(t)| \leq \Omega.$$

For $\boldsymbol{K}_\Omega > \widehat{\boldsymbol{K}}(t)$, if the auto-tuning PID controller:

$$\boldsymbol{\tau} = \left(\widehat{\boldsymbol{K}}(t) + \gamma^{-2}\boldsymbol{I}\right)\boldsymbol{s}, \tag{5.7}$$

using the auto-tuning law as following form:

$$\frac{d\widehat{K}_i}{dt} = \Gamma_i s_i^2(t), \qquad \text{for } i = 1, \cdots, n \tag{5.8}$$

is applied to the trajectory tracking system (3.3), then the closed-loop control system is extended disturbance input-to-state stable(ISS), where s_i is i-th element of composite error vector $\boldsymbol{s}$, $\widehat{K}_i$ and Γ_i are i-th diagonal elements of the diagonal time-varying gain matrix $\widehat{\boldsymbol{K}}(t) > \boldsymbol{0}$ and the update gain matrix $\boldsymbol{\Gamma} > \boldsymbol{0}$, respectively.

Proof. First, we take Lyapunov function as following form:

$$V(\boldsymbol{s}, \widehat{\boldsymbol{K}}, t) = \frac{1}{2}\boldsymbol{s}^T\boldsymbol{M}\boldsymbol{s} + \frac{1}{2}tr\left[\left(\widehat{\boldsymbol{K}}(t) - \boldsymbol{K}_\Omega\right)\boldsymbol{\Gamma}^{-1}\left(\widehat{\boldsymbol{K}}(t) - \boldsymbol{K}_\Omega\right)\right], \quad (5.9)$$

where $tr[\cdot]$ means the trace of given matrix. If the auto tuning PID controller (5.7) is applied to the trajectory tracking system model (3.3), then we can get the time derivative of Lyapunov function along the solution trajectory of closed-loop system as follows:

$$\begin{aligned}\dot{V} &= -\boldsymbol{s}^T\left(\widehat{\boldsymbol{K}}(t) + \frac{1}{2\gamma^2}\boldsymbol{I}\right)\boldsymbol{s} - \frac{\gamma^2}{2}\left|\frac{1}{\gamma^2}\boldsymbol{s} - \boldsymbol{w}\right|^2 + \frac{\gamma^2}{2}|\boldsymbol{w}|^2 \\ &\quad + tr\left[\left(\widehat{\boldsymbol{K}}(t) - \boldsymbol{K}_\Omega\right)\boldsymbol{\Gamma}^{-1}\dot{\widehat{\boldsymbol{K}}}(t)\right] \\ &= -\boldsymbol{s}^T\left(\boldsymbol{K}_\Omega + \frac{1}{2\gamma^2}\boldsymbol{I}\right)\boldsymbol{s} - \frac{\gamma^2}{2}\left|\frac{1}{\gamma^2}\boldsymbol{s} - \boldsymbol{w}\right|^2 + \frac{\gamma^2}{2}|\boldsymbol{w}|^2 \\ &\quad - \boldsymbol{s}^T\left(\widehat{\boldsymbol{K}}(t) - \boldsymbol{K}_\Omega\right)\boldsymbol{s} + tr\left[\left(\widehat{\boldsymbol{K}}(t) - \boldsymbol{K}_\Omega\right)\boldsymbol{\Gamma}^{-1}\dot{\widehat{\boldsymbol{K}}}(t)\right].\end{aligned}$$

Here, if the following matrix trace property is applied to above equation:

$$\boldsymbol{s}^T\left(\widehat{\boldsymbol{K}}(t) - \boldsymbol{K}_\Omega\right)\boldsymbol{s} = tr\left[\left(\widehat{\boldsymbol{K}}(t) - \boldsymbol{K}_\Omega\right)\boldsymbol{s}\boldsymbol{s}^T\right],$$

then above time derivative of Lyapunov function is rearranged as follows:

$$\begin{aligned}\dot{V} &= -\boldsymbol{s}^T\left(\boldsymbol{K}_\Omega + \frac{1}{2\gamma^2}\boldsymbol{I}\right)\boldsymbol{s} - \frac{\gamma^2}{2}\left|\frac{1}{\gamma^2}\boldsymbol{s} - \boldsymbol{w}\right|^2 + \frac{\gamma^2}{2}|\boldsymbol{w}|^2 \\ &\quad + tr\left[\left(\widehat{\boldsymbol{K}}(t) - \boldsymbol{K}_\Omega\right)\left(\boldsymbol{\Gamma}^{-1}\dot{\widehat{\boldsymbol{K}}}(t) - \boldsymbol{s}\boldsymbol{s}^T\right)\right]. \quad (5.10)\end{aligned}$$

Also, if the diagonal elements of $\left(\boldsymbol{\Gamma}^{-1}\dot{\widehat{\boldsymbol{K}}}(t) - \boldsymbol{s}\boldsymbol{s}^T\right)$ are zeros, then the trace term of (5.10) becomes zero because $\left(\widehat{\boldsymbol{K}}(t) - \boldsymbol{K}_\Omega\right)$ is a diagonal matrix. In other words, the auto-tuning law (5.8) is derived from the following relation:

$$\begin{aligned}&\text{if } \frac{d\widehat{K}_i}{dt} = \Gamma_i s_i^2(t), \quad \text{for } i = 1, \cdots, n \\ &\text{then } tr\left[\left(\widehat{\boldsymbol{K}}(t) - \boldsymbol{K}_\Omega\right)\left(\boldsymbol{\Gamma}^{-1}\dot{\widehat{\boldsymbol{K}}}(t) - \boldsymbol{s}\boldsymbol{s}^T\right)\right] = 0.\end{aligned}$$

Therefore, if the auto-tuning PID controller (5.7) is applied to trajectory tracking system, then we can get the following relation from (5.10):

$$\dot{V} \leq -\boldsymbol{s}^T\left(\boldsymbol{K}_\Omega + \frac{1}{2\gamma^2}\boldsymbol{I}\right)\boldsymbol{s} + \frac{\gamma^2}{2}|\boldsymbol{w}|^2. \quad (5.11)$$

Also, since the right hand sides of (5.11) are unbounded functions for $\boldsymbol{s}$ and $\boldsymbol{w}$, respectively, above inequality follows the ISS characteristics of (3.8). Hence,

the trajectory tracking system with an auto-tuning PID controller is extended disturbance input-to-state stable(ISS). □

Actually, if the PID controller can not achieve the target performance, namely, $\boldsymbol{K}_\Omega > \widehat{\boldsymbol{K}}$, then the auto-tuning law suggested in Theorem 10 will help to achieve the target performance. On the contrary, for $\widehat{\boldsymbol{K}} \geq \boldsymbol{K}_\Omega$, the target performance can be accomplished without using an auto-tuning law, in other words, $\dot{\widehat{\boldsymbol{K}}} = \boldsymbol{0}$ for $\widehat{\boldsymbol{K}} \geq \boldsymbol{K}_\Omega$. Also, since the time derivative of Lyapunov function (5.10) is rearranged using $\dot{\widehat{\boldsymbol{K}}} = \boldsymbol{0}$ as follows:

$$\dot{V} \leq -\boldsymbol{s}^T \left(\widehat{\boldsymbol{K}} + \frac{1}{2\gamma^2} \boldsymbol{I} \right) \boldsymbol{s} + \frac{\gamma^2}{2} |\boldsymbol{w}|^2,$$

the ISS can be also proved for $\widehat{\boldsymbol{K}} \geq \boldsymbol{K}_\Omega$. As a matter of fact, the auto-tuning PID controller (5.7) without using an auto-tuning law (5.8) is equal to the conventional PID controller (4.1). In following section, we will discuss about the criterion on whether the auto-tuning law is necessary to achieve the target performance or not.

5.3.2 Criterion for Auto-tuning

To apply the auto-tuning law, we should exactly know the gain matrix $\boldsymbol{K}_\Omega$ guaranteeing target performance (Ω). Since $\boldsymbol{K}_\Omega$ is the smallest gain matrix satisfying $\sup_{0 \leq t \leq t_f} |\boldsymbol{s}(t)| \leq \Omega$ by its definition, we can not know the matrix $\boldsymbol{K}_\Omega$ till the experimental result satisfies the target performance as follows:

$$\sup_{0 \leq t \leq t_f} |\boldsymbol{s}(t)| = \Omega.$$

But we can calculate the size of composite error $|\boldsymbol{s}(t)|$ at any time. Moreover, since the auto-tuning law was composed of the decentralized type in Theorem 10, we suggest the decentralized criterion for auto-tuning as follows:

$$|s_i| > \frac{\Omega}{\sqrt{2n}}, \tag{5.12}$$

where n is the number of configuration coordinates. The relations between the criterion for auto-tuning and target performance are illustrated in Fig. 5.2. As soon as the composite error arrives at the tuning region of (5.12), the auto-tuning law should be implemented to assist the achievement of target performance. Hence, the size of target performance is larger than the non-tuning region as shown in Fig. 5.2.

Although we can not use the constant gain matrix $\boldsymbol{K}_\Omega$ which accomplishes the target performance, an auto-tuning PID controller (5.7) results in the effect of gain $\boldsymbol{K}_\Omega$ for $|s_i| > \frac{\Omega}{\sqrt{2n}}$ as shown in equation (5.11). On the contrary, if the composite error stays in non-tuning region of Fig. 5.2, namely, $|s_i| \leq$

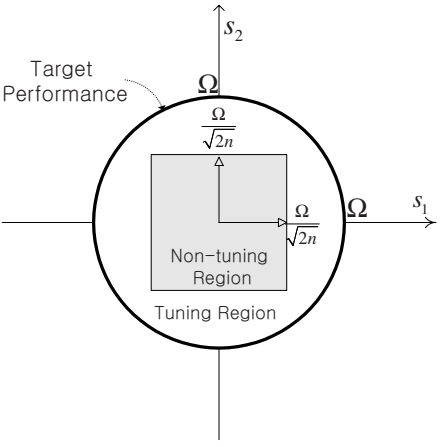

Fig. 5.2. Target performance and non-tuning region

$\frac{\Omega}{\sqrt{2n}}$, then the auto-tuning process is stopped. For this case, we expect that the gain $\widehat{\boldsymbol{K}}$ updated by an auto-tuning law (5.8) will be larger than the matrix $\boldsymbol{K}_\Omega$ achieving the target performance. As a matter of fact, the auto-tuning law has the property of a nonlinear damping suggested in [38, 39]. Strictly speaking, the first term of auto-tuning PID controller (5.7) means the nonlinear damping which helps to stabilize the control system against disturbances and the second term expresses a linear controller. In following section, we will consider the performance enhancement obtained by using the auto-tuning law.

5.3.3 Performance Enhanced by Auto-tuning Law

The upper bound of composite error (4.17) in Theorem 8 can be modified by using an auto-tuning law, in other words, it will be expressed more clearly by the bound of external disturbances and the size of real parameter vector. The performance enhancement acquired by using an auto-tuning PID controller will be suggested in following Theorem. Actually, new upper bound of composite error in following Theorem means the performance limitation of auto-tuning PID controller, however, it requires one assumption for the update gain matrix $\boldsymbol{\Gamma}$ and an initial $\widehat{\boldsymbol{K}}(0)$.

Theorem 11. *Assume that the update gain matrix $\boldsymbol{\Gamma}$ and an initial $\widehat{\boldsymbol{K}}(0)$ are determined sufficiently large to satisfy the following inequality:*

$$\widehat{\boldsymbol{K}}(t) > \frac{1}{2}\boldsymbol{Y}(\boldsymbol{x},t)\boldsymbol{Y}^T(\boldsymbol{x},t). \tag{5.13}$$

If the auto-tuning PID controller (5.7) is applied to the trajectory tracking system model (3.3), then its composite error is upper bounded as following

form:

$$|\boldsymbol{s}(t)| \leq |\boldsymbol{s}(0)|\boldsymbol{e}^{-\frac{1}{2\lambda\gamma^2}t} + \gamma^2\|\boldsymbol{d}\|_\infty + \gamma|\boldsymbol{\theta}|, \tag{5.14}$$

where $\boldsymbol{s}(0)$ is an initial composite error, λ is the maximum eigenvalue of $\boldsymbol{M}$, and $\boldsymbol{\theta}$ is the real parameter vector of Lagrangian system.

Proof. If the auto-tuning PID controller (5.7) is applied to the trajectory tracking system (3.3) using the extended disturbance (5.1) divided into linear parameterization part and external disturbance, then we can get the time derivative of positive real-valued function $\left(\frac{1}{2}\boldsymbol{s}^T\boldsymbol{M}\boldsymbol{s}\right)$ along the solution trajectory of closed-loop control system as follows:

$$\begin{aligned}
\frac{d}{dt}\left(\frac{1}{2}\boldsymbol{s}^T\boldsymbol{M}\boldsymbol{s}\right) &= -\boldsymbol{s}^T\left(\widehat{\boldsymbol{K}} + \frac{1}{\gamma^2}\boldsymbol{I}\right)\boldsymbol{s} + \boldsymbol{s}^T\boldsymbol{Y}\boldsymbol{\theta} + \boldsymbol{s}^T\boldsymbol{d} \\
&= -\frac{1}{2\gamma^2}|\boldsymbol{s}|^2 - \frac{\gamma^2}{2}\left|\frac{1}{\gamma^2}\boldsymbol{s} - \boldsymbol{d}\right|^2 + \frac{\gamma^2}{2}|\boldsymbol{d}|^2 \\
&\quad -\boldsymbol{s}^T\left(\widehat{\boldsymbol{K}} - \frac{1}{2}\boldsymbol{Y}\boldsymbol{Y}^T\right)\boldsymbol{s} - \frac{1}{2}\left|\boldsymbol{Y}^T\boldsymbol{s} - \boldsymbol{\theta}\right|^2 + \frac{1}{2}|\boldsymbol{\theta}|^2 \\
&\leq -\frac{1}{2\gamma^2}|\boldsymbol{s}|^2 - \boldsymbol{s}^T\left(\widehat{\boldsymbol{K}} - \frac{1}{2}\boldsymbol{Y}\boldsymbol{Y}^T\right)\boldsymbol{s} + \frac{\gamma^2}{2}|\boldsymbol{d}|^2 + \frac{1}{2}|\boldsymbol{\theta}|^2.
\end{aligned}$$

Here, if we use the assumption (5.13) and the maximum eigenvalue of Inertia matrix $\boldsymbol{M}$, then above equation can be simplified to:

$$\frac{d}{dt}\left(\frac{\lambda}{2}|\boldsymbol{s}|^2\right) \leq -\frac{1}{2\gamma^2}|\boldsymbol{s}|^2 + \frac{\gamma^2}{2}|\boldsymbol{d}|^2 + \frac{1}{2}|\boldsymbol{\theta}|^2.$$

If we multiply above inequality by $\boldsymbol{e}^{\frac{1}{\lambda\gamma^2}t}$, then it becomes

$$\frac{d}{dt}\left(\frac{\lambda}{2}|\boldsymbol{s}(t)|^2\boldsymbol{e}^{\frac{1}{\lambda\gamma^2}t}\right) \leq \frac{\gamma^2}{2}|\boldsymbol{d}(t)|^2\boldsymbol{e}^{\frac{1}{\lambda\gamma^2}t} + \frac{1}{2}|\boldsymbol{\theta}|^2\boldsymbol{e}^{\frac{1}{\lambda\gamma^2}t}. \tag{5.15}$$

Integrating (5.15) over [0,t], we arrive at the following form:

$$\begin{aligned}
|\boldsymbol{s}(t)|^2 &\leq |\boldsymbol{s}(0)|^2\boldsymbol{e}^{-\frac{1}{\lambda\gamma^2}t} + \frac{\gamma^2}{\lambda}\int_0^t \boldsymbol{e}^{-\frac{1}{\lambda\gamma^2}(t-\tau)}|\boldsymbol{d}(\tau)|^2 d\tau + \frac{|\boldsymbol{\theta}|^2}{\lambda}\int_0^t \boldsymbol{e}^{-\frac{1}{\lambda\gamma^2}(t-\tau)}d\tau \\
&\leq |\boldsymbol{s}(0)|^2\boldsymbol{e}^{-\frac{1}{\lambda\gamma^2}t} + \frac{\gamma^2}{\lambda}\sup_{\tau\in[0,t]}\left\{|\boldsymbol{d}(\tau)|^2\right\}\int_0^t \boldsymbol{e}^{-\frac{1}{\lambda\gamma^2}(t-\tau)}d\tau \\
&\quad + \frac{|\boldsymbol{\theta}|^2}{\lambda}\int_0^t \boldsymbol{e}^{-\frac{1}{\lambda\gamma^2}(t-\tau)}d\tau \\
&= |\boldsymbol{s}(0)|^2\boldsymbol{e}^{-\frac{1}{\lambda\gamma^2}t} + \frac{\gamma^2}{\lambda}\|\boldsymbol{d}\|_\infty^2\lambda\gamma^2(\boldsymbol{e}^{-\frac{1}{\lambda\gamma^2}t} - 1) + \frac{|\boldsymbol{\theta}|^2}{\lambda}\lambda\gamma^2(\boldsymbol{e}^{-\frac{1}{\lambda\gamma^2}t} - 1)
\end{aligned}$$

Using the fact that $\sqrt{a^2+b^2+c^2} \leq |a|+|b|+|c|$, we obtain an explicit upper bound for composite error as follows:

$$|\boldsymbol{s}(t)| \leq |\boldsymbol{s}(0)|e^{-\frac{1}{2\lambda\gamma^2}t} + \gamma^2\|\boldsymbol{d}\|_\infty + \gamma|\boldsymbol{\theta}|.$$

□

In above Theorem, the initial composite error can be set to zero by making the desired trajectory smooth. Hence, the composite error is bounded by the size of plant parameter vector and $\mathcal{L}_\infty$ norm of external disturbance as follows:

$$|\boldsymbol{s}(t)| \leq \gamma^2\|\boldsymbol{d}\|_\infty + \gamma|\boldsymbol{\theta}|,$$

under the assumption (5.13). However, we do not know whether the assumption is satisfied or not. In the assumption, the regressor matrix $\boldsymbol{Y}(\boldsymbol{x}, t)$ is dependent on desired configurations and errors. The auto-tuned gain matrix $\widehat{\boldsymbol{K}}(t)$ is affected by the update gain matrix $\boldsymbol{\Gamma}$ and an initial $\widehat{\boldsymbol{K}}(0)$. Therefore, an initial $\widehat{\boldsymbol{K}}(0)$ should satisfy at least the following inequality:

$$\widehat{\boldsymbol{K}}(0) > \frac{1}{2}\boldsymbol{Y}(\boldsymbol{0}, 0)\boldsymbol{Y}^T(\boldsymbol{0}, 0).$$

As a matter of fact, since $\boldsymbol{Y}(\boldsymbol{0}, 0)$ is equal to the simple regressor obtained by separating parameter vector from gravity torque $\boldsymbol{g}(\boldsymbol{q})$, if there exists no gravity torque, namely, $\boldsymbol{g}(\boldsymbol{q}) = \boldsymbol{0}$, then $\widehat{\boldsymbol{K}}(0) > \boldsymbol{0}$. Also, the update gain matrix should be chosen sufficiently large to satisfy the assumption because it determines the increasing rate of auto-tuned gains.

If there are no external disturbances $\boldsymbol{d} = \boldsymbol{0}$, then upper bound of composite error is bounded only by the size of parameter vector of Lagrangian system:

$$|\boldsymbol{s}(t)| \leq \gamma|\boldsymbol{\theta}|. \tag{5.16}$$

As a matter of fact, above boundedness of composite error means the performance limitation of an auto-tuning PID controller. Also, we can see in (5.16) that the composite error can be adjusted by $\mathcal{L}_2$-gain γ like a linear tuning rule explained in Remark 6. Basically, the auto-tuning PID controller has the performance limitation for trajectory tracking model of Lagrangian system. Hence, the model adaptation is required to overcome this limitation and bring the global asymptotic stability(GAS).

5.4 Model Adaptation

First of all, the regressor should be obtained to use the model adaptation in controller. However, it is not easy to obtain the applicable regressor for general Lagrangian systems because the plant parameter vector can be maximum $10n$-dimensional one $\boldsymbol{\theta} \in \Re^{10n}$, according to the report in [35]. This is a serious disadvantage for the controller using a model adaptation. However, if the regressor can be obtained anyhow, then the adaptive motion control scheme can be applied to the trajectory tracking system. Also, the controller using model adaptation overcomes the performance limitation of PID control itself as suggested in following Theorem.

Theorem 12. *Assume that there exists an auto-tuning PID controller (5.7) in Theorem 10. If the adaptive auto-tuning PID controller as following form:*

$$\boldsymbol{\tau} = \left(\widehat{\boldsymbol{K}}(t) + \frac{1}{\gamma^2}\boldsymbol{I}\right)\boldsymbol{s} + \boldsymbol{Y}(\boldsymbol{x},t)\widehat{\boldsymbol{\theta}}(t) \tag{5.17}$$

with the plant parameter update law:

$$\dot{\widehat{\boldsymbol{\theta}}}(t) = \boldsymbol{\Lambda}^{-1}\boldsymbol{Y}^T(\boldsymbol{x},t)\boldsymbol{s} \tag{5.18}$$

is applied to the trajectory tracking system (3.3), then the closed-loop control system is external disturbance input-to-state stable(ISS), where $\boldsymbol{\Lambda}$ is the gain matrix for parameter update.

Proof. First, let us consider a Lyapunov function as follow:

$$V_{Adaptive}(\boldsymbol{s},\widehat{\boldsymbol{K}},\widehat{\boldsymbol{\theta}},t) = V(\boldsymbol{s},\widehat{\boldsymbol{K}},t) + \frac{1}{2}(\boldsymbol{\theta}-\widehat{\boldsymbol{\theta}}(t))^T\boldsymbol{\Lambda}(\boldsymbol{\theta}-\widehat{\boldsymbol{\theta}}(t)), \tag{5.19}$$

where $\boldsymbol{\Lambda}$ is a constant, symmetric and positive definite matrix and $V(\boldsymbol{s},\widehat{\boldsymbol{K}},t)$ is (5.9). If the adaptive auto-tuning PID controller (5.17) is applied to the trajectory tracking system (3.3), then we get the time derivative of Lyapunov function (5.19) along the solution trajectory of closed-loop system with the control law (5.17) as follows:

$$\begin{aligned}
\dot{V}_{Adaptive} &= -\boldsymbol{s}^T\left(\widehat{\boldsymbol{K}}(t) + \frac{1}{\gamma^2}\boldsymbol{I}\right)\boldsymbol{s} + \boldsymbol{s}^T\boldsymbol{d} + \boldsymbol{s}^T\boldsymbol{Y}\left(\boldsymbol{\theta}-\widehat{\boldsymbol{\theta}}(t)\right) \\
&\quad + tr\left[\left(\widehat{\boldsymbol{K}}(t) - \boldsymbol{K}_\Omega\right)\boldsymbol{\Gamma}^{-1}\dot{\widehat{\boldsymbol{K}}}(t)\right] - (\boldsymbol{\theta}-\widehat{\boldsymbol{\theta}}(t))^T\boldsymbol{\Lambda}\dot{\widehat{\boldsymbol{\theta}}}, \\
&= -\boldsymbol{s}^T\left(\boldsymbol{K}_\Omega + \frac{1}{2\gamma^2}\boldsymbol{I}\right)\boldsymbol{s} - \frac{\gamma^2}{2}\left|\frac{1}{\gamma^2}\boldsymbol{s} - \boldsymbol{d}\right|^2 + \frac{\gamma^2}{2}|\boldsymbol{d}|^2 \\
&\quad + tr\left[(\widehat{\boldsymbol{K}}(t) - \boldsymbol{K}_\Omega)\left\{\boldsymbol{\Gamma}^{-1}\dot{\widehat{\boldsymbol{K}}}(t) - \boldsymbol{s}\boldsymbol{s}^T\right\}\right] \\
&\quad + (\boldsymbol{\theta}-\widehat{\boldsymbol{\theta}}(t))^T(\boldsymbol{Y}^T\boldsymbol{s} - \boldsymbol{\Lambda}\dot{\widehat{\boldsymbol{\theta}}}).
\end{aligned} \tag{5.20}$$

If the auto-tuning law (5.8) and parameter update law (5.18) are applied to above (5.20), then we can get the following similar to (3.8):

$$\dot{V}_{Adaptive} \leq -\boldsymbol{s}^T\left(\boldsymbol{K}_\Omega + \frac{1}{2\gamma^2}\boldsymbol{I}\right)\boldsymbol{s} + \frac{\gamma^2}{2}|\boldsymbol{d}|^2. \tag{5.21}$$

Since the right hand side of above inequality (5.21) is unbounded function for $\boldsymbol{s}$ and $\boldsymbol{d}$, respectively, hence, we conclude that the adaptive auto-tuning PID controller brings the external disturbance input-to-state stability(ISS). □

Additionally, if there exist no external disturbances, in other words, $\boldsymbol{d} = \boldsymbol{0}$, then we can see that the adaptive auto-tuning PID controller offers the global

asymptotic stability(GAS) for the trajectory tracking model of Lagrangian system. However, this adaptive plus auto-tuning PID control scheme can be applied only when the regressor is known. For most Lagrangian systems, the PID control scheme has been used without using model adaptation because it was difficult or impossible to obtain the exact regressor for many Lagrangian systems. Therefore, only an auto-tuning PID controller (5.7) will be implemented to show the validity of automatic performance tuning method in following section.

5.5 Experimental Results

To show the effectiveness of an auto-tuning PID controller, we employ three link robotic manipulator as the representative Lagrangian system. This robotic manipulator consists of three direct drive motors: the first axis motor has 200[Nm] capability, the second one 55[Nm] and the third one 18[Nm]. The desired configuration profiles of Fig. 5.3.(a) are obtained by solving inverse kinematics for 3 line segments whose lengths are all 0.7[m]. Also, the given trajectories require the fast motion (maximum velocity $\approx$ 3 $[rad/s]$) of robotic manipulator as shown in Fig. 5.3.(b). First, we determine the static gains of auto-tuning PID controller (5.7) as $\boldsymbol{K}_P = 20\boldsymbol{I}$, $\boldsymbol{K}_I = 100\boldsymbol{I}$ and $\gamma = 0.5$ satisfying the design guidelines (C1),(C2),(C3). Now, the controller has the following form: for $i = 1, 2, 3$,

$$\begin{aligned} \tau_i &= (\widehat{K}_i(t) + 4)s_i \\ s_i &= \dot{e}_i + 20e_i + 100\int e_i dt \\ \frac{d\widehat{K}_i(t)}{dt} &= \Gamma s_i^2, \qquad \text{if } |s_i| > \frac{\Omega}{\sqrt{2n}}, \end{aligned}$$

where τ_i is the i-th element of input torque vector $\boldsymbol{\tau}$ and $n = 3$. Also, initial auto-tuned gains are determined as $\widehat{K}_i(0) = 0.1$ because the robotic manipulator is not affected by the gravity. Second, since the composite error is approximately proportional to the configuration error with proportional constant K_P, the target performance can be approximately determined as follows:

$$\Omega = \sqrt{2n} \times |s_i|_t \approx \sqrt{2n} \times K_P \times |e_i|_t. \tag{5.22}$$

where $|s_i|_t$ and $|e_i|_t$ are the target composite error and configuration error, respectively. For instance, if we are to obtain the performance of $|e_i|_t < 0.02$ $[rad]$ for each driving axis, then the target performance should be determined as $\Omega = 1.0$ by (5.22). Also, the update gain $\Gamma = 1000$ is used in an auto-tuning law. Fig. 5.3.(c) and (d) show experimental results: the configuration error and its velocity error. In figures, the errors are large at initial time, however, they are reduced till the target performance is achieved by an auto-tuning law.

As a matter of fact, the auto-tuning law is executed at the exterior of two dotted lines in Fig. 5.4.(a). After the auto-tuning process is finished, the auto-tuned gains arrive at $\widehat{K}_1 = 136.98$, $\widehat{K}_2 = 65.60$ and $\widehat{K}_3 = 6.83$ as we can see in Fig. 5.4.(c). To examine the auto-tuning process in detail, the horizontal ranges of $0 \sim 1$ second in Fig. 5.4.(a) and (c) are enlarged as shown in that figure (b) and (d). The auto-tuning for first axis is started at 0.11 second and ended at 0.26 second because the error goes over the criterion (dotted line : $1/\sqrt{6} = 0.408$) for the first time as shown in Fig. 5.4.(b). Also, the error of second axis goes over the criterion between 0.13 and 0.24 second. Finally, since the error of third axis goes over the criterion downward twice, the auto-tuning process is implemented twice as shown in Fig. 5.4.(d). The experimental result of Fig. 5.4.(a) shows that the target performance is achieved after 0.6 second when the auto-tuning is finished.

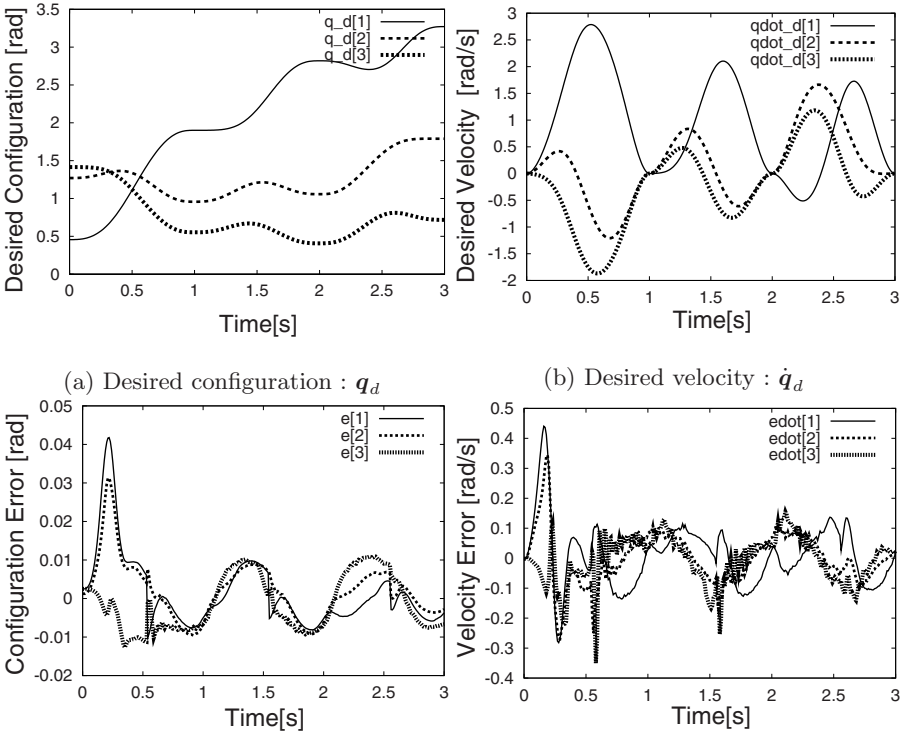

(a) Desired configuration : $\boldsymbol{q}_d$

(b) Desired velocity : $\dot{\boldsymbol{q}}_d$

(c) Configuration error : $\boldsymbol{e}$

(d) Velocity error : $\dot{\boldsymbol{e}}$

Fig. 5.3. Performance of auto-tuning PID controller

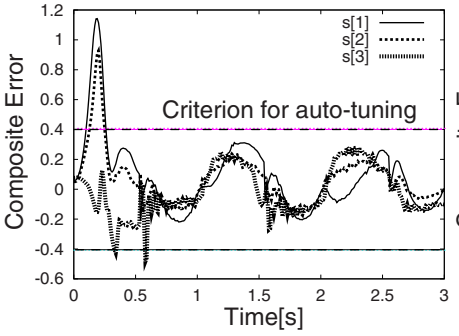

(a) Composite error : $\boldsymbol{s}$

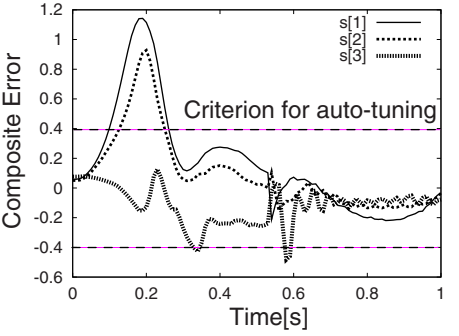

(b) Composite error ($\boldsymbol{s}$) for $0 \sim 1[s]$

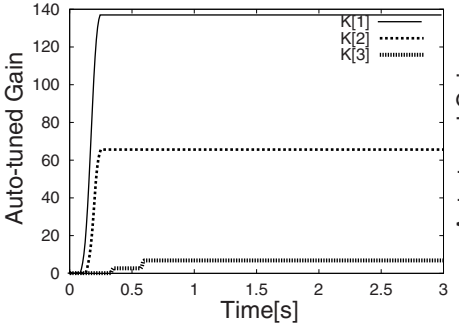

(c) Auto-tuned gains : $\widehat{\boldsymbol{K}}$

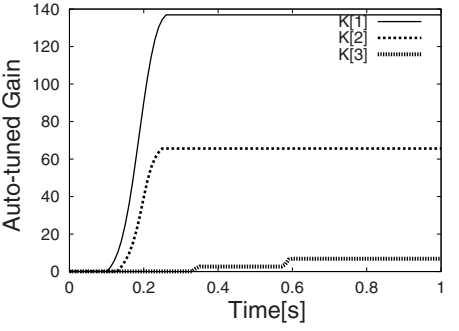

(d) Auto-tuned gains ($\widehat{\boldsymbol{K}}$) for $0 \sim 1[s]$

Fig. 5.4. Composite error and auto-tuned gains

5.6 Summary

Since the equilibrium point can not be defined for the control system involving performance limitation, the quasi-equilibrium region was newly introduced to guarantee the existence of PID controller achieving target performance. Second, we proposed the auto-tuning PID controller achieving target performance. The auto-tuning law was derived from the direct adaptive control scheme based on ISS and the analysis result of performance limitation. Through experiments, we showed the effectiveness of automatic performance tuning method.

6

Output Feedback PID Control

6.1 Introduction

In previous chapters and [10, 11, 13, 14, 15], an inverse optimal PID controller was derived as a form of full state feedback one from the extended disturbance input-to-state stability and $\mathcal{H}_\infty$ performance index. From now on, we are to make the PID state observer for an inverse optimal PID controller. There are two reasons why the PID control systems are not equipped with sensing devices for all states: the one is because of their costs and the other is that sensors show different characteristics according to a kind of sensors. For instance, the tachometer and encoder have been used to measure the derivative and configuration coordinates (*e.g.* velocity and position information) for Lagrangian systems, respectively, however, an analog sensor such as tachometer is more contaminated by measurement noises than the digital sensor such as encoder. In this case, since the performance limitation of control system is subject to the performance of tachometer against sensor noise, most Lagrangian systems are equipped with only the noise-free configuration measurement devices such as the rotary encoder or linear encoder. Therefore, it is necessary for a PID state observer to estimate PID full states from the measurement output.

The nonlinear observers for Lagrangian systems were suggested in [44, 19], also, their regions of attraction. Since these nonlinear observers require the exact model for Lagrangian system, however, they may not be available if the dynamic parameters of Lagrangian system are not identified exactly. Second, another nonlinear observer to estimate the angular velocity and momentum was proposed using Euler-quaternion in [54]. Third, the PD linear observer was suggested in [6, 7]. They showed that the output feedback PD controller (PD controller with PD linear observer) yields the semi-global uniform ultimate boundedness for Lagrangian systems and, in particular, the observer derivative gain is required to be sufficiently large in order to guarantee it. Actually, since this is the property of high-gain observer, the well-known high-gain observer theory is used to define newly the PID state observer.

Y. Choi, W.K. Chung: PID Trajectory Tracking Control for Mechanical Systems, LNCIS 298, pp. 89–100, 2004.

As a representative observer for nonlinear systems, the high-gain observer was introduced for the first time in [21]. The high-gain observer robustly estimates the derivatives of output signal. However, the high-gain observer does not include the integrals of output signal, though it is required to make an output feedback PID control system. In this chapter, the PID state observer is suggested as an estimator for derivatives and integrals of measurement outputs. The separation principle between the high-gain observer and the full state feedback controller was suggested in [4], based on the separation principle suggested in [62]. The observer design condition to recover the stability achieved by a full state feedback PID control system is also suggested in this chapter.

If the PID state observer is used, then an inverse optimal PID controller suggested in [14] can be rewritten by replacing a state vector with its estimate under the assumption that the observation is exact, *i.e.*, the certainty equivalence principle, as follows:

$$\begin{aligned}\boldsymbol{\tau} &= \boldsymbol{R}^{-1}\boldsymbol{B}^T\boldsymbol{P}\hat{\boldsymbol{x}} \\ &= \left(\boldsymbol{K} + \frac{1}{\gamma^2}\boldsymbol{I}\right)\left(\hat{\boldsymbol{x}}_3 + \boldsymbol{K}_P\hat{\boldsymbol{x}}_2 + \boldsymbol{K}_I\hat{\boldsymbol{x}}_1\right), \end{aligned} \tag{6.1}$$

where $\boldsymbol{K}, \boldsymbol{K}_P, \boldsymbol{K}_I$ are constant, diagonal and positive definite matrices satisfying $\boldsymbol{K}_P^2 > 2\boldsymbol{K}_I > \boldsymbol{0}$, γ means $\mathcal{L}_2$-gain and $\hat{\boldsymbol{x}}$ expresses the estimate for a real state vector $\boldsymbol{x}$ which is defined as following form:

$$\boldsymbol{x} \triangleq \begin{bmatrix}\boldsymbol{x}_1 \\ \boldsymbol{x}_2 \\ \boldsymbol{x}_3\end{bmatrix} = \begin{bmatrix}\int \boldsymbol{e} \\ \boldsymbol{e} \\ \dot{\boldsymbol{e}}\end{bmatrix} \in \Re^{3n}.$$

From now on, we call (6.1) an output feedback PID controller, where $\hat{\boldsymbol{x}}_1 \in \Re^n$ represents the estimate of integral configuration error vector, $\hat{\boldsymbol{x}}_2 \in \Re^n$ that of configuration error vector itself and $\hat{\boldsymbol{x}}_3 \in \Re^n$ that of derivative one.

This chapter is organized as follows. The next section suggests the normal form of Lagrangian systems. In section 6.3, the PID state observer is derived from the robustness against disturbances, and its closed-loop stability is investigated and the reduced-order ID state observer is also suggested.

6.2 Normal Form of Lagrangian Systems

The state-space description for Lagrangian systems has been suggested in [14, 47] as follows:

$$\dot{\boldsymbol{x}} = \boldsymbol{A}(\boldsymbol{x}, t)\boldsymbol{x} + \boldsymbol{B}(\boldsymbol{x}, t)\boldsymbol{w} + \boldsymbol{B}(\boldsymbol{x}, t)\boldsymbol{u}, \tag{6.2}$$

where $\boldsymbol{w}$ is the extended disturbance and $\boldsymbol{u}$ the control input vector having this relation $\boldsymbol{u} = -\boldsymbol{\tau}$ with an inverse optimal PID controller. However, this

state-space description can not be used to make an observer because it is a nonlinear equation, *e.g.*, the system matrix $\boldsymbol{A}(\boldsymbol{x}, t)$ includes the state vector again. Hence, we are to use the normal form which is the simplest one among the representation methods for nonlinear systems. Now, let us take the normal form for Lagrangian system as follows:

$$\begin{aligned} \dot{\boldsymbol{x}} &= \boldsymbol{A}_o \boldsymbol{x} + \boldsymbol{B}_o \phi(\boldsymbol{x}_2, \boldsymbol{x}_3, \boldsymbol{\tau}, t) \\ \boldsymbol{y} &= \boldsymbol{C}_o \boldsymbol{x} \end{aligned} \tag{6.3}$$

where,

$$\begin{aligned} \boldsymbol{A}_o &= \begin{bmatrix} \boldsymbol{0} & \boldsymbol{I} & \boldsymbol{0} \\ \boldsymbol{0} & \boldsymbol{0} & \boldsymbol{I} \\ \boldsymbol{0} & \boldsymbol{0} & \boldsymbol{0} \end{bmatrix} \\ \boldsymbol{B}_o &= \begin{bmatrix} \boldsymbol{0} \\ \boldsymbol{0} \\ \boldsymbol{I} \end{bmatrix} \\ \boldsymbol{C}_o &= \begin{bmatrix} \boldsymbol{0} & \boldsymbol{I} & \boldsymbol{0} \end{bmatrix} \\ \phi(\boldsymbol{x}_2, \boldsymbol{x}_3, \boldsymbol{\tau}, t) &= \ddot{\boldsymbol{q}}_d(t) + \boldsymbol{M}^{-1}(\boldsymbol{q}) \left[\boldsymbol{C}(\boldsymbol{q}, \dot{\boldsymbol{q}}) \dot{\boldsymbol{q}} + \boldsymbol{g}(\boldsymbol{q}) - \boldsymbol{\tau} \right] \end{aligned} \tag{6.4}$$

and $\boldsymbol{I}$ is an $n \times n$ identity matrix. Also, we should notice that only configuration error vector is measured by encoders, *i.e.*, $\boldsymbol{y} = \boldsymbol{x}_2 \in \Re^n$, and the nonlinear function $\phi(\boldsymbol{x}_2, \boldsymbol{x}_3, \boldsymbol{\tau}, t)$ is not a function of $\boldsymbol{x}_1$, because the configuration coordinates $(\boldsymbol{q} = \boldsymbol{q}_d(t) - \boldsymbol{x}_2)$ and their derivatives $(\dot{\boldsymbol{q}} = \dot{\boldsymbol{q}}_d(t) - \boldsymbol{x}_3)$ are functions of $\boldsymbol{x}_2$, $\boldsymbol{x}_3$ and time t.

6.3 PID State Observer

In this section, the PID state observer is defined as a kind of high-gain observer in [34]. Actually, the PID state observer is different from the high-gain observer only in that the middle states are measured, not first states among integrator block chains of normal form (6.3), *i.e.*, $\boldsymbol{y} = \boldsymbol{x}_2$. Now, let us define the PID state observer according to the form of Luenberger observer as follows:

$$\dot{\hat{\boldsymbol{x}}} = \boldsymbol{A}_o \hat{\boldsymbol{x}} + \boldsymbol{H} \left[\boldsymbol{y} - \boldsymbol{C}_o \hat{\boldsymbol{x}} \right], \tag{6.5}$$

where $\boldsymbol{H}$ is an observer gain matrix and, in particular, we should notice that this is a linear state observer. Also, the observer gain matrix should be designed so that the observer can estimate the PID states accurately.

6.3.1 Observer Gain

First of all, if we define the state estimation error vector as $\tilde{\boldsymbol{x}} = \boldsymbol{x} - \hat{\boldsymbol{x}}$, then the estimation error dynamics can be obtained by subtracting (6.5) from (6.3) as follow:

$$\dot{\tilde{\boldsymbol{x}}} = [\boldsymbol{A}_o - \boldsymbol{H}\boldsymbol{C}_o]\,\tilde{\boldsymbol{x}} + \boldsymbol{B}_o\phi(\boldsymbol{x}_2, \boldsymbol{x}_3, \boldsymbol{\tau}, t). \tag{6.6}$$

Here, since the nonlinear term $\phi(.)$ corresponds to the disturbance term with which we can not deal, the observer gain should be designed with an additional goal of rejecting the effect of disturbance term $\phi(.)$ on the estimation error $\tilde{\boldsymbol{x}}$. Also, when it is not possible for the transfer matrix from disturbance to estimation error to make zero, we should design the observer gain $\boldsymbol{H}^T = \left[h_0\boldsymbol{I}, h_1\boldsymbol{I}, h_2\boldsymbol{I}\right]$ such that this transfer matrix can be very close to zero. Now, let us consider the transfer matrix from ϕ to $\tilde{\boldsymbol{x}}$ in (6.6) as follow:

$$\begin{aligned}\boldsymbol{G}_{\phi\tilde{x}}(s) &= (s\boldsymbol{I}_{3n\times 3n} - \boldsymbol{A}_o + \boldsymbol{H}\boldsymbol{C}_o)^{-1}\boldsymbol{B}_o \\ &= \begin{bmatrix} \frac{1-h_0}{s(s^2+h_1 s+h_2)}\boldsymbol{I} \\ \frac{1}{s^2+h_1 s+h_2}\boldsymbol{I} \\ \frac{s+h_1}{s^2+h_1 s+h_2}\boldsymbol{I} \end{bmatrix},\end{aligned}$$

where s means Laplace operator. Since the first term of above transfer matrix has the integrator, the first element h_0 of observer gain matrix should be chosen as one, *i.e.*, $h_0 = 1$. Similar to the high-gain observer, the remaining transfer functions can be also made small by choosing $h_2 \gg h_1 \gg 1$. In particular, if the remaining observer gains are chosen as follows:

$$h_1 = \frac{\alpha_1}{\varepsilon} \quad \text{and} \quad h_2 = \frac{\alpha_2}{\varepsilon^2} \tag{6.7}$$

where ε is an observer gain parameter ($0 < \varepsilon \ll 1$), α_1 and α_2 are positive real constants, then above transfer matrix is rearranged as follows:

$$\boldsymbol{G}_{\phi\tilde{x}}(s) = \begin{bmatrix} \boldsymbol{0} \\ \frac{\varepsilon^2}{\varepsilon^2 s^2+\alpha_1\varepsilon s+\alpha_2}\boldsymbol{I} \\ \frac{\varepsilon^2 s+\alpha_1\varepsilon}{\varepsilon^2 s^2+\alpha_1\varepsilon s+\alpha_2}\boldsymbol{I} \end{bmatrix} \quad \rightarrow \quad \therefore \quad \lim_{\varepsilon\to 0}\boldsymbol{G}_{\phi\tilde{x}}(s) = \boldsymbol{0}.$$

This disturbance rejection property of PID state observer (6.5) can be obtained by designing the gain matrix like a high-gain observer. Also, it is important to perceive that the PID state observer includes both an exact integrator and an approximate differentiator at the same time. This can be seen immediately by considering the transfer matrix from the measurement output $\boldsymbol{y}$ to the estimate $\hat{\boldsymbol{x}}$ for a PID state observer (6.5) as follow:

$$\begin{aligned}\boldsymbol{G}_{y\hat{x}}(s) &= (s\boldsymbol{I}_{3n\times 3n} - \boldsymbol{A}_o + \boldsymbol{H}\boldsymbol{C}_o)^{-1}\boldsymbol{H} \\ &= \begin{bmatrix} \frac{1}{s}\boldsymbol{I} \\ \frac{\varepsilon\alpha_1 s+\alpha_2}{\varepsilon^2 s^2+\varepsilon\alpha_1 s+\alpha_2}\boldsymbol{I} \\ \frac{\alpha_2 s}{\varepsilon^2 s^2+\varepsilon\alpha_1 s+\alpha_2}\boldsymbol{I} \end{bmatrix}.\end{aligned}$$

Here, if the observer gain parameter ε approaches zero for above transfer matrix as follow:

$$\lim_{\varepsilon \to 0} \boldsymbol{G}_{y\hat{x}}(s) = \begin{bmatrix} \frac{1}{s}\boldsymbol{I} \\ \boldsymbol{I} \\ s\boldsymbol{I} \end{bmatrix},$$

then $\hat{\boldsymbol{x}}_2$ and $\hat{\boldsymbol{x}}_3$ approach $\boldsymbol{y}$ and $\dot{\boldsymbol{y}}$, respectively. Since the measurement output is the configuration error, *i.e.*, $\boldsymbol{y} = \boldsymbol{x}_2 = \boldsymbol{e}$, therefore, we can confirm that a PID state observer (6.5) estimates the integral error, current error and derivative error according as $\varepsilon \to 0$.

Remark 9. The linear PD state observer for Lagrangian systems was suggested for the first time in [7], though it was not a PID state observer. Also, it was proved that the PD output feedback controller using the PD state observer could yield the semi-global uniform ultimate boundedness.

6.3.2 Stability

When the output feedback PID controller (6.1) using the PID state observer (6.5) is applied to Lagrangian systems, the closed-loop stability is examined in this section. To begin with, since the nonlinear function $\phi(\boldsymbol{x}_2, \boldsymbol{x}_3, \boldsymbol{\tau}, t)$ is not a function of $\boldsymbol{x}_1$, the $\boldsymbol{x}_1$ part of the state vector can be neglected when the total closed-loop stability is considered. Now, let us introduce the transformation into the form without $\tilde{\boldsymbol{x}}_1$ to use the singular perturbation theory, when ε is very small, with the following relation:

$$\varphi = \boldsymbol{D}(\varepsilon)\tilde{\boldsymbol{x}} \tag{6.8}$$

where

$$\boldsymbol{D}(\varepsilon) = \begin{bmatrix} \boldsymbol{0} & \boldsymbol{I} & \boldsymbol{0} \\ \boldsymbol{0} & \boldsymbol{0} & \varepsilon\boldsymbol{I} \end{bmatrix} \in \Re^{2n \times 3n},$$

then the estimation error dynamics (6.6) is transformed as follows:

$$\varepsilon\dot{\varphi} = \boldsymbol{A}_s\varphi + \varepsilon^2 \boldsymbol{B}_s \phi(\boldsymbol{x}_2, \boldsymbol{x}_3, \boldsymbol{\tau}, t), \tag{6.9}$$

where

$$\boldsymbol{A}_s \triangleq \varepsilon \boldsymbol{D}(\varepsilon)\left[\boldsymbol{A}_o - \boldsymbol{H}\boldsymbol{C}_o\right]\boldsymbol{D}^{+}(\varepsilon) = \begin{bmatrix} -\alpha_1\boldsymbol{I} & \boldsymbol{I} \\ -\alpha_2\boldsymbol{I} & \boldsymbol{0} \end{bmatrix}$$

$$\boldsymbol{B}_s \triangleq \frac{1}{\varepsilon}\boldsymbol{D}(\varepsilon)\boldsymbol{B}_o = \begin{bmatrix} \boldsymbol{0} \\ \boldsymbol{I} \end{bmatrix},$$

and $\boldsymbol{D}^{+}$ is the pseudoinverse of $\boldsymbol{D}$. The transformed estimation error dynamics (6.9) shows clearly that reducing ε decreases the effect of the disturbance $\phi(.)$. Also, it is clear that the dynamics of estimation error will be much faster than that of $\boldsymbol{x}$ when an observer gain parameter ε is sufficiently small. According to a survey reported in [17, 34], during this transient period, the estimation

error $\tilde{\boldsymbol{x}}$ may exhibit peaking behavior where the transient response takes the impulsive-like form $(1/\varepsilon)e^{-at/\varepsilon}$ as ε approaches zero for some $a > 0$. Actually, it is an intrinsic feature of the high-gain observer that rejects the effect of the disturbance $\phi(.)$ in (6.9). Also, it is known that this peaking phenomenon can be overcome by saturating either control inputs or state estimates. After peaking period, the estimation error becomes the order of $O(\varepsilon)$ and the output feedback PID controller becomes $O(\varepsilon)$ close to the full state one.

If the output feedback PID controller (6.1) is applied to the Lagrangian system (6.2) and the transformed estimation error dynamics (6.9), then the closed-loop system described by using state variables $\boldsymbol{x}$ and φ can be obtained according to an observer gain parameter ε as follows:

$$\dot{\boldsymbol{x}} = \boldsymbol{A}\boldsymbol{x} + \boldsymbol{B}\boldsymbol{w} - \boldsymbol{B}\boldsymbol{R}^{-1}\boldsymbol{B}^T\boldsymbol{P}(\boldsymbol{x} - \boldsymbol{D}^+(\varepsilon)\varphi) \tag{6.10}$$

$$\varepsilon\dot{\varphi} = \boldsymbol{A}_s\varphi + \varepsilon^2\boldsymbol{B}_s\phi(\boldsymbol{x}_2, \boldsymbol{x}_3, \boldsymbol{R}^{-1}\boldsymbol{B}^T\boldsymbol{P}(\boldsymbol{x} - \boldsymbol{D}^+(\varepsilon)\varphi), t), \tag{6.11}$$

where the solution trajectories of above closed-loop system starting from $\boldsymbol{x}(0)$ and $\varphi(0)$ are denoted by $\boldsymbol{x}(t,\varepsilon)$ and $\varphi(t,\varepsilon)$, respectively. According to the singular perturbation theory in [33], each stability of reduced system and boundary-layer one derived from the closed-loop system (6.10) and (6.11) is examined in following Remarks. Using these stability proofs, the total stability for closed-loop system is proved in following Theorem.

Remark 10. The reduced system derived from the closed-loop one has the extended disturbance ($\boldsymbol{w}$) input-to-state ($\boldsymbol{x}$) stability.

Proof. Since $\varphi = \boldsymbol{0}$ is the unique solution of (6.11) when $\varepsilon = 0$, the reduced system is obtained by putting $\varphi = \boldsymbol{0}$ in (6.10) as follow:

$$\frac{d\boldsymbol{x}}{dt} = (\boldsymbol{A} - \boldsymbol{B}\boldsymbol{R}^{-1}\boldsymbol{B}^T\boldsymbol{P})\boldsymbol{x} + \boldsymbol{B}\boldsymbol{w}.$$

For a reduced system, since an output feedback PID controller (6.1) becomes equal to an inverse optimal PID controller, as proved in Theorem 3 in [14], the Lyapunov function defined as $V(\boldsymbol{x}, t) \triangleq \frac{1}{2}\boldsymbol{x}^T\boldsymbol{P}(\boldsymbol{x}, t)\boldsymbol{x}$ shows the following relation:

$$\begin{aligned}\frac{dV}{dt} &= V_t + \boldsymbol{V}_x\left\{(\boldsymbol{A} - \boldsymbol{R}^{-1}\boldsymbol{B}^T\boldsymbol{P})\boldsymbol{x} + \boldsymbol{B}\boldsymbol{w}\right\} \\ &\leq -\frac{1}{2}\boldsymbol{x}^T\left(\boldsymbol{Q} + \boldsymbol{P}\boldsymbol{B}\boldsymbol{K}\boldsymbol{B}^T\boldsymbol{P}\right)\boldsymbol{x} + \gamma^2|\boldsymbol{w}|^2,\end{aligned} \tag{6.12}$$

where $\boldsymbol{Q} > \boldsymbol{0}$, $V_t = \frac{\partial V}{\partial t}$ and $\boldsymbol{V}_x \triangleq \frac{\partial V}{\partial \boldsymbol{x}^T}$ is a row vector. Therefore, we can see from (6.12) that the reduced system has the extended disturbance input-to-state stability. □

Remark 11. The boundary-layer system derived from the closed-loop one has the asymptotic stability.

Proof. The boundary-layer system is obtained by applying (6.11) to the change of time variable $\sigma = t/\varepsilon$ then setting $\varepsilon = 0$ as follow:

$$\frac{d\varphi}{d\sigma} = \boldsymbol{A}_s\varphi.$$

For a boundary-layer system, let us define the Lyapunov function as $W(\varphi) \triangleq \frac{1}{2}\varphi^T\boldsymbol{P}_s\varphi$, with the following matrix satisfying Lyapunov equation $\boldsymbol{P}_s\boldsymbol{A}_s + \boldsymbol{A}_s^T\boldsymbol{P}_s = -\boldsymbol{I}_{2n\times 2n}$:

$$\boldsymbol{P}_s = \begin{bmatrix} \frac{\alpha_2+1}{2\alpha_1}\boldsymbol{I} & -\frac{1}{2}\boldsymbol{I} \\ -\frac{1}{2}\boldsymbol{I} & \frac{(1+\alpha_2)-\alpha_1^2}{2\alpha_1\alpha_2}\boldsymbol{I} \end{bmatrix},$$

where positive constants α_1 and α_2 should be chosen satisfying this relation $\frac{(1+\alpha_2)^2}{1+2\alpha_2} > \alpha_1^2$ to guarantee $\boldsymbol{P}_s > \boldsymbol{0}$. Then, we can see that the boundary-layer system has the asymptotic stability because the time derivative of Lyapunov function has the following form:

$$\begin{aligned} \frac{dW}{d\sigma} &= \boldsymbol{W}_\varphi\boldsymbol{A}_s\varphi \\ &= -\frac{1}{2}\varphi^T\varphi, \end{aligned} \tag{6.13}$$

where $\boldsymbol{W}_\varphi \triangleq \frac{\partial W}{\partial \varphi^T}$ is a row vector. □

Theorem 13. *Let $\boldsymbol{K} = k\boldsymbol{I}$ and $\boldsymbol{K}_P = k_P\boldsymbol{I}$. If the observer gain parameter ε is chosen within*

$$0 < \varepsilon < \frac{1}{k_P}, \tag{6.14}$$

then the closed-loop system (6.10) and (6.11) has the extended disturbance $(\boldsymbol{w}, \phi)$ input-to-state $(\boldsymbol{x}, \varphi)$ stability.

Proof. First, let us take the total Lyapunov function of following form:

$$Z(\boldsymbol{x}, \varphi, t) = (1-\nu)V(\boldsymbol{x}, t) + \nu W(\varphi), \quad \text{for } 0 < \nu < 1$$

then the time derivative of Lyapunov function is obtained along the solution trajectories of closed-loop system (6.10) and (6.11) as follow:

$$\begin{aligned} \frac{dZ}{dt} = (1-\nu)&\left(V_t + \boldsymbol{V}_x\left\{(\boldsymbol{A} - \boldsymbol{R}^{-1}\boldsymbol{B}^T\boldsymbol{P})\boldsymbol{x} + \boldsymbol{B}\boldsymbol{w}\right\}\right) \\ &+(1-\nu)\boldsymbol{V}_x\boldsymbol{B}\boldsymbol{R}^{-1}\boldsymbol{B}^T\boldsymbol{P}\boldsymbol{D}^{-1}(\varepsilon)\varphi \\ &+\frac{\nu}{\varepsilon}\boldsymbol{W}_\varphi\boldsymbol{A}_s\varphi + \nu\varepsilon\boldsymbol{W}_\varphi\boldsymbol{B}_s\phi. \end{aligned}$$

If both (6.12) and (6.13) are used with $\boldsymbol{V}_x\boldsymbol{B} = \boldsymbol{x}^T\boldsymbol{P}\boldsymbol{B}$ and $\boldsymbol{W}_\varphi\boldsymbol{B}_s = \varphi^T\boldsymbol{P}_s\boldsymbol{B}_s$, then above equation is modified to the following form:

$$\begin{aligned}\frac{dZ}{dt} \le & -\frac{(1-\nu)}{2}\boldsymbol{x}^T\left(\boldsymbol{Q}+\boldsymbol{PBKB}^T\boldsymbol{P}\right)\boldsymbol{x}+(1-\nu)\gamma^2|\boldsymbol{w}|^2 \\ & +(1-\nu)\boldsymbol{x}^T\boldsymbol{PBR}^{-1}\boldsymbol{B}^T\boldsymbol{PD}^{-1}(\varepsilon)\varphi \\ & -\frac{\nu}{2\varepsilon}\varphi^T\varphi+\nu\varepsilon\varphi^T\boldsymbol{P}_s\boldsymbol{B}_s\phi. \end{aligned} \tag{6.15}$$

Second, if Young's inequality is utilized as following form:

$$\begin{aligned}\varphi^T\boldsymbol{P}_s\boldsymbol{B}_s\phi &\le \frac{k_P}{2\varepsilon}\varphi^T\varphi+\frac{2\varepsilon}{k_P}\phi^T\boldsymbol{B}_s^T\boldsymbol{P}_s\boldsymbol{P}_s\boldsymbol{B}_s\phi \\ &= \frac{k_P}{2\varepsilon}\varphi^T\varphi+\frac{2\varepsilon\delta}{k_P}\phi^T\phi,\end{aligned}$$

by using $\boldsymbol{B}_s^T\boldsymbol{P}_s\boldsymbol{P}_s\boldsymbol{B}_s=\delta\boldsymbol{I}$ with

$$\delta=\frac{1}{4}+\left(\frac{(1+\alpha_2)-\alpha_1^2}{2\alpha_1\alpha_2}\right)^2,$$

then above inequality (6.15) can be arranged as the following form:

$$\begin{aligned}&\frac{dZ}{dt} \le \\ &-\frac{1}{2}\begin{bmatrix}\boldsymbol{x}\\ \varphi\end{bmatrix}^T\begin{bmatrix}(1-\nu)(\boldsymbol{Q}+\boldsymbol{PBKB}^T\boldsymbol{P}) & -(1-\nu)\boldsymbol{PBR}^{-1}\boldsymbol{B}^T\boldsymbol{PD}^{+}(\varepsilon)\\ -(1-\nu)\boldsymbol{D}^{+T}(\varepsilon)\boldsymbol{PBR}^{-1}\boldsymbol{B}^T\boldsymbol{P} & \frac{\nu(1-\varepsilon k_P)}{\varepsilon}\boldsymbol{I}\end{bmatrix}\begin{bmatrix}\boldsymbol{x}\\ \varphi\end{bmatrix} \\ &+(1-\nu)\gamma^2|\boldsymbol{w}|^2+\frac{2\nu\varepsilon^2\delta}{k_P}|\phi|^2,\end{aligned} \tag{6.16}$$

where $\boldsymbol{w}$ and ϕ are the extended disturbances for the reduced system and the estimation error dynamics, respectively. Third, the matrix related with an augmented state vector $\left[\boldsymbol{x}^T,\varphi^T\right]^T$ should be positive definite to prove the extended disturbance $(\boldsymbol{w},\phi)$ input-to-state $(\boldsymbol{x},\varphi)$ stability. Hence, the following inequality obtained from (6.16) should be satisfied:

$$\boldsymbol{Q}+\boldsymbol{PBKB}^T\boldsymbol{P}>\frac{\varepsilon(1-\nu)}{\nu(1-\varepsilon k_P)}\boldsymbol{PBR}^{-1}\boldsymbol{B}^T\boldsymbol{PD}^{+}(\varepsilon)\boldsymbol{D}^{+T}(\varepsilon)\boldsymbol{PBR}^{-1}\boldsymbol{B}^T\boldsymbol{P}. \tag{6.17}$$

Since $\boldsymbol{Q}>\boldsymbol{0}$ and $\boldsymbol{R}^{-1}\boldsymbol{B}^T\boldsymbol{PD}^{+}(\varepsilon)\boldsymbol{D}^{+T}(\varepsilon)\boldsymbol{PBR}^{-1}$ in (6.17) can be simplified to the following form:

$$\left(\boldsymbol{K}_P^2+\frac{1}{\varepsilon^2}\boldsymbol{I}\right)\left(\boldsymbol{K}+\frac{1}{\gamma^2}\boldsymbol{I}\right)^2,$$

if the following condition is satisfied

$$\boldsymbol{K}\ge\frac{\varepsilon(1-\nu)}{\nu(1-\varepsilon k_P)}\left(\boldsymbol{K}_P^2+\frac{1}{\varepsilon^2}\boldsymbol{I}\right)\left(\boldsymbol{K}+\frac{1}{\gamma^2}\boldsymbol{I}\right)^2, \tag{6.18}$$

then we say that the inequality (6.17) is always satisfied. Also, by letting $\boldsymbol{K}_P = k_P\boldsymbol{I}$ and $\boldsymbol{K} = k\boldsymbol{I}$, above equation (6.18) can be more simplified to the following form:

$$\left[(1-\nu)k_P^2(k+1/\gamma^2)^2 + \nu k k_P\right]\varepsilon^2 - \nu k\varepsilon + (1-\nu)(k+1/\gamma^2)^2 \le 0. \quad (6.19)$$

To have the real ε-boundary from above inequality, the discriminant should not be at least negative like this:

$$\begin{aligned} D &\triangleq \nu^2k^2 - 4\left[ak_P^2 + \nu k k_P\right]a \\ &= \nu^2k^2 - 4\nu k k_P a - 4k_P^2a^2 \\ &= (\nu k - 2k_P a)^2 - 8k_P^2a^2 \\ &= (\nu k - (2+2\sqrt{2})k_P a)(\nu k + (2\sqrt{2}-2)k_P a) \ge 0 \end{aligned}$$

where $a = (1-\nu)(k+1/\gamma^2)^2 > 0$. Since ν, k, k_P, a are all positive real constants, we can find the following ν-boundary from above inequality:

$$\begin{aligned} &\left\{\nu k \ge (2+2\sqrt{2})k_P a\right\} \bigcap \{0 < \nu < 1\} \\ \rightarrow \quad &\therefore \ \frac{(2+2\sqrt{2})k_P(k+1/\gamma^2)^2}{k + (2+2\sqrt{2})k_P(k+1/\gamma^2)^2} \le \nu < 1. \end{aligned} \quad (6.20)$$

For the ν-region of (6.20), the discriminant has the region of $0 \le D < k^2$. Also, the real ε-boundary can be obtained from (6.19) as follows:

$$\frac{\nu k - \sqrt{D}}{2k_P^2a + 2\nu k k_P} \le \varepsilon \le \frac{\nu k + \sqrt{D}}{2k_P^2a + 2\nu k k_P}. \quad (6.21)$$

Fourth, when $\nu = \frac{(2+2\sqrt{2})k_P(k+1/\gamma^2)^2}{k+(2+2\sqrt{2})k_P(k+1/\gamma^2)^2}$, $D = 0$ and ε has the multiple root at $\varepsilon = \frac{1+\sqrt{2}}{(3+2\sqrt{2})k_P}$ as we can see in (6.21). Also, according as $\nu \to 1$, $D \to k^2$ and the ε-region is extended to $0 < \varepsilon < \frac{1}{k_P}$ as we can see in (6.21). These are illustrated in Fig. 6.1.

In other words, if the observer gain parameter within ε-region of (6.14) is chosen as shown in Fig. 6.1, then the ν parameter in Lyapunov function $Z(\boldsymbol{x}, \varphi, t)$ exists within ν-region of (6.20) so that the condition (6.17) can be satisfied. Therefore, we can conclude that the closed-loop system (6.10) and (6.11) has the extended disturbance $(\boldsymbol{w}, \phi)$ input-to-state $(\boldsymbol{x}, \varphi)$ stability. □

In above Theorem, we showed that an output feedback PID controller using the PID state observer can recover the disturbance input-to-state stability (ISS) achieved by using a full state feedback PID controller (an inverse optimal PID controller), if one condition for an observer gain can be satisfied. For instance, if the gain $k_P = 20$ was used as in [14], then the observer gain parameter ε should be determined within $0 < \varepsilon < 0.05$ to guarantee the ISS by Theorem 13. Actually, the smaller ε, the better PID state observer performance. However, very small ε causes the difficulty in implementing the PID

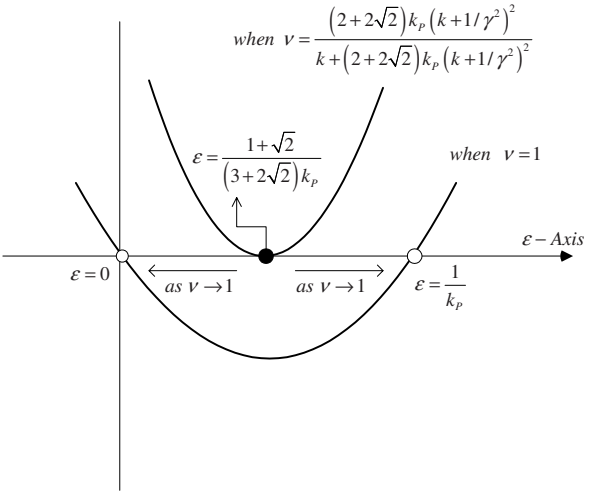

Fig. 6.1. The ε-boundary according to ν values

state observer because the observer gains become too large. Since it can be unnecessary to estimate the part of states corresponding to the measurement output, the reduced-order observer is suggested in following section.

6.3.3 Reduced-Order ID State Observer

Since the configuration error vector is the measurement output, *i.e.*, $\boldsymbol{y} = \boldsymbol{x}_2$, we can make the reduced-order observer that estimates only $\boldsymbol{x}_1$ and $\boldsymbol{x}_3$. To begin with, let us define new state vector as follows:

$$\begin{aligned} \eta_1 &= \boldsymbol{x}_1 - h_{r1}\boldsymbol{y} \\ \eta_2 &= \boldsymbol{x}_3 - h_{r2}\boldsymbol{y}, \end{aligned}$$

where h_{r1} and h_{r2} are new observer gains, then the reduced-order dynamics can be obtained from (6.3) using $\eta \triangleq [\eta_1^T \;\; \eta_2^T]^T$ and $\boldsymbol{x}_r \triangleq [\boldsymbol{x}_1^T \;\; \boldsymbol{x}_3^T]^T$ as follows:

$$\begin{aligned} \dot{\eta} &= \boldsymbol{A}_r\eta + \boldsymbol{B}_r\boldsymbol{y} + \boldsymbol{B}_{ro}\phi(\boldsymbol{y}, \eta_2, \boldsymbol{\tau}, t) \\ \boldsymbol{x}_r &= \boldsymbol{C}_r\eta + \boldsymbol{D}_r\boldsymbol{y}, \end{aligned} \tag{6.22}$$

where

$$
\begin{aligned}
\boldsymbol{A}_r &= \begin{bmatrix} \boldsymbol{0} & -h_{r1}\boldsymbol{I} \\ \boldsymbol{0} & -h_{r2}\boldsymbol{I} \end{bmatrix} \\
\boldsymbol{B}_r &= \begin{bmatrix} (1-h_{r1}h_{r2})\boldsymbol{I} \\ -h_{r2}^2\boldsymbol{I} \end{bmatrix} \\
\boldsymbol{C}_r &= \begin{bmatrix} \boldsymbol{I} & \boldsymbol{0} \\ \boldsymbol{0} & \boldsymbol{I} \end{bmatrix} \\
\boldsymbol{D}_r &= \begin{bmatrix} h_{r1}\boldsymbol{I} \\ h_{r2}\boldsymbol{I} \end{bmatrix} \\
\boldsymbol{B}_{ro} &= \begin{bmatrix} \boldsymbol{0} \\ \boldsymbol{I} \end{bmatrix}.
\end{aligned}
$$

For a reduced-order system (6.22), let us define the reduced-order observer as follows:

$$
\begin{aligned}
\dot{\hat{\eta}} &= \boldsymbol{A}_r\hat{\eta} + \boldsymbol{B}_r\boldsymbol{y} \\
\hat{\boldsymbol{x}}_r &= \boldsymbol{C}_r\hat{\eta} + \boldsymbol{D}_r\boldsymbol{y},
\end{aligned}
\tag{6.23}
$$

where $\hat{\eta}$ and $\hat{\boldsymbol{x}}_r$ are the estimates for η and $\boldsymbol{x}_r$. Also, if we define the estimation errors as $\tilde{\boldsymbol{x}}_r = \boldsymbol{x}_r - \hat{\boldsymbol{x}}_r$ and $\tilde{\eta} = \eta - \hat{\eta}$, then the estimation error dynamics is obtained by subtracting (6.23) from (6.22) as following form:

$$
\begin{aligned}
\dot{\tilde{\eta}} &= \boldsymbol{A}_r\tilde{\eta} + \boldsymbol{B}_{ro}\phi(\boldsymbol{y}, \eta_2, \boldsymbol{\tau}, t) \\
\tilde{\boldsymbol{x}}_r &= \boldsymbol{C}_r\tilde{\eta}.
\end{aligned}
$$

Since the transfer function from disturbance ϕ to the reduced-order estimation error $\tilde{\boldsymbol{x}}_r$ is calculated as follow:

$$
\begin{aligned}
\boldsymbol{G}_{\phi\tilde{x}_r}(s) &= \boldsymbol{C}_r[s\boldsymbol{I}_{2n\times 2n} - \boldsymbol{A}_r]^{-1}\boldsymbol{B}_{ro} \\
&= \begin{bmatrix} -\frac{h_{r1}}{s(s+h_{r2})}\boldsymbol{I} \\ \frac{1}{s+h_{r2}}\boldsymbol{I} \end{bmatrix},
\end{aligned}
$$

if we choose the observer gains as follows:

$$
h_{r1} = 0 \quad \text{and} \quad h_{r2} = \frac{\alpha}{\varepsilon}
\tag{6.24}
$$

with a small $\varepsilon \ll 1$, then above transfer function is arranged as follows:

$$
\boldsymbol{G}_{\phi\tilde{x}_r}(s) = \begin{bmatrix} \boldsymbol{0} \\ \frac{\varepsilon}{\varepsilon s+\alpha}\boldsymbol{I} \end{bmatrix} \quad \rightarrow \quad \therefore \lim_{\varepsilon\to 0} \boldsymbol{G}_{\phi\tilde{x}_r}(s) = \boldsymbol{0}.
$$

Hence, the effect of disturbance ϕ is gradually diminished for a reduced-order estimation error $\tilde{\boldsymbol{x}}_r$ according as $\varepsilon \to 0$.

On the other hand, we can see that the reduced-order observer (6.23) includes both an exact integrator and an approximate differentiator. Let us consider the reduced-order observer from $\boldsymbol{y}$ to $\hat{\boldsymbol{x}}_r$ as follow:

$$\begin{aligned} \boldsymbol{G}_{y\hat{x}_r}(s) &= \boldsymbol{C}_r(s\boldsymbol{I}_{2n\times 2n} - \boldsymbol{A}_r)^{-1}\boldsymbol{B}_r + \boldsymbol{D}_r \\ &= \begin{bmatrix} \frac{1}{s}\boldsymbol{I} \\ \frac{\alpha s}{\varepsilon s+\alpha}\boldsymbol{I} \end{bmatrix}. \end{aligned}$$

Here, if the observer gain parameter ε approaches zero as follow:

$$\lim_{\varepsilon\to 0} \boldsymbol{G}_{y\hat{x}_r}(s) = \begin{bmatrix} \frac{1}{s}\boldsymbol{I} \\ s\boldsymbol{I} \end{bmatrix}, \tag{6.25}$$

then $\hat{\boldsymbol{x}}_{r1}$ and $\hat{\boldsymbol{x}}_{r2}$ approach $\int \boldsymbol{e}dt$ and $\dot{\boldsymbol{e}}$, respectively. Differently from the PID state observer, since this observer (6.23) estimates only both integral error and derivative error, we call it the reduced-order ID state observer.

6.4 Notes

The PID state observer and its reduced-order one were suggested for Lagrangian systems. Also, we proved that an output feedback PID controller using the PID state observer can also recover the extended disturbance input-to-state stability (ISS) achieved by using a full state feedback one, if one condition for an observer gain parameter is satisfied. In a broad sense, the separation principle between an inverse optimal PID controller and PID state observer should be made as discussed in references such as [4, 5, 17, 62]. Our future work should be to reveal the separation principle for PID control and observer systems.

7

Concluding Remarks

This book has answered to several possible questions which can be raised in applying a trajectory tracking PID control to mechanical systems, ***e****.g.*, can it be an optimal control? If yes, what is it? Can its performance tuning rules be derived analytically? Is there its automatic performance tuning law? Can an output feedback PID control be effectively used under what condition? *etc.* Also. this book extends the PID control theory to an optimal control, auto-tuning control, and output feedback control. Those are simply summarized in following paragraphs.

First, this book found out algebraic relationships between the individual PID gains and $\mathcal{H}_\infty$ performance index. It was proved that an inverse optimal PID control exists if and only if the mechanical system is extended disturbance input-to-state stable (ISS).

Second, the performance tuning rules of PID control were derived from the performance limitation. Two simple performance tuning rules were suggested as the name of square rule and linear rule, and then, the compound rule was suggested as one rule unifying both square rule and linear one.

Third, an automatic performance tuning rule of PID control was derived from both quasi-equilibrium region and direct adaptive control. This automatic performance tuning rule can help to accomplish the target performance.

Fourth, the PID state observer was suggested to achieve the output feedback PID controller. Also, it was proved that the output feedback PID control system including a PID state observer can be disturbance input-to-state stable with one condition for observer gain.

Although this book has dealt with possible many subjects which can be raised for continuous PID control systems, we still need the theoretical development for the sampled-data PID control and discrete PID control because the PID control is mostly performed in a digital form. Also, PID control has produced many kinds of PID control plus something methods for mechanical systems, *e.g.*, PID plus feed-forward dynamic term, PID plus disturbance observer, PID plus friction compensator, *etc.* These methods have each meaning according to the control objectives of various mechanical systems. It has

Y. Choi, W.K. Chung: PID Trajectory Tracking Control for Mechanical Systems, LNCIS 298, pp. 101–102, 2004.

been also very important to study PID control plus something for mechanical systems, in these cases, this book can help to study and analyze them.

References

1. Angeli, D. (1999). Input-to-state stability of PD-controlled robotic systems. *Automatica*, **35**, 1285–1290.
2. Arimoto, S. and Miyazaki, F. (1984). Stability and robustness of PID feedback control for robot manipulators of sensory capability. *Robotics Research edited by M. Brady and R. Paul*, pages 783–799.
3. Astrom, K. and Hagglund, T. (1995). *PID Controllers: Theory, Design, and Tuning*. Instrument Society of America: Research Triangle Park.
4. Atassi, A. N. and Khalil, H. K. (1999). A separation principle for the stabilization of a class of nonlinear systems. *IEEE Trans. on Automatic Control*, **44**(9), 1672–1687.
5. Atassi, A. N. and Khalil, H. K. (2001). A separation principle for the control of a class of nonlinear systems. *IEEE Trans. on Automatic Control*, **46**(5), 742–746.
6. Berghuis, H. and Nijmeijer, H. (1993). A passivity approach to controller-observer design for robots. *IEEE Trans. on Robotics and Automation*, **9**(6), 740–754.
7. Berghuis, H. and Nijmeijer, H. (1994). Robust control of robots via linear estimated state feedback. *IEEE Trans. on Automatic Control*, **39**(10), 2159–2162.
8. Bryson, A. E. and Ho, Y. C. (1975). *Applied Optimal Control*. A Halsted Press Book.
9. Chellaboina, V., Haddad, W. M., and Hayakawa, T. (2001). Direct adaptive control for nonlinear matrix second-order dynamical systems with state-dependent uncertainty. *Proc. of the American Control Conference*, pages 4247–4252.
10. Choi, Y. and Chung, W. K. (2001). On the optimality and performance of PID controller for robotic manipulators. *Proc. of IEEE Int. Conf. on Robotics and Automation*, pages 1142–1148.
11. Choi, Y. and Chung, W. K. (2003). PID performance tuning methods for a robotic manipulator based on ISS. *Asian Journal of Control*, **5**(2), 206–216.
12. Choi, Y., Chung, W. K., and Youm, Y. (1997). Robust control of manipulators using Hamiltonian optimization. *Proc. of IEEE Int. Conf. on Robotics and Automation*, pages 2538–2364.
13. Choi, Y., Chung, W. K., and Youm, Y. (2001a). On the optimal PID performance tuning for robotic manipulators. *Proc. of IEEE/RSJ Int. Conf. on Intelligent Robots and Systems*, pages 1656–1661.

14. Choi, Y., Chung, W. K., and Suh, I. H. (2001b). Performance and $\mathcal{H}_\infty$ optimality of PID trajectory tracking controller for Lagrangian systems. *IEEE Trans. on Robotics and Automation*, **17**(6), 857–869.
15. Choi, Y., Oh, Y., Oh, S. R., and Chung, W. K. (2003). Auto-tuning PID controller for robotic manipulators. *Proc. of the American Control Conference*, pages 350–355.
16. Craig, J. J. (1989). *Introduction to Robotics : Mechanics and Control*. Addison Wesley.
17. Dabroom, A. M. and Khalil, H. K. (2001). Output feedback sampled-data control of nonlinear systems using high-gain observer. *IEEE Trans. on Automatic Control*, **46**(11), 1712–1725.
18. Dawson, D., Grabbe, M., and Lewis, F. L. (1991). Optimal control of a modified computed-torque controller for a robotic manipulator. *International J. of Robotics and Automation*, **6**, 161–165.
19. de Wit, C. C., Fixot, N., and Astrom, K. J. (1992). Trajectory tracking in robot manipulators via nonlinear estimated state feedback. *IEEE Trans. on Robotics and Automation*, **8**(1), 138–144.
20. Doyle, J. C., Glover, K., Khargonekar, P. P., and Francis, B. A. (1989). State space solutions to standard $\mathcal{H}_2$ and $\mathcal{H}_\infty$ control problems. *IEEE Trans. on Automatic Control*, **34**(8), 831–847.
21. Esfandiari, F. and Khalil, K. H. (1992). Output feedback stabilization of fully linearizable systems. *Int, J. of Control*, **56**, 1007–1037.
22. Golub, G. H. and Loan, C. F. V. (1996). *Matrix Computations 3rd Edition*. The Johns Hopkins Univ. Press.
23. Gu, E. Y. L. (2000). Configuration manifolds and their applications to robot dynamic modeling and control. *IEEE Trans. on Robotics and Automation*, **16**(5), 517–527.
24. Haddad, W. M. and Hayakawa, T. (2000a). Direct adaptive control for nonlinear systems with bounded energy $\mathcal{L}_2$ disturbances. *IEEE Conf. on Decision and Control*, pages 2419–2423.
25. Haddad, W. M. and Hayakawa, T. (2000b). Direct adaptive control for nonlinear uncertain systems with exogenous disturbances. *Proc. of the American Control Conference*, pages 4425–4429.
26. He, J. B., Wang, Q. G., and Lee, T. H. (2000). PI/PID controller tuning via LQR approach. *Chemical Engineering Science*, **55**, 2429–2439.
27. Horn, R. A. and Johnson, C. R. (1985). *Matrix Analysis*. Cambridge Univ. Press.
28. Ioannou, P. A. and Sun, J. (1996). *Robust Adaptive Control*. Prentice Hall.
29. Isidori, A. and Astolfi, A. (1992). Disturbance attenuation and $\mathcal{H}_\infty$–control via measurement feedback in nonlinear systems. *IEEE Trans. on Automatic Control*, **37**, 1283–1293.
30. Johansson, R. (1990). Adaptive control of robot manipulator motion. *IEEE Trans. on Robotics and Automation*, **6**(4), 483–490.
31. Kelly, R. (1995). A tuning procedure for stable PID control of robot manipulators. *Robotica*, **13**, 141–148.
32. Kelly, R. (1998). Global positioning of robot manipulators via PD control plus a class of nonlinear integral actions. *IEEE Trans. on Automatic Control*, **43**(7), 934–937.
33. Khalil, H. K. (1992). *Nonlinear Systems*. Macmillan.

34. Khalil, H. K. (1999). *High-gain Observers in Nonlinear Feedback Control*. edited by H. Nijmeijer and T. I. Fossen, Springer.
35. Khosla, P. K. (1989). Categorization of parameters in the dynamics robot model. *IEEE Trans. on Robotics and Automation*, **5**(3), 261–268.
36. Krstic, M. and Li, Z. H. (1998). Inverse optimal design of input-to-state stabilizing nonlinear controllers. *IEEE Trans. on Automatic Control*, **43**(3), 336–350.
37. Krstic, M. and Tsiotras, P. (1999). Inverse optimal stabilization of a rigid spacecraft. *IEEE Trans. on Automatic Control*, **44**(5), 1042–1049.
38. Krstic, M., Kanellakopoulos, I., and Kokotovic, P. V. (1995). *Nonlinear and Adaptive Control Design*. John Wiley & Sons.
39. Krstic, M., Sun, J., and Kokotovic, P. V. (1996). Robust control of nonlinear systems with input unmodeled dynamics. *IEEE Trans. on Automatic Control*, **41**(6), 913–920.
40. Lee, K. and Kim, J. (2000). Controller gain tuning of a simultaneous multi-axis PID control system using the Taguchi method. *Control Engineering Practice*, pages 949–958.
41. Macki, J. and Strauss, A. (1982). *Introduction to Optimal Control Theory*. Springer-Verlag.
42. Magnus, J. R. and Neudecker, H. (1988). *Matrix Differential Calculus with Applications in Statistics and Econometrics*. John Wiley & Sons.
43. Meressi, T., Chen, D., and Paden, B. (1993). Application of kharitonov's theorem to mechanical systems. *IEEE Trans. on Automatic Control*, **38**(3), 488–491.
44. Nicosia, S. and Tomei, P. (1990). Robot control by using only joint position measurements. *IEEE Trans. on Automatic Control*, **35**(9), 1058–1061.
45. Ortega, R. and Spong, M. W. (1988). Adaptive motion control of rigid robots: A tutorial. *IEEE Conf. on Decision and Control*, pages 1575–1584.
46. Ortega, R., Loria, A., and Kelly, R. (1995). A semi-globally stable output feedback PI^2D regulator for robot manipulators. *IEEE Trans. on Automatic Control*, **40**(8), 1432–1436.
47. Park, J. and Chung, W. K. (2000a). Analytic nonlinear $\mathcal{H}_\infty$ inverse-optimal control for Euler-Lagrange system. *IEEE Trans. on Robotics and Automation*, **16**, 847–854.
48. Park, J. and Chung, W. K. (2000b). Design of a robust $\mathcal{H}_\infty$ PID control for industrial manipulators. *Trans. ASME J. of Dyn. Syst., Meas. and Contr.*, pages 803–812.
49. Park, J., Chung, W. K., and Youm, Y. (1998). Analytic nonlinear $\mathcal{H}_\infty$ optimal control for robot manipulators. *Proc. of IEEE Int. Conf. on Robotics and Automation*, pages 2709–2715.
50. Qu, Z. and Dorsey, J. (1991). Robust tracking control of robots by a linear feedback law. *IEEE Trans. on Automatic Control*, **36**(9), 1081–1084.
51. Ramirez, J. A., Cervantes, I., and Kelly, R. (2000). PID regulation of robot manipulators: Stability and Performance. *System & Control Letter*, **41**, 73–83.
52. Rocco, P. (1996). Stability of PID control for industrial robot arm. *IEEE Trans. on Robotics and Automation*, **12**(4), 606–614.
53. Roup, A. V. and Bernstein, D. S. (2000). Stabilization of a class of nonlinear systems using direct adaptive control. *Proc. of the American Control Conference*, pages 3148–3152.
54. Salcudean, S. (1991). A globally convergent angular velocity observer for rigid body motion. *IEEE Trans. on Automatic Control*, **36**(12), 1493–1497.

55. Sciavicco, L. and Siciliano, B. (1996). *Modeling and Control of Robot Manipulators*. McGraw-Hill.
56. Slotine, J.-J. E. (1988). Putting physics in control - the example of robotics. *IEEE Control Systems Magazine*, pages 12–17.
57. Sontag, E. D. (1989). Smooth stabilization implies coprime factorization. *IEEE Trans. on Automatic Control*, **34**(4), 435–443.
58. Sontag, E. D. and Wang, Y. (1995). On characterizations of the input-to-state stability property. *System & Control Letter*, **24**, 351–359.
59. Su, W., de Souza, C. E., and Xie, L. (1999). $\mathcal{H}_\infty$ control for asymptotically stable nonlinear systems. *IEEE Trans. on Automatic Control*, **44**(5), 989–993.
60. Takegaki, M. and Arimoto, S. (1981). A new feedback method for dynamic control of manipulators. *Trans. ASME J. of Dyn. Syst., Meas. and Contr.*, **102**, 119–125.
61. Tang, Y., Tomizuka, M., Guerrero, G., and Montemayor, G. (2000). Decentralized robust control of mechanical systems. *IEEE Trans. on Automatic Control*, **45**(4), 771–776.
62. Teel, A. and Praly, L. (1994). Global stabilizability and observability imply semi-global stabilization by output feedback. *System & Control Letter*, **22**, 313–325.
63. Tomei, P. (1991). Adaptive PD controller for robot manipulators. *IEEE Trans. on Robotics and Automation*, **7**(4), 565–570.
64. van der Schaft, A. (1992). $\mathcal{L}_2$-gain analysis of nonlinear systems and nonlinear state feedback $\mathcal{H}_\infty$ control. *IEEE Trans. on Automatic Control*, **37**(6), 770–784.
65. van der Schaft, A. (2000). *$\mathcal{L}_2$-gain and Passivity Techniques in Nonlinear Control*. Springer-Verlag.
66. Yu, C. C. (1999). *Autotuning of PID Controllers: Relay Feedback Approach*. Springer.
67. Zhou, K., Doyle, J. C., and Glover, K. (1995). *Robust and Optimal Control*. Prentice Hall.
68. Ziegler, J. G. and Nichols, N. B. (1942). Optimum settings for automatic controllers. *ASME Trans.*, **64**, 759–768.

Index